



Calhoun: The NPS Institutional Archive
DSpace Repository

Theses and Dissertations

1. Thesis and Dissertation Collection, all items

1984-12

Analysis of control system from a viewpoint of desired pole placement and desired degree of robustness

Chang, Jinhwa

<http://hdl.handle.net/10945/19130>

Downloaded from NPS Archive: Calhoun



Calhoun is the Naval Postgraduate School's public access digital repository for research materials and institutional publications created by the NPS community. Calhoun is named for Professor of Mathematics Guy K. Calhoun, NPS's first appointed -- and published -- scholarly author.

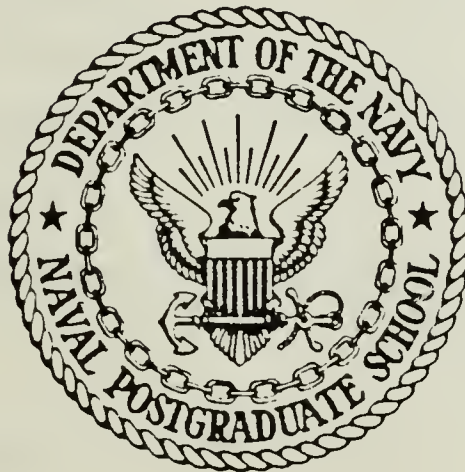
Dudley Knox Library / Naval Postgraduate School
411 Dyer Road / 1 University Circle
Monterey, California USA 93943

<http://www.nps.edu/library>

PUDLEY KNOX LIBRARY
NAVAL POSTGRADUATE SCHOOL
MONTEREY, CALIFORNIA 93943

NAVAL POSTGRADUATE SCHOOL

Monterey, California



THESIS

ANALYSIS OF CONTROL SYSTEM FROM A VIEWPOINT
OF DESIRED POLE PLACEMENT AND
DESIRED DEGREE OF ROBUSTNESS

by

Jinhwa Chang

December 1984

Thesis Advisor:

Daniel J. Collins

Approved for public release; distribution unlimited.

T222034

UNCLASSIFIED

SECURITY CLASSIFICATION OF THIS PAGE (When Data Entered)

REPORT DOCUMENTATION PAGE		READ INSTRUCTIONS BEFORE COMPLETING FORM
1. REPORT NUMBER	2. GOVT ACCESSION NO.	3. RECIPIENT'S CATALOG NUMBER
4. TITLE (and Subtitle) Analysis of Control System From A Viewpoint of Desired Pole Placement and Desired Degree of Robustness		5. TYPE OF REPORT & PERIOD COVERED Master's Thesis December 1984
		6. PERFORMING ORG. REPORT NUMBER
7. AUTHOR(s) Jinhwa Chang		8. CONTRACT OR GRANT NUMBER(s)
9. PERFORMING ORGANIZATION NAME AND ADDRESS Naval Postgraduate School Monterey, CA 93943		10. PROGRAM ELEMENT, PROJECT, TASK AREA & WORK UNIT NUMBERS
11. CONTROLLING OFFICE NAME AND ADDRESS Naval Postgraduate School Monterey, CA 93943		12. REPORT DATE December 1984
		13. NUMBER OF PAGES 82
14. MONITORING AGENCY NAME & ADDRESS (if different from Controlling Office)		15. SECURITY CLASS. (of this report) Unclassified
		15a. DECLASSIFICATION/DOWNGRADING SCHEDULE
16. DISTRIBUTION STATEMENT (of this Report) Approved for public release; distribution unlimited.		
17. DISTRIBUTION STATEMENT (of the abstract entered in Block 20, if different from Report)		
18. SUPPLEMENTARY NOTES		
19. KEY WORDS (Continue on reverse side if necessary and identify by block number) Analysis Control System, Desired Pole Placement, Robustness		
20. ABSTRACT (Continue on reverse side if necessary and identify by block number) A design method for solving the problem of robustness to cross-coupling perturbations in multivariable control systems for the X22A V/STOL aircraft is presented. The method uses numerical optimization procedures to manipulate the system feedback gains as direct design variables. The desired performance by pole placement and robustness by modification of the minimum singular values of the system return difference matrix.		

Channels affected by cross-coupling perturbation may be recognized by the character of their transfer function Bode plots. The mechanism used by the pole placement and robustness routine in obtaining a robust design is evident from the gain changes associated with the transfer function diagram and the zero shifts shown on pole-zero plots. The pole placement and robustness routine uses gain equalization and zero assignment to modify the characteristics of the system in the areas of low singular values, producing a robust design.

Approved for public release; distribution is unlimited

Analysis of Control System from a Viewpoint
of Desired Pole Placement
and Desired Degree of Robustness

by

Jinhwa Chang
Major, Republic of Korea Air Force
B.S., Republic of Korea Air Force Academy, 1975

Submitted in partial fulfillment of the
requirements for the degree of

MASTER OF SCIENCE IN AERONAUTICAL ENGINEERING

from the

NAVAL POSTGRADUATE SCHOOL
December 1984

ABSTRACT

A design method for solving the problem of robustness to cross-coupling perturbations in multivariable control systems for the X22A V/STOL aircraft is presented. The method uses numerical optimization procedures to manipulate the system feedback gains as direct design variables. The manipulation is accomplished in a manner that produces desired performance by pole placement and robustness by modification of the minimum singular values of the system return difference matrix.

Channels affected by cross-coupling perturbation may be recognized by the character of their transfer function Bode plots. The mechanism used by the pole placement and robustness routine in obtaining a robust design is evident from the gain changes associated with the transfer function diagram and the zero shifts shown on pole-zero plots. The pole placement and robustness routine uses gain equalization and zero assignment to modify the characteristics of the system in the areas of low singular values, producing a robust design.

TABLE OF CONTENTS

I.	INTRODUCTION	10
II.	ROBUSTNESS: SINGLE-INPUT SINGLE-OUTPUT SYSTEMS (SISO)	12
III.	MULTIVARIABLE SYSTEMS ROBUSTNESS	20
IV.	POLE PLACEMENT ONLY DESIGN PROCEDURE	26
V.	POLE PLACEMENT AND ROBUSTNESS DESIGN PROCEDURE	27
VI.	APPLICATIONS (X22A LONGITUDINAL PROBLEM)	31
	A. INPUT TRANSFER FUNCTION $F*G$ ANALYSIS	33
	B. OUTPUT TRANSFER FUNCTION $G*F$ ANALYSIS	53
VII.	CONCLUSIONS	79
	LIST OF REFERENCES	81
	INITIAL DISTRIBUTION LIST	82

LIST OF TABLES

1.	X22A V/STOL a/c Parameter Definitions	32
2.	Pole Only Desired Pole and Computed Pole	33
3.	Pole Placement and Robustness Design Pole Locations	35
4.	F*G Transfer Functions Bode Plot Results	48
5.	G*F Pole placement and Robustness Design Pole Locations	57
6.	G*F Transfer Functions Bode Plot Results	69

LIST OF FIGURES

2.1	Classical Bode Plot	13
2.2	Nyquist Plot of Stable System	14
2.3	Additively Perturbed System	15
2.4	Additive Nyquist Plot	16
2.5	Nyquist for Inequality Additive Condition	17
2.6	Multiplicative System	18
2.7	Nyquist Plot for Multiplicative System	19
3.1	Nyquist D Contour	21
3.2	Basic Multi-input Multi-output System	22
3.3	Additive Perturbation	23
3.4	Multiplicative Perturbation	25
5.1	Universal Gain and Phase Singular Value Plot	28
6.1	System Block Diagram	32
6.2	Pole Placement Only Singular Value Plots	34
6.3	Robustness Design Singular Value Plots	36
6.4	Pole Placement Only Design Time Response	37
6.5	F*G Robustness Design Time Response	38
6.6	Pole Placement Only Design F*G 1:1	40
6.7	Robustness Design F*G 1:1	41
6.8	Pole Placement Only Design F*G 1:2	42
6.9	Robustness Design F*G 1:2	43
6.10	Pole Placement Only Design F*G 2:1	44
6.11	Robustness Design F*G 2:1	45
6.12	Pole Placement Only Design F*G 2:2	46
6.13	Robustness Design F*G 2:2	47
6.14	Pole-Zero Map for 1:1 and 1:2	49
6.15	Pole-Zero Map for 1:3 and 1:4	50
6.16	Pole-Zero Map for 2:1 and 2:2	51

6.17	Pole-Zero Map for 2:3 and 2:4	52
6.18	Pole Placement Only Design F*G Closedloop 1:2 . . .	54
6.19	Robustness Design F*G Closedloop 1:2	55
6.20	Pole placement only G*F Singular Value Plots . . .	56
6.21	Robustness Design G*F Singular Value Plots	58
6.22	G*F Robustness Design Time Response	59
6.23	Pole Placement Only Design G*F 1:1	60
6.24	Robustness Design G*F 1:1	61
6.25	Pole Placement Only Design G*F 1:2	63
6.26	Robustness Design G*F 1:2	64
6.27	Pole Placement Only Design G*F 2:1	65
6.28	Robustness Design G*F 2:1	66
6.29	Pole Placement Only Design G*F 2:2	67
6.30	Robustness Design G*F 2:2	68
6.31	Pole-Zero Map for 1:1 and 1:2	70
6.32	Pole-Zero Map for 1:3 and 1:4	71
6.33	Pole-Zero Map for 2:1 and 2:2	72
6.34	Pole-Zero Map for 2:3 and 2:4	73
6.35	Pole Placement Only Design G*F Closedloop 1:2 . . .	74
6.36	Robustness Design G*F Closedloop 1:2	75
6.37	Robust Design F*G Output Singular Value Plots . . .	77
6.38	Robust design G*F Input Singular Value Plots . . .	78

ACKNOWLEDGEMENTS

For over nine years the Republic of Korea Air Force has allowed me to make practical application of the science of flight as a Combat Pilot. I wish to express my appreciation to the Korea Air Force and United States Naval postgraduate school for the opportunity to further expand my knowledge of aviation by pursuing this degree.

I would also like to express a sincere thanks to Professor D.J. Collins as my thesis adviser. Without his support this effort would never have been completed.

I would also like to thank my wife, Heasung and children, Soona and Sunghwan. As anyone knows who has undertaken an effort of this magnitude without their love and support this would have been impossible. They have "gone it alone" quite often so that this paper could be completed.

Above all thanks to Him who started it all.

I. INTRODUCTION

In practice, the control system designer rarely has the freedom to feed back the entire state of the system to achieve the desired system performance. Thus, an important problem from a practical standpoint is the determination of constant, output feed back gains for the control of systems with unmeasured states.

The pole placement only and pole placement and robustness design procedure uses placement to establish a designer selected performance level and then a minimum singular value level to establish robustness. The pole placement only was relatively easy to implement through a numerical optimization routine. By using this numerical procedure it is also simple to incorporate robustness into the procedure along with the performance requirement. The technique, which utilizes a modern optimization routine, can significantly assist the designer in obtaining robustness in the face of cross coupling perturbations. It has been shown that the cross coupling problem can be detected by using classical open loop Bode diagrams as well as modern control analysis based on singular values. As currently employed, the pole placement and robustness program is used to obtain pole placement and robustness for a given set of starting gains and a selected optimization routine from the ADS program.

The pole placement and robustness design procedure is a straight forward numerical optimization procedure for the practical application modern MIMO system analysis. The new aspects of the procedure are the implementation of both pole placement and robustness criteria within the same design program.

The pole placement and robustness design routine developed for this thesis has been used on X-22A A/C problem. In these studies the pole placement and robustness design code has proven capable of meeting the desired goals of pole placement and robustness and also brought to light some interesting aspects of the cross-coupling perturbation problem.

The remainder of the thesis will present background material on Robustness(SISO system) in Chapter Two and Robustness of MIMO systems in chapter Three. Pole placement only design procedure in chapter Four, Pole placement and Robustness design in chapter Five, along with a discussion of Applications for X-22A a/c problem by input transfer function $F*G$ analysis and output transfer function $G*F$ analysis. Conclusions will be presented in the final chapter. The computer programs used in the present analysis were developed in [Ref. 9].

II. ROBUSTNESS: SINGLE-INPUT SINGLE-OUTPUT SYSTEMS (SISO)

A review of the concept of robustness and stability in the framework of a conventional SISO system will be done before pursuing the concepts in a more complicated fashion in the following chapters. A simple interpretation of robustness is the ability of the system to tolerate design perturbations. These perturbations could be in the form of actuator failures, plant parameter uncertainty, unmodeled dynamics or nonlinear terms, or any one of many other perturbations to the nominal design of the system.

The primary reason for feedback systems is the control of uncertainty within the system. By appropriate use of feedback, properties that would lead to an unstable system may be controlled. When stability and robustness aspects are considered for a SISO system, frequency domain design concepts, using either Nyquist or Bode plots, are normally used. Robustness in SISO systems is formulated naturally by the concept of gain and phase margins, both of which are readily available on the Nyquist or Bode diagram.

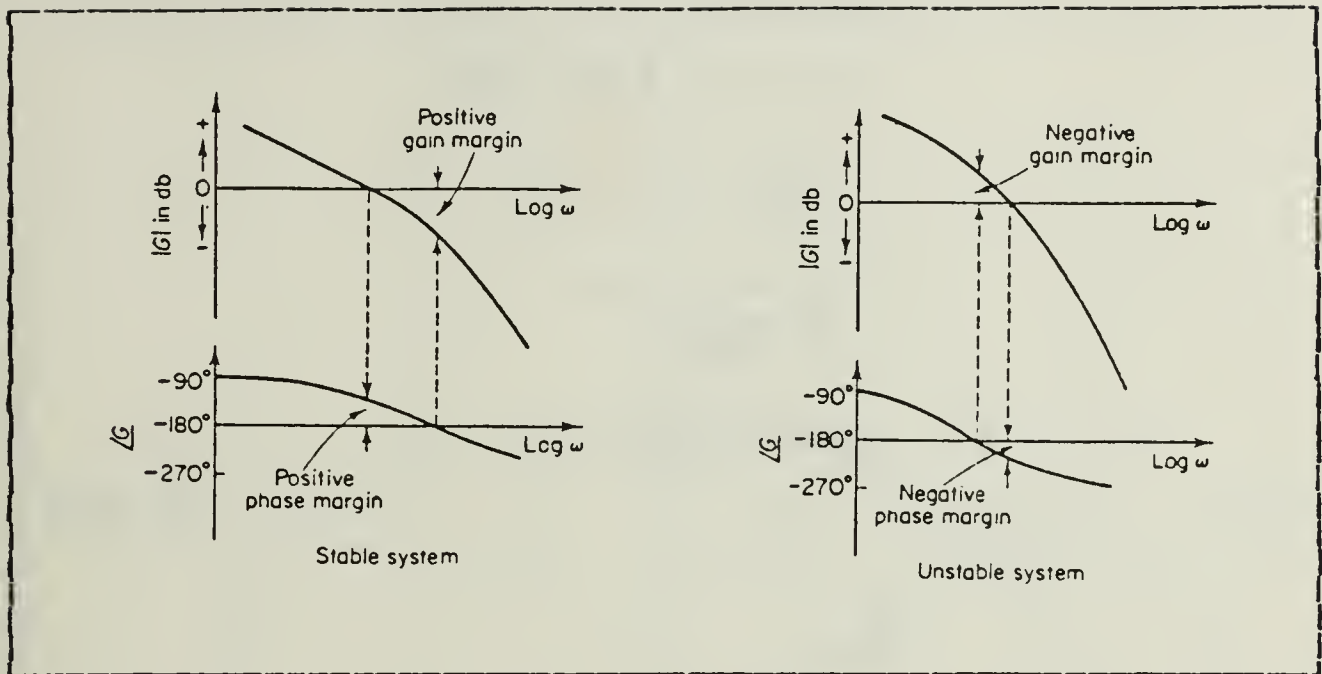


Figure 2.1. Classical Bode Plot.

Gain and phase margin can be defined in terms of the open-loop frequency domain plots in either the Bode or Nyquist format. Figure 2.1 depicts a classical Bode plot showing gain and phase margin determination from the plot. The Nyquist plot may also be used to obtain this information. Nyquist criterion states that if the open-loop transfer function $G(s)H(s)$ has n poles in the right half plane and the limit of $G(s)H(s) = \text{constant}$ as $s \rightarrow \infty$ then for a stable system the locus of $G(s)H(s)$ will encircle the $-1+j0$ point n times in the counterclockwise direction as s varies along the Nyquist contour. If there are no poles in the right half s plane then the locus will not encircle the $-1 + j0$ point. The diagram in Figure 2.2 illustrates a nominally stable system. The gain and phase margin may be determined directly from the diagram.

Any change in the loop transfer function, provided the order of $G(s)H(s)$ does not change, that changes the number of times the locus of $G(s)H(s)$ encircles the $(-1,0)$ point in

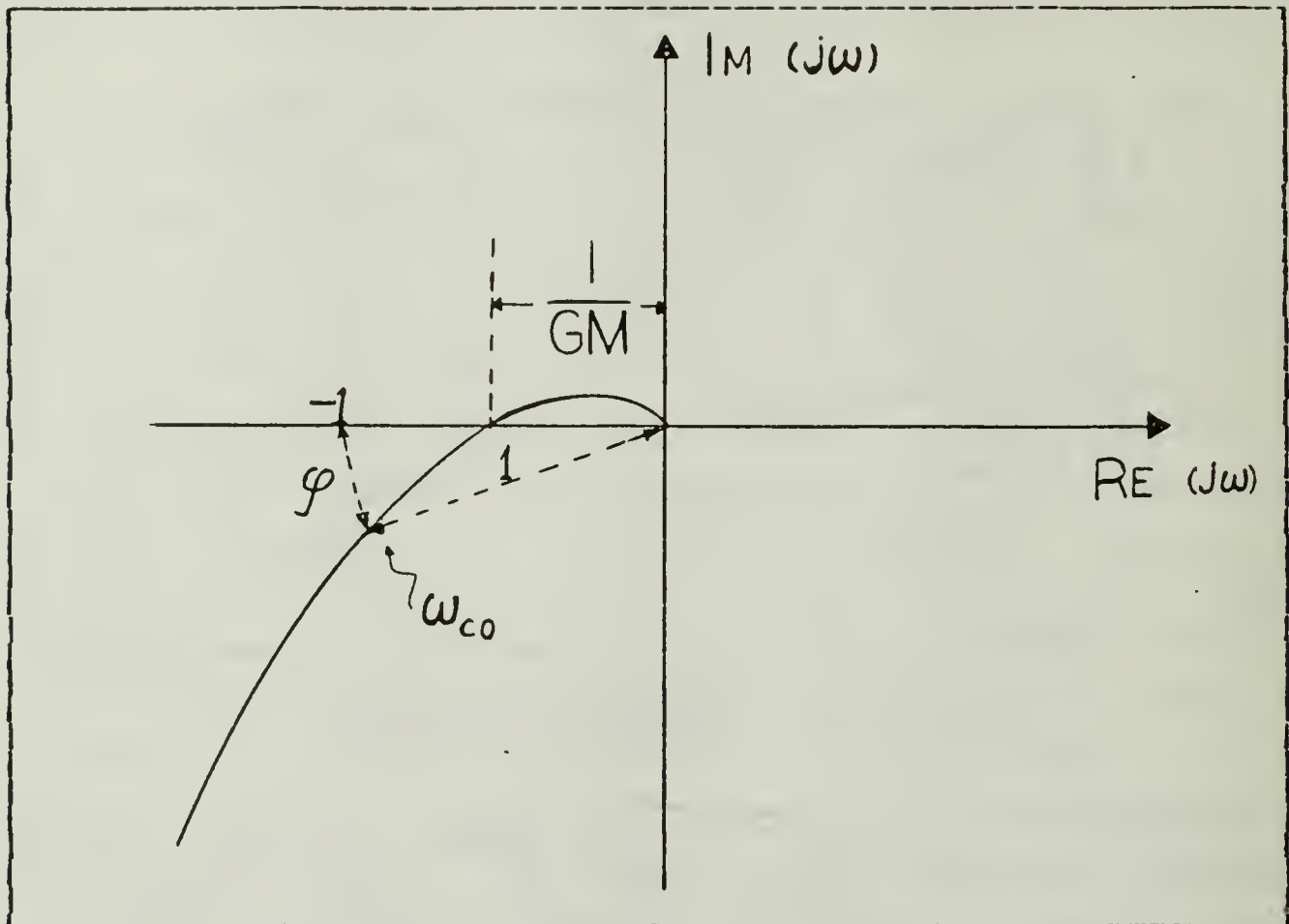


Figure 2.2 Nyquist Plot of Stable System.

the Nyquist plot causes the system to become unstable. This leads to the conclusion that the minimum distance of the locus of $G(s)H(s)$ to the $(-1,0)$ point is a measure of the system stability. This distance concept carries over directly to the Multi-Input Multi-Output (MIMO) system as will be shown in the next chapter. Examples of a multiplicative perturbation and an additive perturbation illustrate this idea. Figure 2.3 is an additively perturbed system. Figure 2.4 shows the Nyquist plot for this system. Assuming that the plant is itself stable and the perturbations are also stable the diagram may then be used to determine how

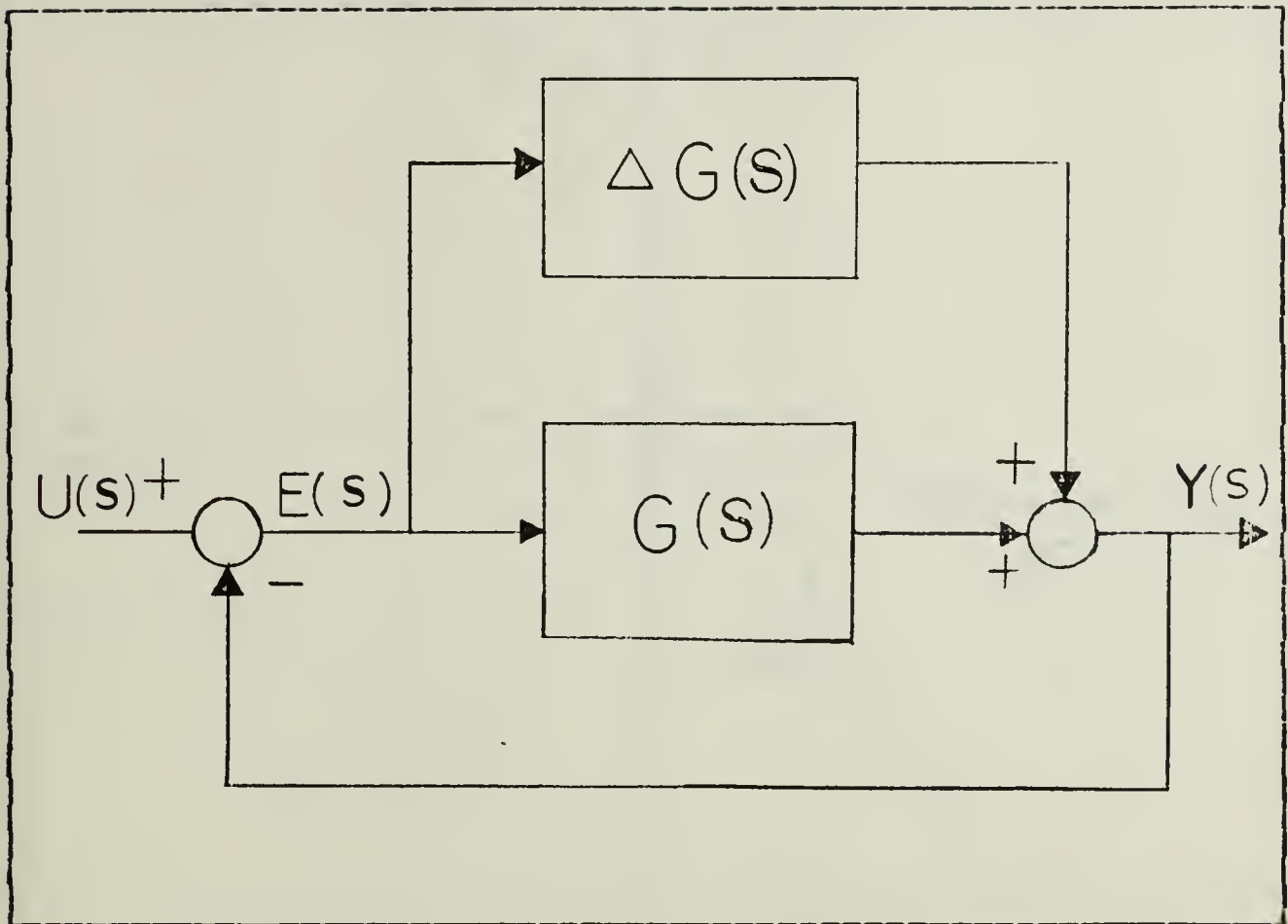


Figure 2.3 Additively Perturbed System.

near the system is to instability for the given perturbation.

Since the system is stable the $(-1,0)$ point is encircled the correct number of times by the nominal plant. If the locus of $g(j\omega)$ in the diagram is warped until it passes beyond the $(-1,0)$ point then clearly the number of encirclements of this point will change and the system will become unstable, assuming the order of the plant is not changed by the perturbation. To keep the locus of points from moving beyond the $(-1,0)$ point equation 2.1 must hold.

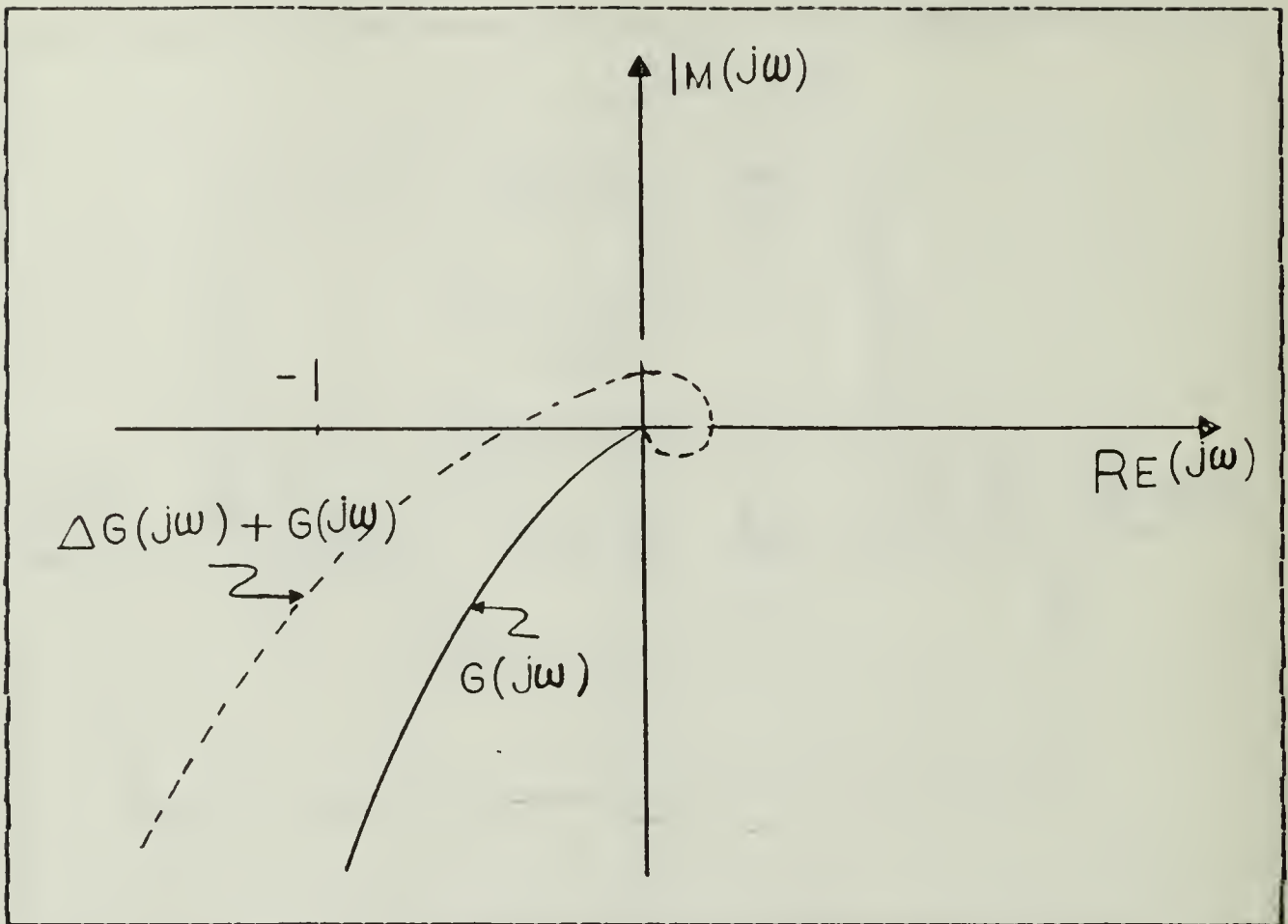


Figure 2.4 Additive Nyquist Plot.

$$|\Delta g(j\omega)| < |1 + g(j\omega)| \quad (2.1)$$

This condition is illustrated in Figure 2.5. The right-hand side of equation 2.1 is just the magnitude of the return difference transfer function of the nominal system. The multiplicative case is depicted in Figure 2.6 with its associated Nyquist plot in Figure 2.7. The requirement for stability is similar to the additive case and may be stated in equation 2.2

$$|\Delta g(j\omega)| < |1 + (g(j\omega))^{-1}| \quad (2.2)$$

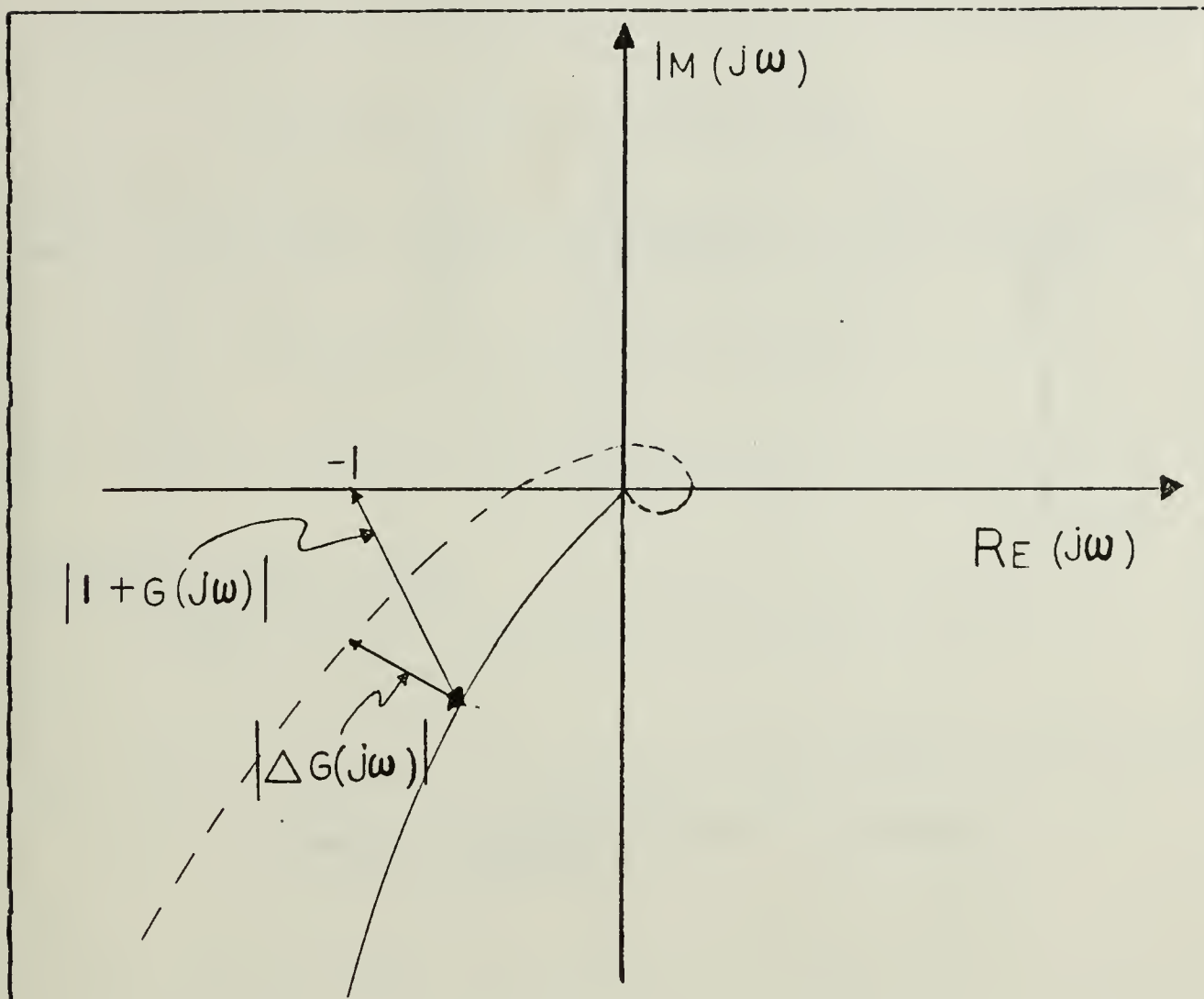


Figure 2.5 Nyquist for Inequality Additive Condition.

The above arguments will be applied again in Chapter 3 to develop multivariable stability and robustness properties. With this basic review of the concepts of stability and robustness in the classical SISO system complete, the next chapter will extend some of these basic concepts to the MIMO system.

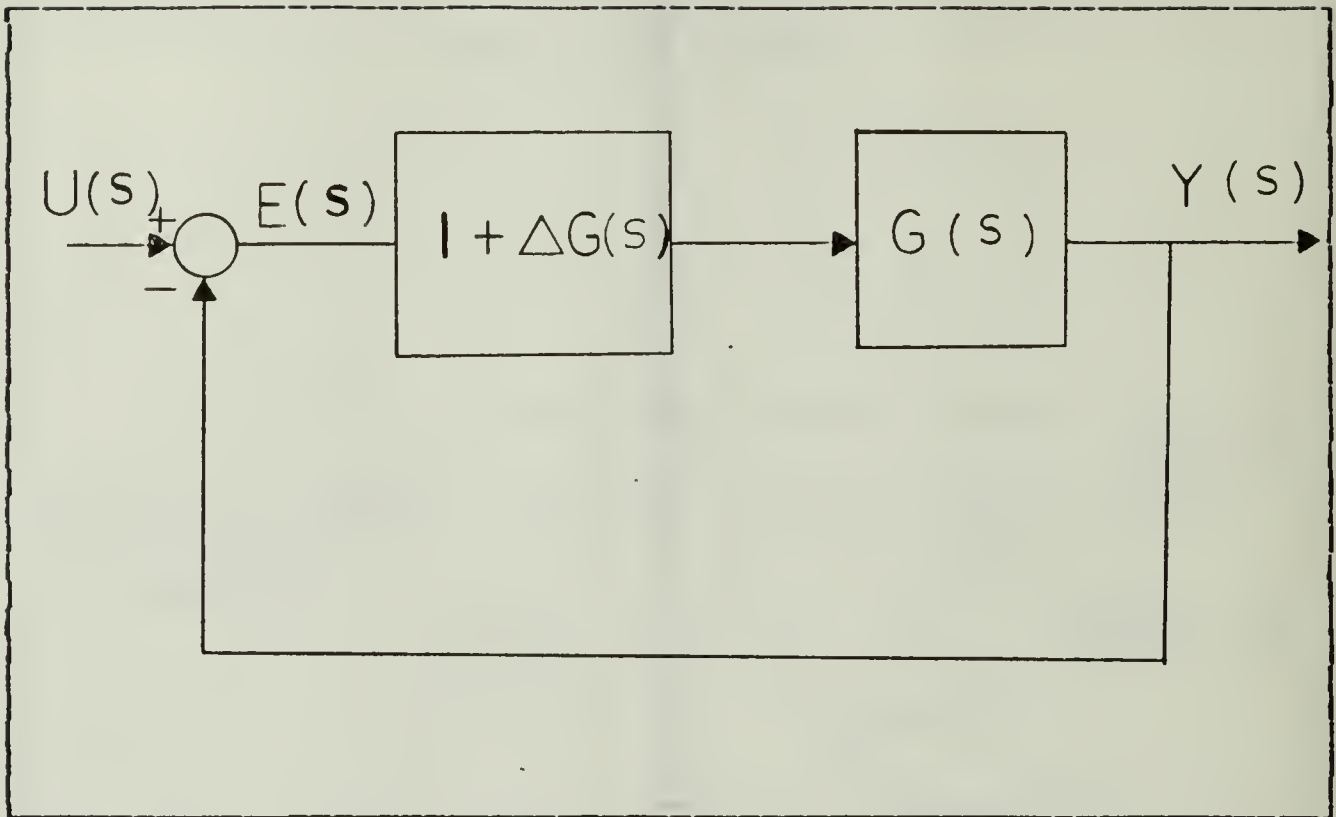


Figure 2.6 Multiplicative System.

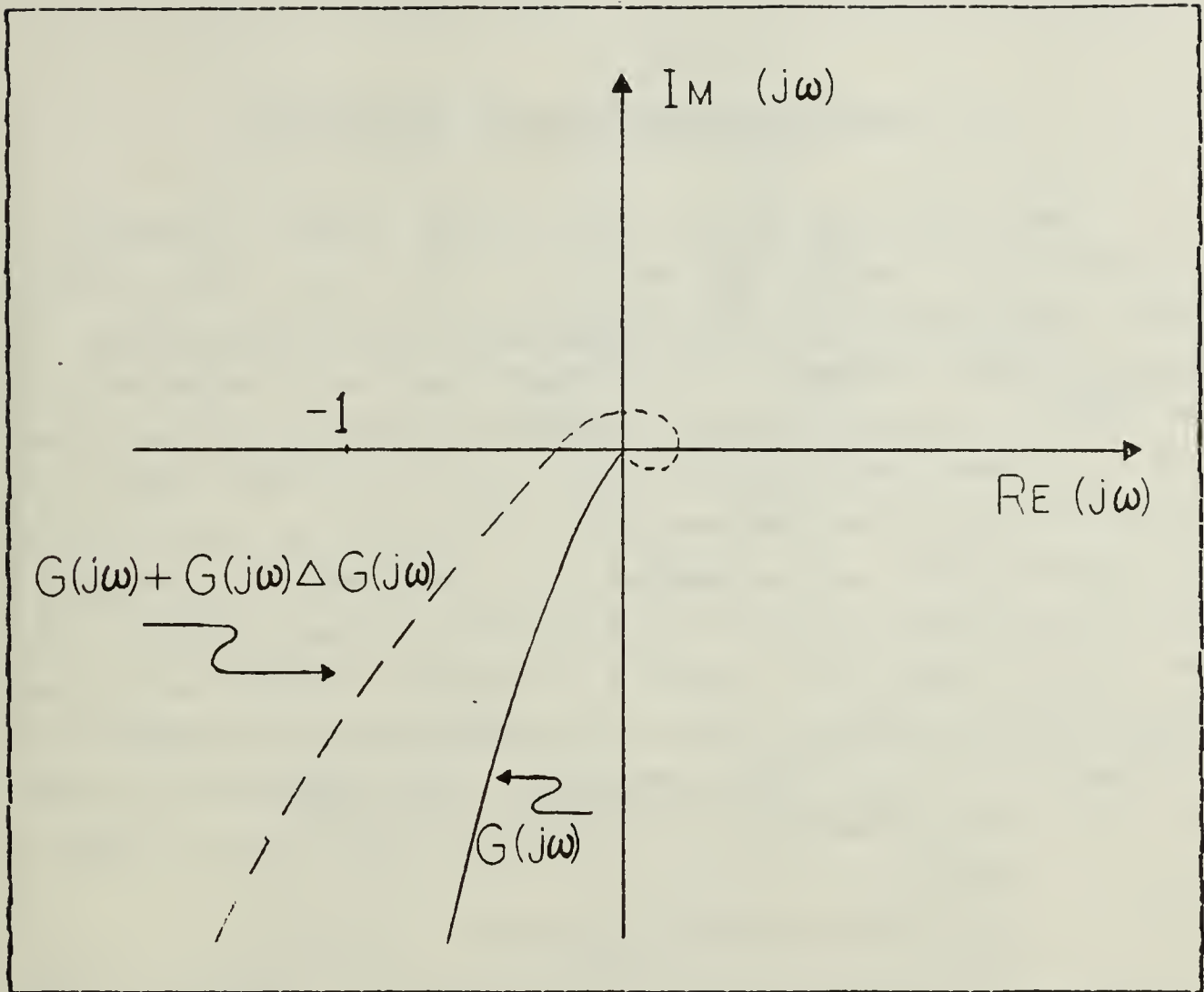


Figure 2.7 Nyquist Plot for Multiplicative System.

III. MULTIVARIABLE SYSTEMS ROBUSTNESS

A generalization of the SISO Nyquist theory discussed in the previous chapter has been made for the MIMO problem. This generalization leads directly to the application of singular value concept. The generalization is expressed in the form of the multivariable Nyquist theorem which requires that a closed loop stable system have the same number of counterclockwise encirclements of the origin by the locus of the $\det(I+G(j\omega))$ as the number of open loop poles that are in the right half plane. This theorem is formally stated as; Let $N[f(s)]$ denote the number of clockwise encirclements of $(-1,0)$ by the locus of $f(s)$ as s traverses the contour D of Figure 3.1 in a clockwise sense. The closed-loop system will be stable if and only if for all R sufficiently large

$$N[f(s)] = -P$$

where N = number of encirclements

$$f(s) = -1 + \det[I+G(s)] = \varphi_{cl}(s) / \varphi_{ol}(s) - 1 \text{ and}$$

P = the number of closed right-half plane zeros of $\varphi_{ol}(s)$.

The application of the Nyquist theorem comes through the fact that a multivariable system will not be robust to modelling errors if the return difference matrix, $I + G$, is nearly singular for some frequency. If $I + G$ is nearly singular a small change in G may make $I + G$ exactly singular. This causes the $\det(I + G)$ to become zero and the Nyquist encirclement count to change indicating an unstable system. It is possible for very small changes in $I+G$ to produce large changes in the determinant of $I+G$. The matrix $I+G$

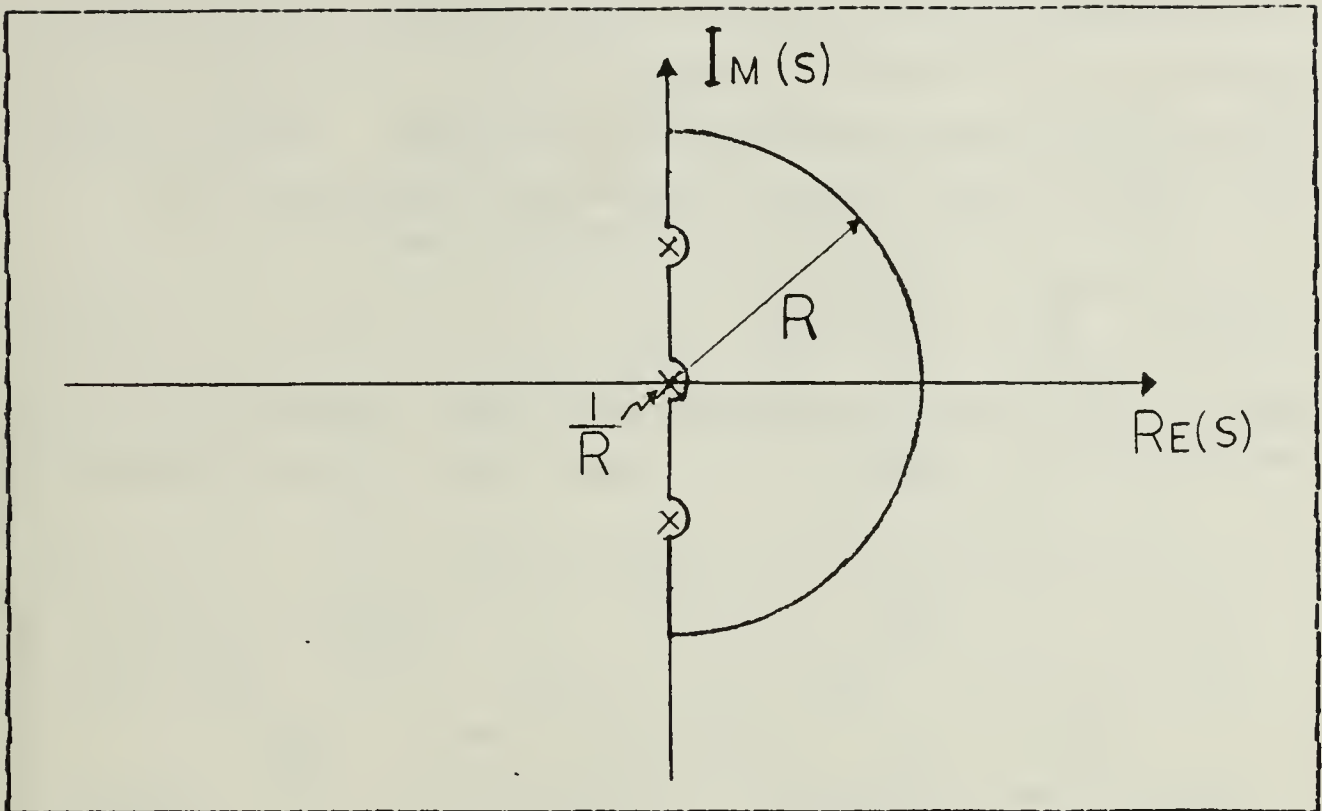


Figure 3.1 Nyquist D Contour.

$$\begin{bmatrix} 10/s+a & 9.99/s+a \\ 10/s+a & 10/s+a \end{bmatrix}$$

has determinant $0.1/(s+a)^2$. If the element p is changed by only one percent to $9.9/s+a$ the determinant becomes $1.1/(s+a)^2$ which is a significant change in the determinant-value. Therefore, it is evident that $\det(I + G)$ is not an accurate measure of how near the return difference is to singularity. Researchers, in the field of controls [Ref. 1], [Ref. 2], [Ref. 3], [Ref. 4] have used singular value analysis to determine how near the return difference matrix is to singularity.

Since the number of encirclements of the Nyquist diagram changes as $f(s)$ passes through the -1 point or when $\det(I+G)$ is zero it is important to find how near the return difference matrix $I+G$ is to being singular. This nearness to singularity can be interpreted as the distance of matrix $I+G$

to the critical point, -1 . A quantity which can be used to express the nearness to singularity of the matrix is the minimum matrix singular value denoted by $\underline{\sigma}$. Given a matrix \underline{A} the singular value may be expressed by equation 3.1

$$\underline{\sigma}(\underline{A}) = \min_i (\lambda_i (\underline{A}^H \underline{A})) \quad (3.1)$$

where $\lambda_i (\underline{A}^H \underline{A})$ is the eigenvalue of the complex conjugate transpose of \underline{A} times \underline{A} . A basic MIMO linear system is

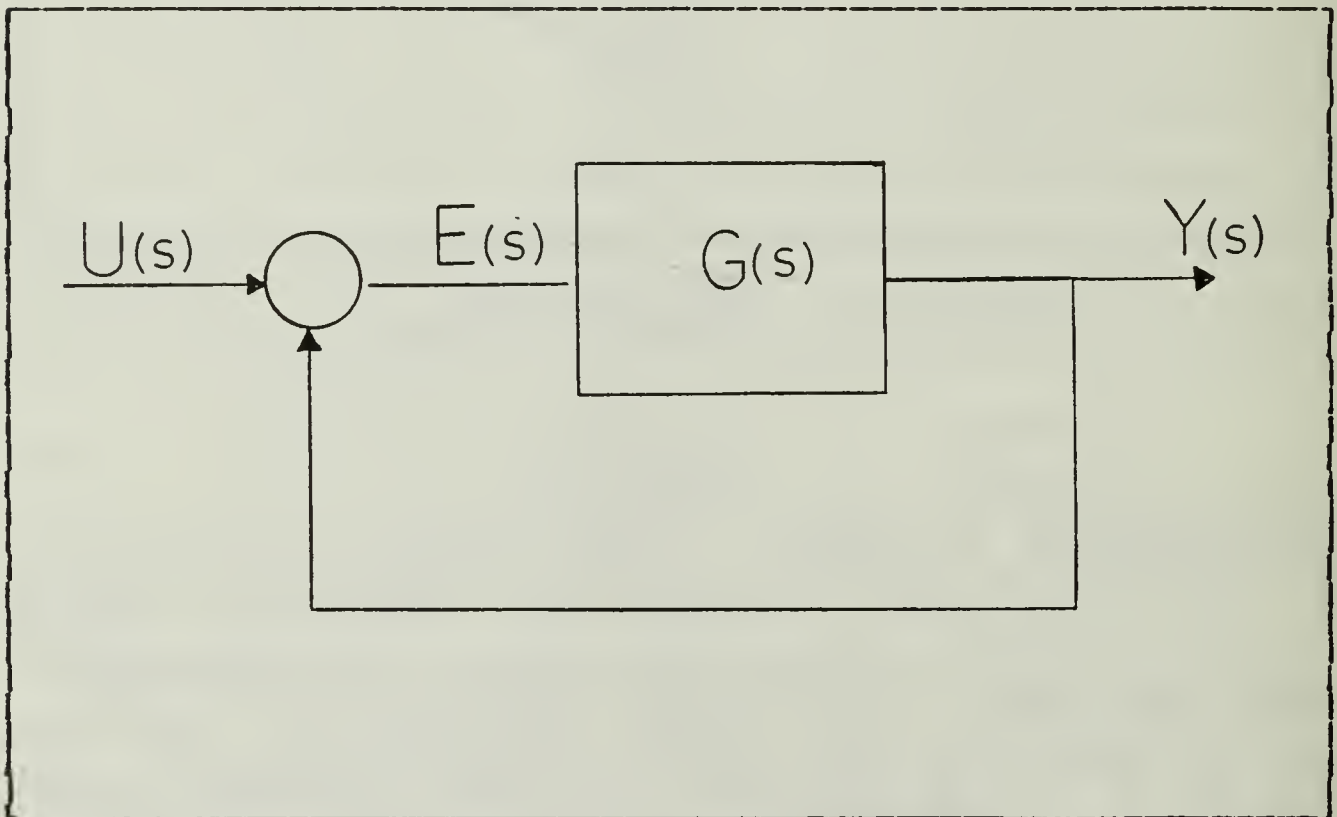


Figure 3.2 Basic Multi-input Multi-output System.

depicted in Figure 3.2. An additive perturbation to the plant is shown in Figure 3.3. If the plant is stable before the perturbation is added to the system the Nyquist theorem will be satisfied and the locus of GH will not encircle the $-1,0$ critical point. When the perturbation is added to the system as long as the Nyquist locus is not forced to

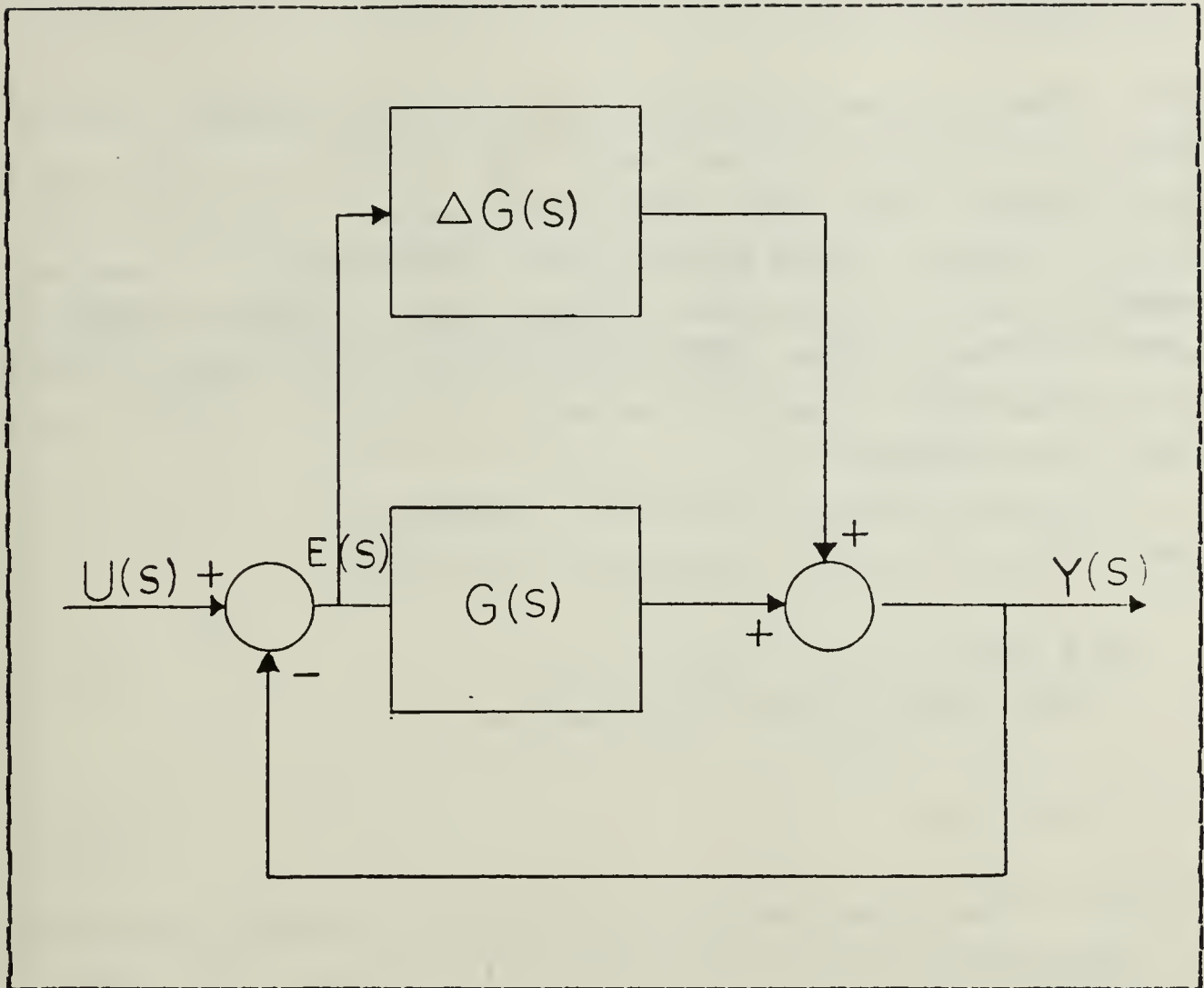


Figure 3.3 Additive Perturbation.

encircle the -1 point the system, will remain stable. A sufficient condition, recalling the SISO discussion in chapter 2, for the perturbed Nyquist plot not to change encirclements is that the norm of the perturbation ΔG remain less than the norm of the return difference matrix as expressed in equation 3.2.

$$\| \Delta G(j\omega) \| < 1 / \| (I + G)^{-1} \| \quad (3.2)$$

The condition $\omega \geq 0$ will that the locus of the $\det(I + G)$ does not pass through the -1 point. If the 1 or Euclidean norm is assumed for this condition the equation 3.2 may be expressed in terms of singular values as equation 3.3.

$$\overline{\sigma}(\Delta G) \leq \underline{\sigma}(I + G) \quad (3.3)$$

This result states that as long as the maximum singular value of the perturbation matrix ΔG is below the minimum norm value of the return difference matrix the system will remain stable. The problem of guaranteeing robustness becomes that of finding the largest norm of the perturbation quantity, the largest singular value, for which the smallest norm or singular value of the return difference matrix will remain non-singular.

The multiplicative form for a system such as Figure 3.4 gives the similar norm equation in equation 3.4

$$\|\Delta G(j\omega)\| < 1 / \|(I + G)^{-1}\| \quad (3.4)$$

$\omega \geq 0$. which may be expressed as

$$\overline{\sigma}(\Delta G) \leq \underline{\sigma}(I + G^{-1}) \quad (3.5)$$

Singular value decomposition software is readily available to determine how near the matrix $I+G$ or $I+G^{-1}$ is to singularity.

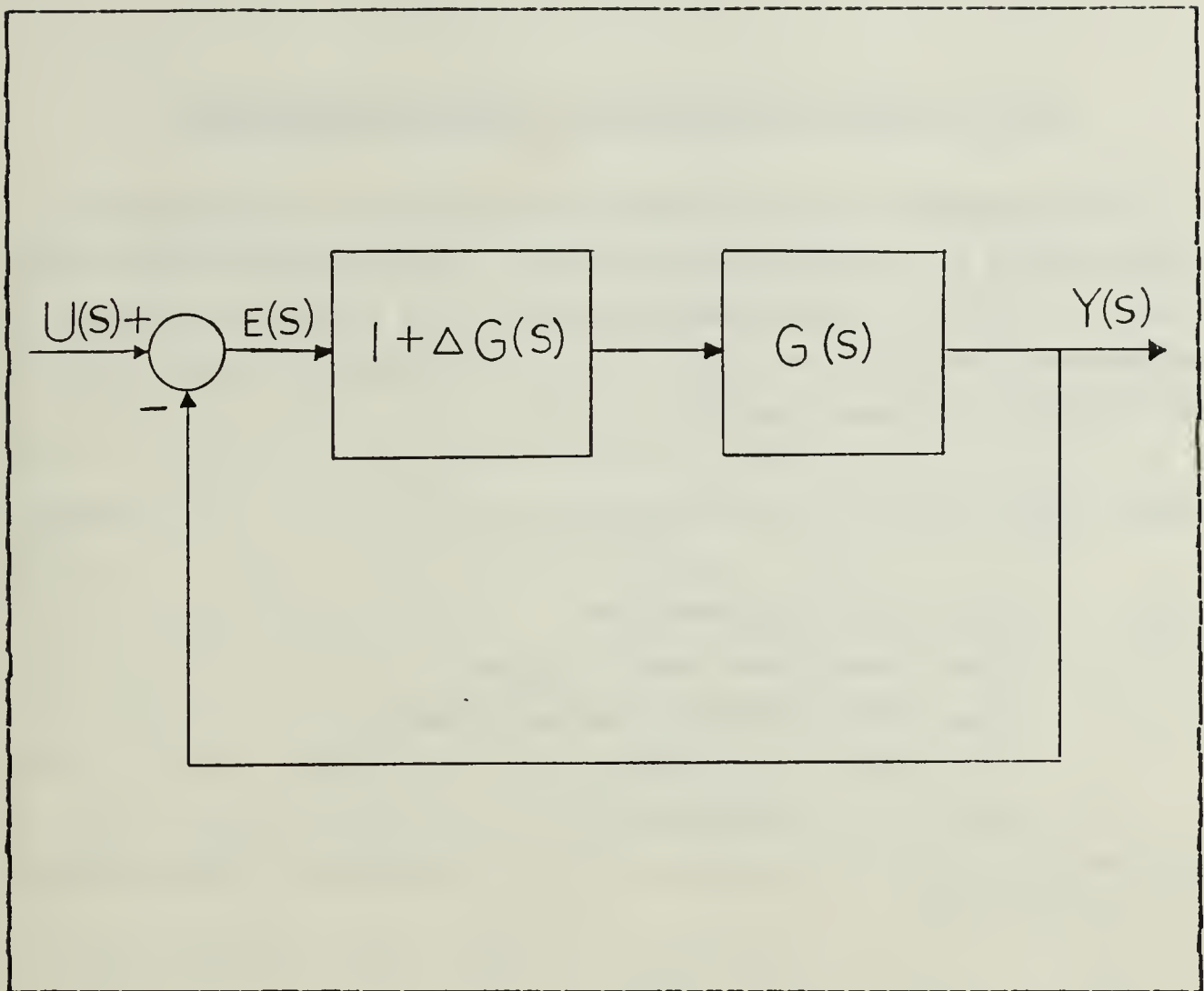


Figure 3.4 Multiplicative Perturbation.

IV. POLE PLACEMENT ONLY DESIGN PROCEDURE

The designer may use either objective, constraint or a combination of functions to secure the desired pole locations. As currently implemented in the program the cost or objective portion of the pole placement procedure is constructed as equation 4.1

$$OBJ = \sum_{i=1}^{\ell} (\lambda_{RD_i} - \lambda_{R_i})^2 + (\lambda_{ID_i} - \lambda_{I_i})^2 \quad (4.1)$$

where λ_R = real eigenvalue
 λ_I = imaginary eigenvalue
 λ_{RD} = desired eigenvalue location
 λ_{ID} = desired eigenvalue location

The constraint formulation is a function that must be kept negative or the constraint is violated. It is written as equation 4.2

$$g(j) = \sqrt{(\lambda_{RD_i} - \lambda_{R_i})^2 + (\lambda_{ID_i} - \lambda_{I_i})^2} - r \quad (4.2)$$

where r is a tolerance circle established as a function of pole placement position. Since the aim of the optimizer is to keep g negative any time the λ function of the constraint is greater than r the constraint will become active, i.e. violated. The optimizer will then attempt to move the constraint to the inactive status by adjusting the design parameters of the system. For obtaining the feedback gains and desired poles use the 'CONXSV' program [Ref. 9], weight function 1 equal 1 the other weight functions are set to 0. After obtaining the feedback gains the NPS 'OPTSYS' program was used to plot the Bode, Nyquist diagram and pole zeros plot.

V. POLE PLACEMENT AND ROBUSTNESS DESIGN PROCEDURE

Consideration of implementation of the frequency domain or robustness portion of the design procedure begins with the concept of MIMO phase and gain margins. Several useful theorems on singular value analysis of multiloop systems are presented in [Ref. 3]. One of these theorems relates the matrix singular value of the return difference function to a parameter, α , and further shows that as long as the maximum singular value of the perturbation function $(L^{-1} - I)$ remains less than this α , the system remains stable. The value of α is then related to gain and phase margins of the MIMO system. The relationship developed is given in equations 5.1 and 5.2:

$$\text{gain margin} = \text{GM} = 1/(1+\alpha_o) \quad (5.1)$$

$$\text{phase margin} = \text{PM} = +\cos^{-1}(1-\alpha_o^2/2) \quad (5.2)$$

provided that equation 5.3 holds.

$$\underline{\sigma}(I+G) \geq \alpha_o \quad (5.3)$$

for some $\alpha_o \leq 1$

These phase and gain margins are guaranteed in every loop simultaneously.

Universal gain and phase margin curves, [Ref. 5], based on the minimum singular values of the return difference matrix are developed from equation 5.4.

$$(L^{-1}-I) = \max \sqrt{(1-1/k_n)^2 + 2/k_n (1-\cos \varphi_n)} \quad (5.4)$$

for all n with $k_n > 0$. These curves shown in Figure 5.1 allow the designer to pick a singular value that corresponds to a specific gain and phase margin for a given system.

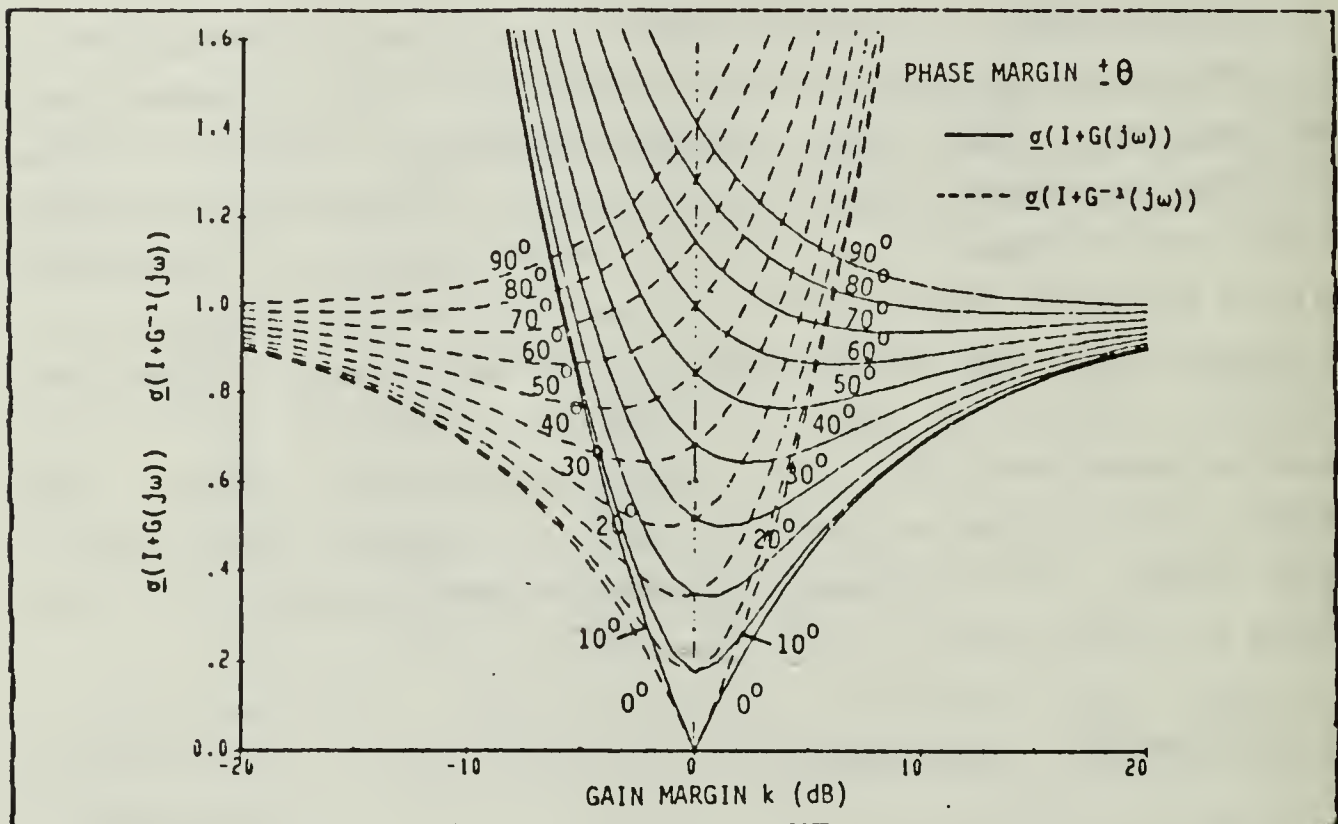


Figure 5.1 Universal Gain and Phase Singular Value Plot.

Since the universal curve in Figure 5.1 provides a convenient method of specifying gain and phase margins in terms of singular values the robustness portion of the pole placement and robustness design procedure uses the minimum singular value level of the return difference matrix to determine the robustness. The minimum singular value level is formulated as an objective or constraint function in equation 5.5

$$J = \sum_{\lambda} (\max(0, (\sigma_D - \sigma(j\omega, p)))^2 \quad (5.5)$$

The optimization procedure may be used to change feedback gains until the minimum singular value is raised above this desired design level. Although the same formulation can be used as a negative constraint function it has not been implemented as such within this program. There are numerous ways the singular value formulation could be implemented within the program by changes of the code if design requirements forced such changes.

The pole placement and robustness design program is based on the ADS code to implement the design variable selection procedures. The pole placement and robustness program is used to provide designs for state or output feedback problem.

For the state or output feedback design program the user must input the plant matrices A, B, C and initial starting values for the feedback matrix F. The matrices correspond to the following linear differential system:

$$\dot{\underline{x}} = \underline{A}\underline{x} + \underline{B}\underline{u} \quad (5.6)$$

$$\underline{y} = \underline{C}\underline{x} \quad (5.7)$$

$$\underline{u} = -\underline{F}\underline{x} \quad (5.8)$$

As the design program is currently coded the user may run output feedback or state feedback design by specifying the C matrix as the diagonal(I) matrix for state feedback. The program relies on initial starting values of the feedback gains, F.

The ability to select acceptable starting values for the feedback gains will make the procedure more efficient in operation. As currently employed, the program is used to obtain pole placement and robustness for a given set of starting gains and a selected optimization routine from the

ADS program. If the optimizer is not able to meet the desired design goals on this program run two options are available. First, change to a different optimization routine from the list of available ADS routines and rerun the problem. This was usually successful in improving the design. Second, the designer uses a new set of starting values for the feedback gains and repeats the design procedure. Both options might be used on particularly difficult cases.

The pole placement and robustness design algorithm computes input additive, output additive, input multiplicative, and output multiplicative singular values. The versatility of the pole placement and robustness design is obtained by incorporating a state of the art optimizer routine ADS, with currently available singular value computation routines.

VI. APPLICATIONS (X22A LONGITUDINAL PROBLEM)

This chapter will deal with a more practical application of the numerical optimization program. In this problem the combined pole placement only, robustness design procedure will be applied to the linear longitudinal dynamic channels of an X22A V/STOL a/c [Ref. 8]. The model is that of the longitudinal dynamics of an X22A V/STOL a/c at low altitude and airspeed = 65 knots. The dynamic model of the system is

$$\dot{\underline{x}} = \underline{A} \underline{x} + \underline{B} \underline{u} \quad (6.1)$$

$$\underline{x} = (u, w, q, \theta) \quad (6.2)$$

$$\underline{u} = (\delta_e, \delta_f) \quad (6.3)$$

where

$$\underline{A} = \begin{bmatrix} -0.18 & -0.03 & 9.57 & -31.87 \\ -0.2 & -0.55 & 109.43 & 2.78 \\ -0.01 & -0.02 & -0.1 & 0 \\ 0 & 0 & 1. & 0 \end{bmatrix}$$

and where

$$\underline{B} = \begin{bmatrix} -0.36 & 0.52 \\ 0. & -1. \\ 0.33 & 0.02 \\ 0. & 0. \end{bmatrix}$$

with full state available for feedback. Table 1 is a summary of parameters. The system is not open-loop stable.

The control law is formulated to satisfy the desired performance specification. Equation 6.4 is the basic control law.

TABLE 1

X22A V/STOL a/c Parameter Definitions

Variable	Units	Description
U	ft/sec	Body axis forward velocity perturbation
W	ft/sec	Vertical velocity perturbation
Q	rad/sec	Pitch rate
θ	rad	Pitch attitude
δ_e	inch	Elevator position
δ_t	inch	Throttle position

$$\underline{u} = -F\underline{x}$$

(6.4)

The design studies presented up to this point have been based on breaking the system loop at the input as shown in

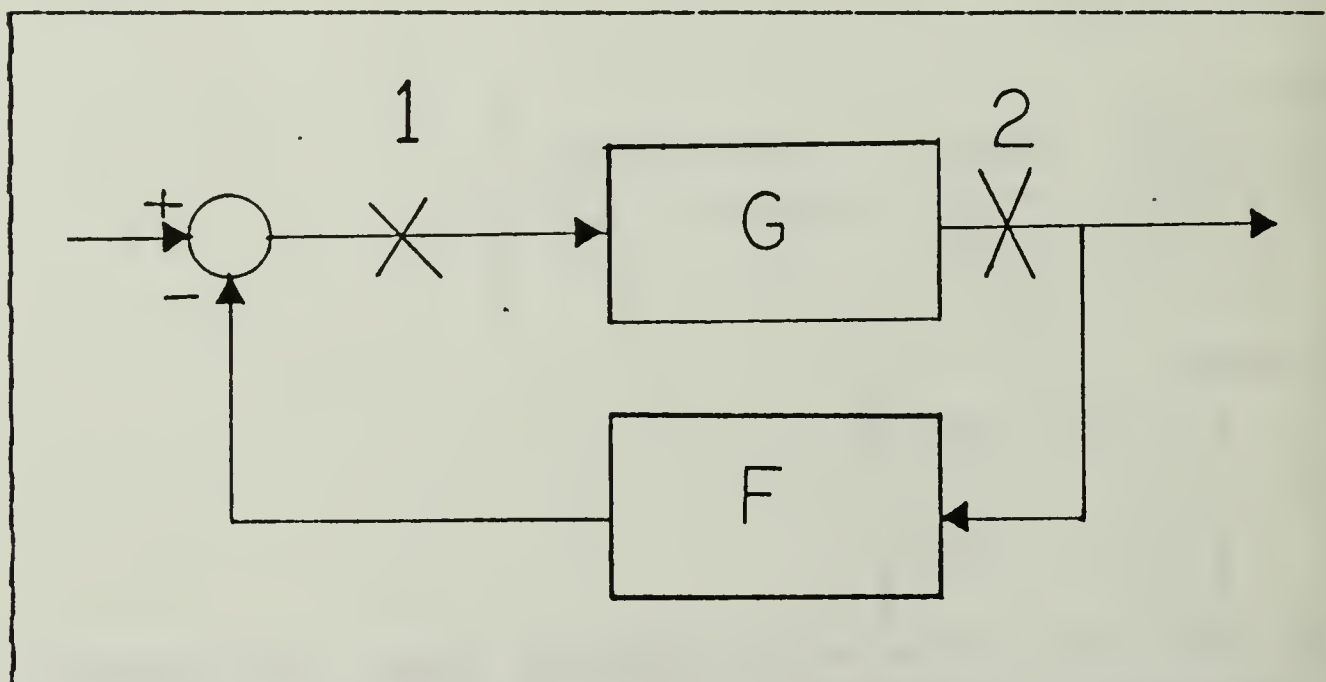


Figure 6.1 System Block Diagram.

Figure 6.1. In multivariable theory the location of the break in the loop changes the return difference for the system and the transfer function formulation. In Figure 6.1, number 1 depicts a system with an input loop break point while number 2 depicts an output loop break point for output return difference determination. The return difference function for point 1 is written as $I+FG$ while the return difference for point 2 is $I+GF$. In figure number 1 the transfer function FG is

$$FG = F' * (SI - A) * B$$

$$F' = F * C$$

and GF is $GF = C * (SI - A) * B'$

$$B' = B * F$$

A. INPUT TRANSFER FUNCTION $F * G$ ANALYSIS

Using the NPGS 'CONXSV' program [Ref. 9], to get the desired feedback constants, the pole placement only program was first run to get the desired pole and the computed

TABLE 2
Pole Only Desired Pole and Computed Pole

Desired pole		Computed pole	
-1.2	1.6j	-1.19889	1.59415j
-1.2	-1.6j	-1.19889	-1.59415j
-1.0		-0.98902	
-0.5		-0.49770	

pole (see Table 2). The feedback matrix F is

$$F = \begin{bmatrix} -0.10853 & 0.50675 & 13.97235 & 7.73604 \\ 0.19809 & -0.10997 & -90.41902 & 12.42874 \end{bmatrix}$$

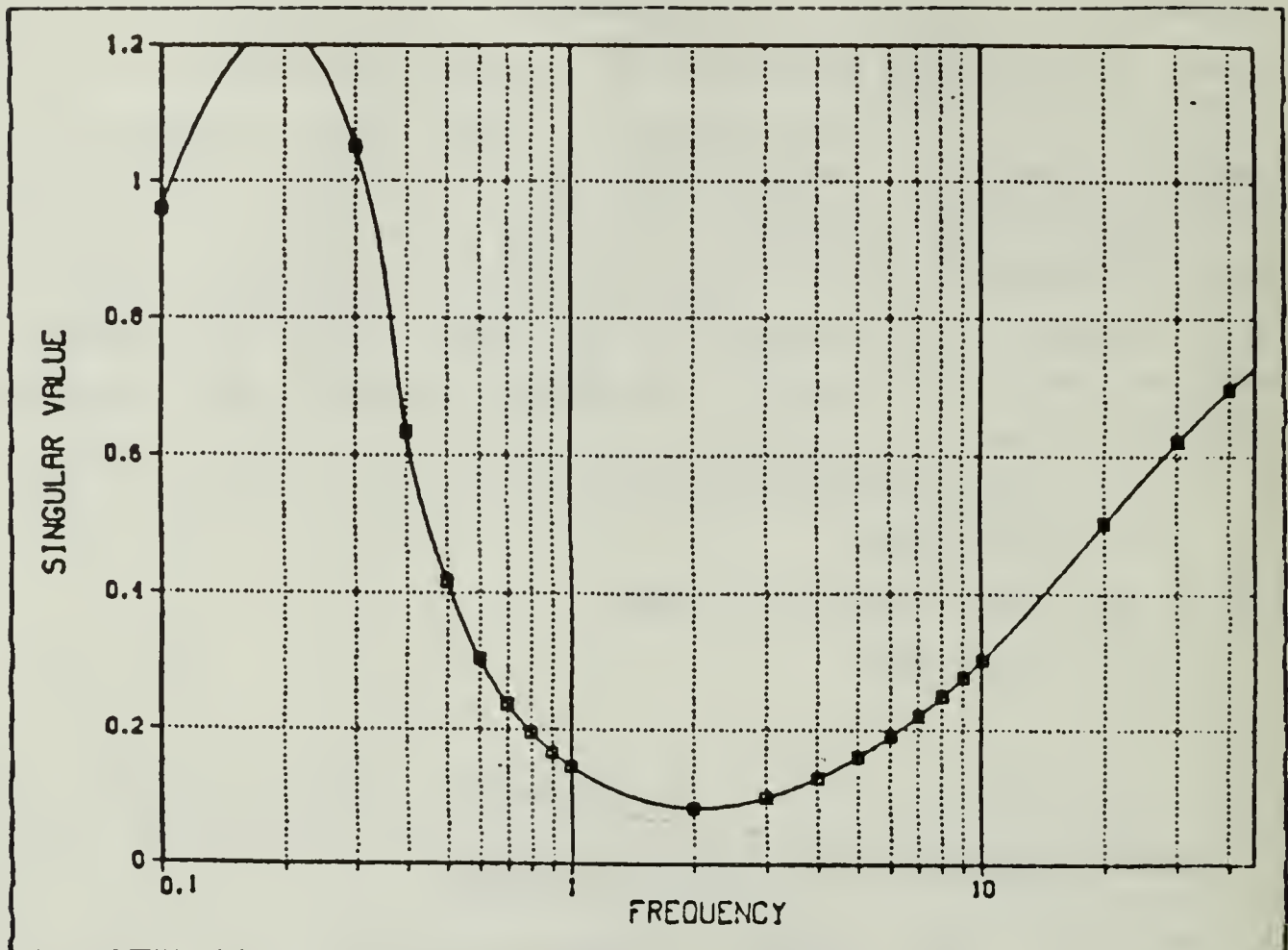


Figure 6.2 Pole Placement Only Singular Value Plots.

the objective function is 0.0002 and the additive minimum singular value vs frequency is seen in Figure 6.2. This plot shows that pole placement only design has very low minimum singular values for the return difference matrix. Pole placement only goes as low as -22 db or 0.0827 rad near 2 rad/sec in frequency. Using the universal gain and phase diagram as discussed in Chapter 5 this equates to a gain margin of about 0.95 db to 1.15 db and a phase margin of 4.7 degrees. These phase and gain margins are quite small, showing the need to run a pole placement and robustness design program. It is assumed that the eigenvalues (pole locations) of the system, as developed in [Ref. 7], are the

required poles for the performance criteria. Once the pole locations are set, robustness criteria must be selected. From the universal gain and phase margin curve discussed earlier, singular value levels were selected for this problem. The singular value level chosen was 0.6 rad. This corresponds to a gain margin of -4.0 db to 8 db and a phase margin of about 35 degrees.

For a singular value level of 0.6 rad the pole placement and robustness design routine places the poles as shown in Table 3. The slight differences in these pole locations

TABLE 3

Pole Placement and Robustness Design Pole Locations

Desired pole	Computed pole
-1.2 1.6j	-1.19297 1.59533j
-1.2 -1.6j	-1.19297 -1.59533j
-1.0	-0.99886
-0.5	-0.45480

have an insignificant effect on the performance.

The feedback constant F is

$$F = \begin{bmatrix} -0.07493 & -0.08746 & 8.0529 & 16.30763 \\ 0.27085 & -0.23019 & -2.2919 & 37.66504 \end{bmatrix}$$

The objective function is 0.0000 and the additive minimum singular value vs frequency is seen in Figure 6.3. This plot shows that in the robustness design the gain adjustment moves the minimum singular value from about 0.08 rad, with very poor phase and gain margins, to a level of 0.645 rad, above the desired values of gain and phase. After obtaining the feedback gains the NPGS 'OPTSYS' program was used to obtain the necessary data, time response plot, Bode plot, and pole-zero map. The pole placement only design closed loop time response plot is shown in Figure

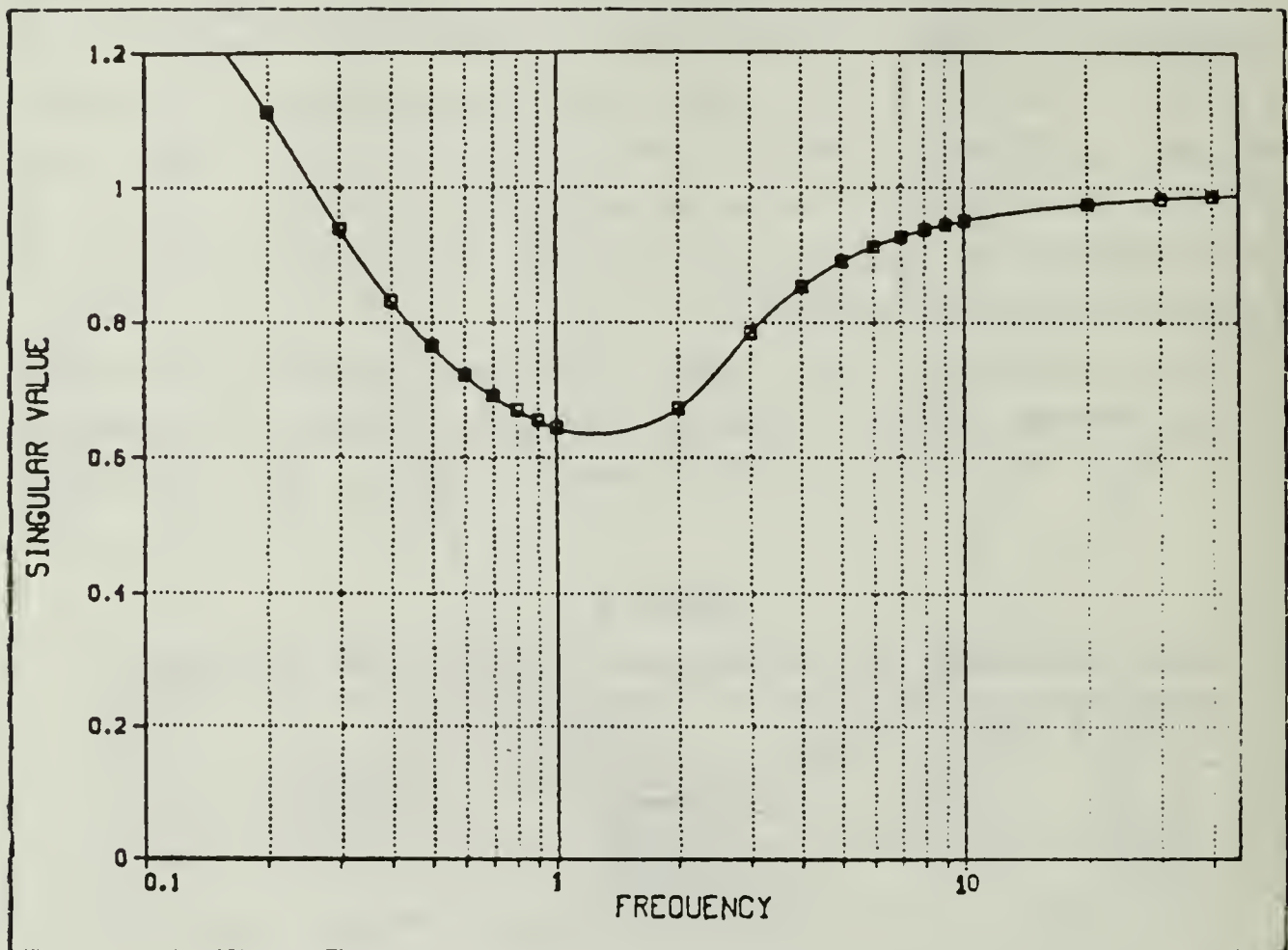
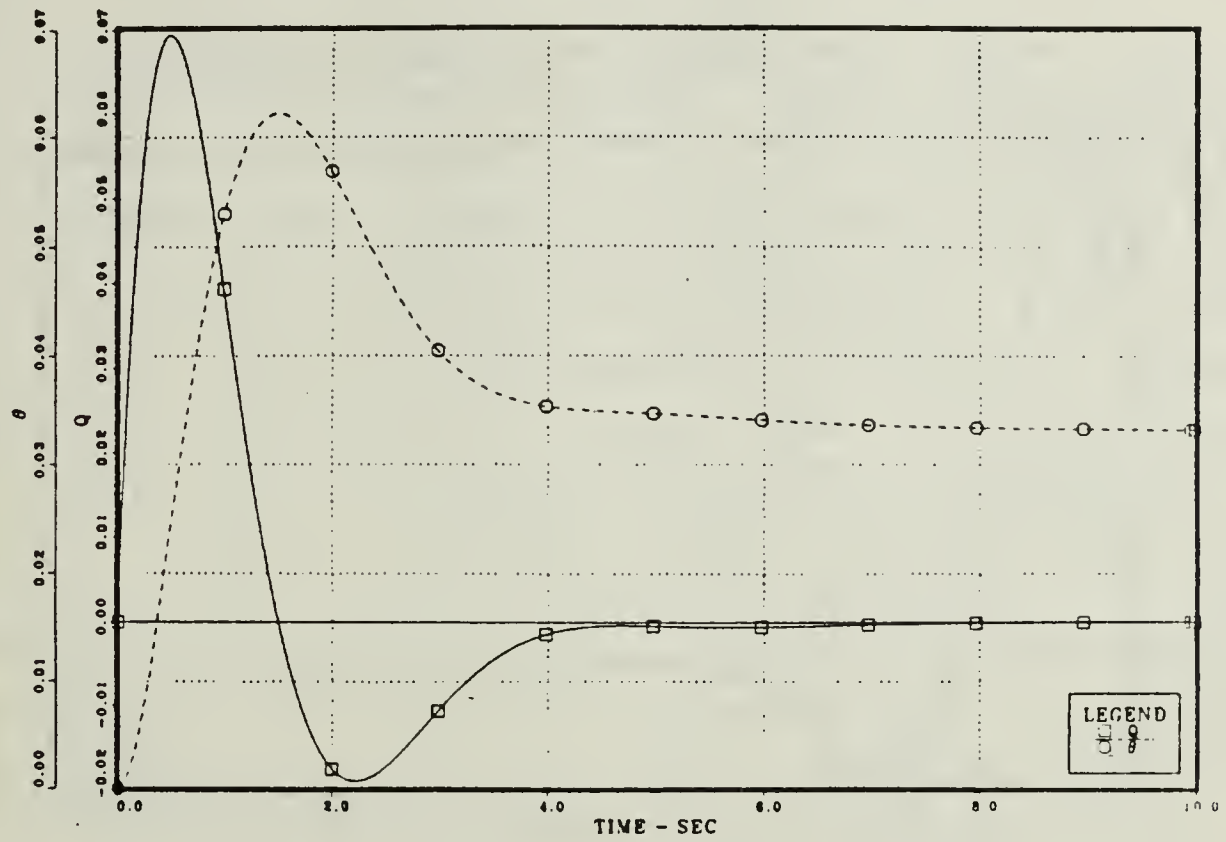


Figure 6.3 Robustness Design Singular Value Plots.

6.4. It shows good pitch rate and pitch attitude responses to δ_e step input, but slow responses to the forward velocity perturbation and vertical velocity perturbation to δ_t step input. The input transfer function $F*G$ robustness design time response plot is shown in Figure 6.5. This indicates a better time response for pitch rate and pitch attitude inputs than pole placement only design, also good vertical velocity perturbation response to δ_e step input, but sluggish response for the forward velocity perturbation [Ref. 8]. Comparing the loop Bode plots of the pole placement and robustness design transfer function, $F*G$, shows an increase in robustness.

ϕ_e Step Input Transient Response



ϕ_t Step Input Transient Response

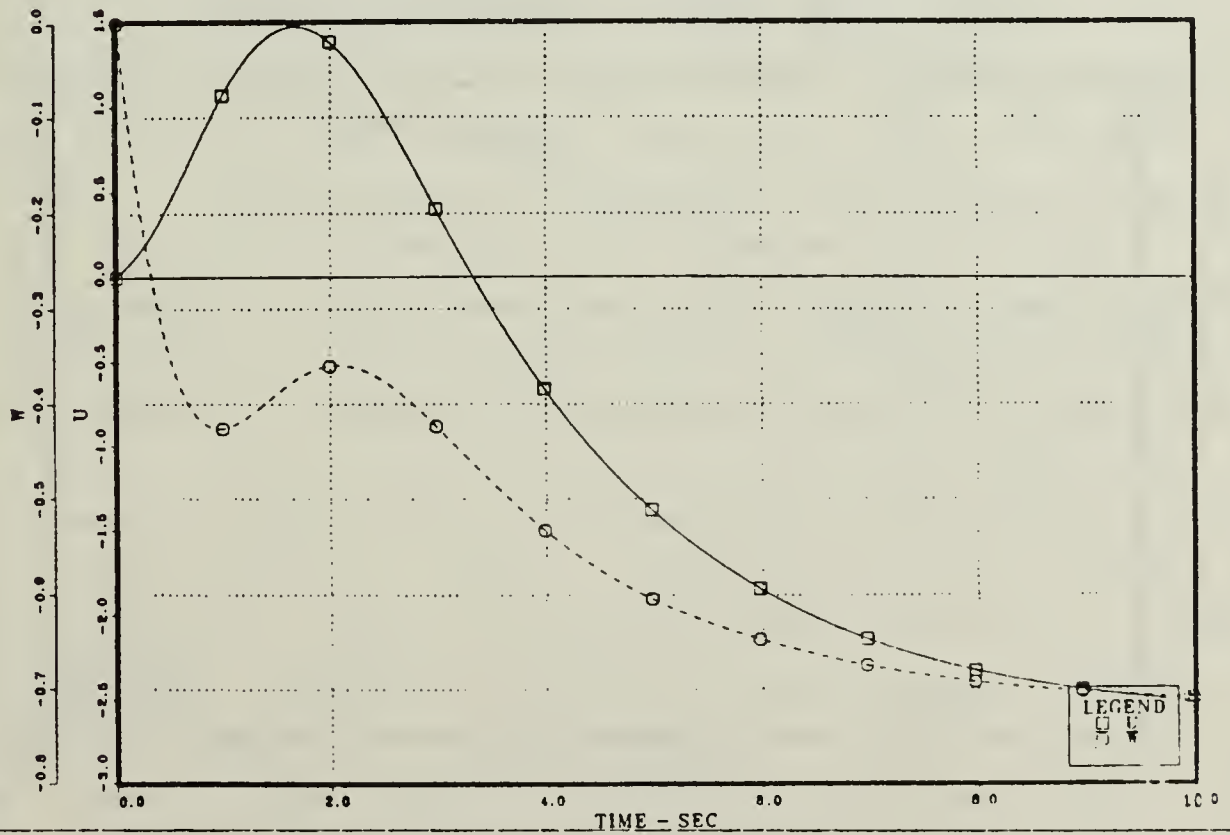
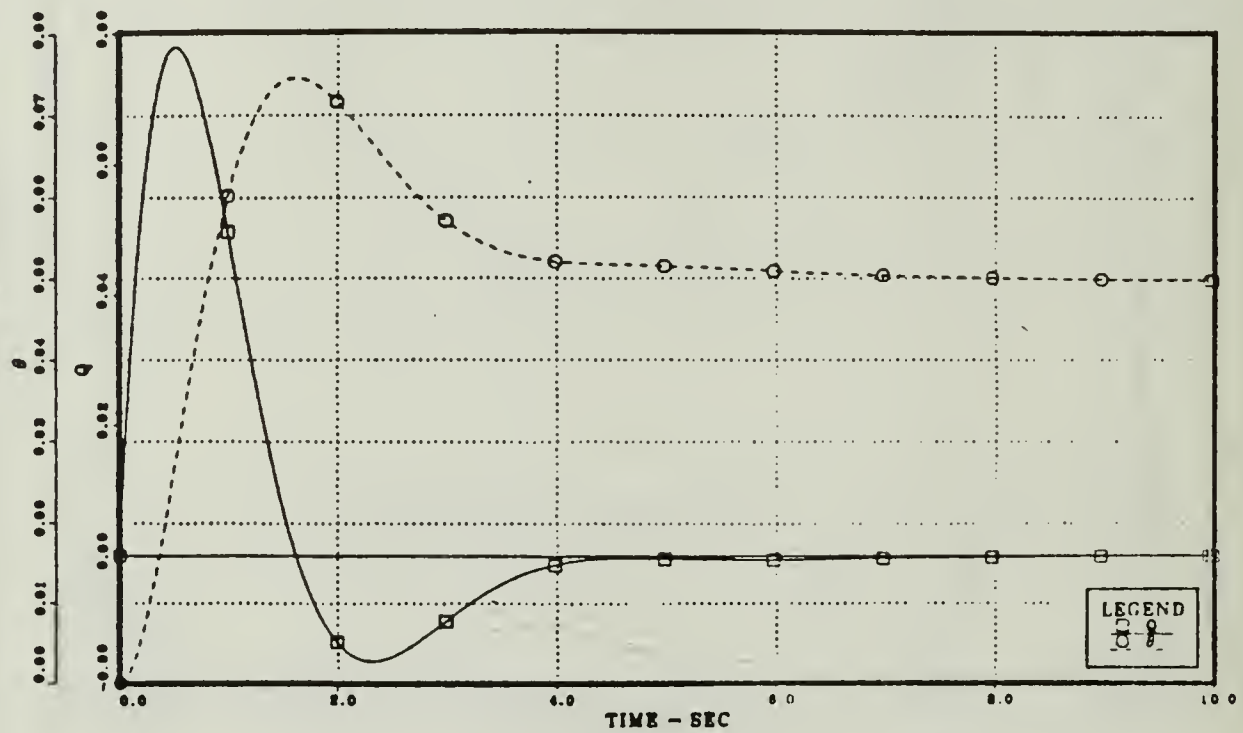


Figure 6.4 Pole Placement Only Design Time Response.

ϕ_e Step Input Transient Response



ϕ_t Step Input Transient Response

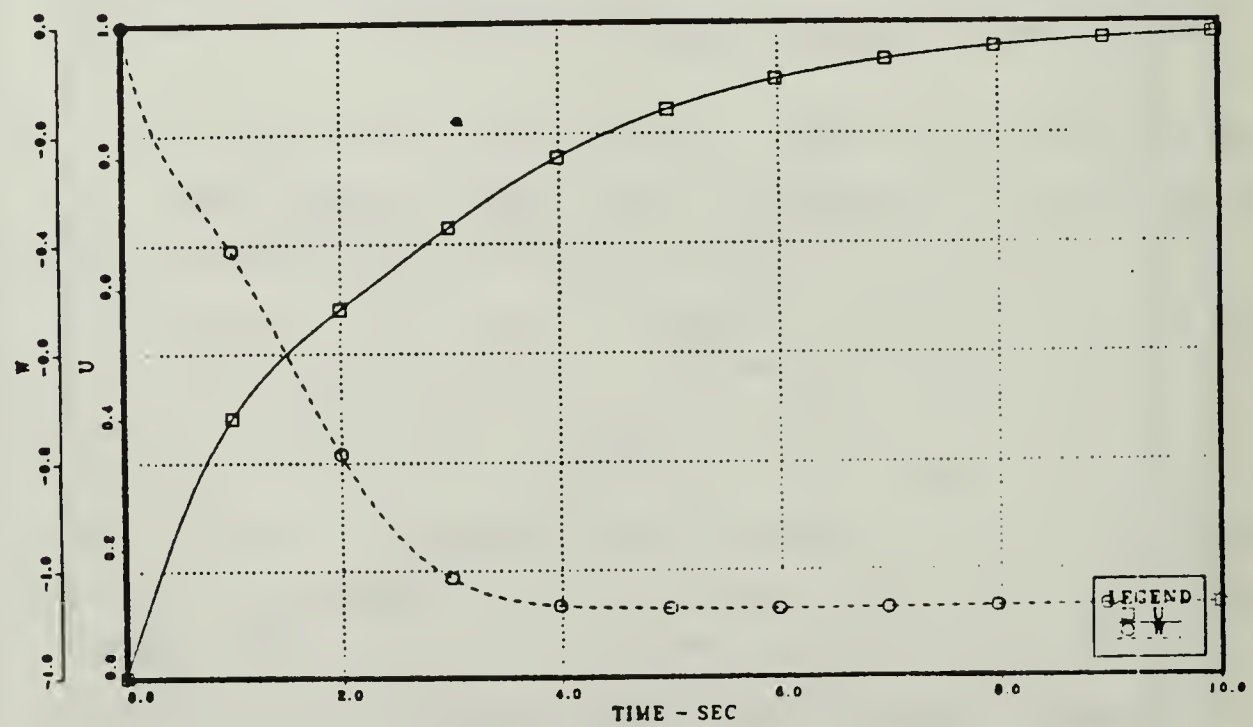


Figure 6.5 P*G Robustness Design Time Response.

Considering a SISO Bode analysis, the channel input 1 output 1 bode plot are shown in Figure 6.6 and 6.7. The bandwidth(BW) shows a small decrease, 3 rad/sec, and an increase, in the phase margin(PM), of 22 degrees. The DC gain drops from 34.3 db to 25.7 db, a 9 db decrease and the slope changes very abruptly in the pole only design (see Figure 6.4). The robustness design seen in figure 6.5 drops the curve down 20 db due to the two zeros at 0.3 rad/sec, which move toward the two poles at 1.27 rad/sec, and the other zero moves closer to another pole 0.16 rad/sec during the optimization. This channel only shows a smoothing of the curve. Consider the channel input 1 output 2 bode plots shown in Figures 6.8 and 6.9. This channel shows a large shift in the bandwidth(BW) from 30 rad/sec to 2.83 rad/sec. The DC gains are similar and increase the gain margin 24 db, but decrease phase margin 90 degrees. Figure 6.8 shows that the frequency response curve slope changes detrimentally, but, the robustness design, as shown in figure 6.9 shows a decrease in the slope down 20 db curve by zeros move the one pole 0.17 rad/sec for pole-zero cancel and the other one zero moves on the minimum singular value frequency 1 rad/sec. The reduction of bandwidth and increase in gain margin yields an increased tolerance to perturbation. The channel input 2 output 1 bode plots are shown in Figures 6.10 and 6.11. The DC gain decreases 10 db and bandwidth shifts left 0.1 rad/sec, increasing the phase margin 43.7 degrees. The zero shift has the effect of smoothing the frequency response curve in the vicinity of the frequency of the minimum singular value. The channel input 2 output 2 bode plots are shown in Figures 6.12 and 6.13. These figures show the same response as the channel 1;2 but a bandwidth shift right of 0.47 rad/sec and the same DC gains for a smooth curve, caused by the zero location shift in the same manner as the other channels(channels 1;1,2;1,2;2).

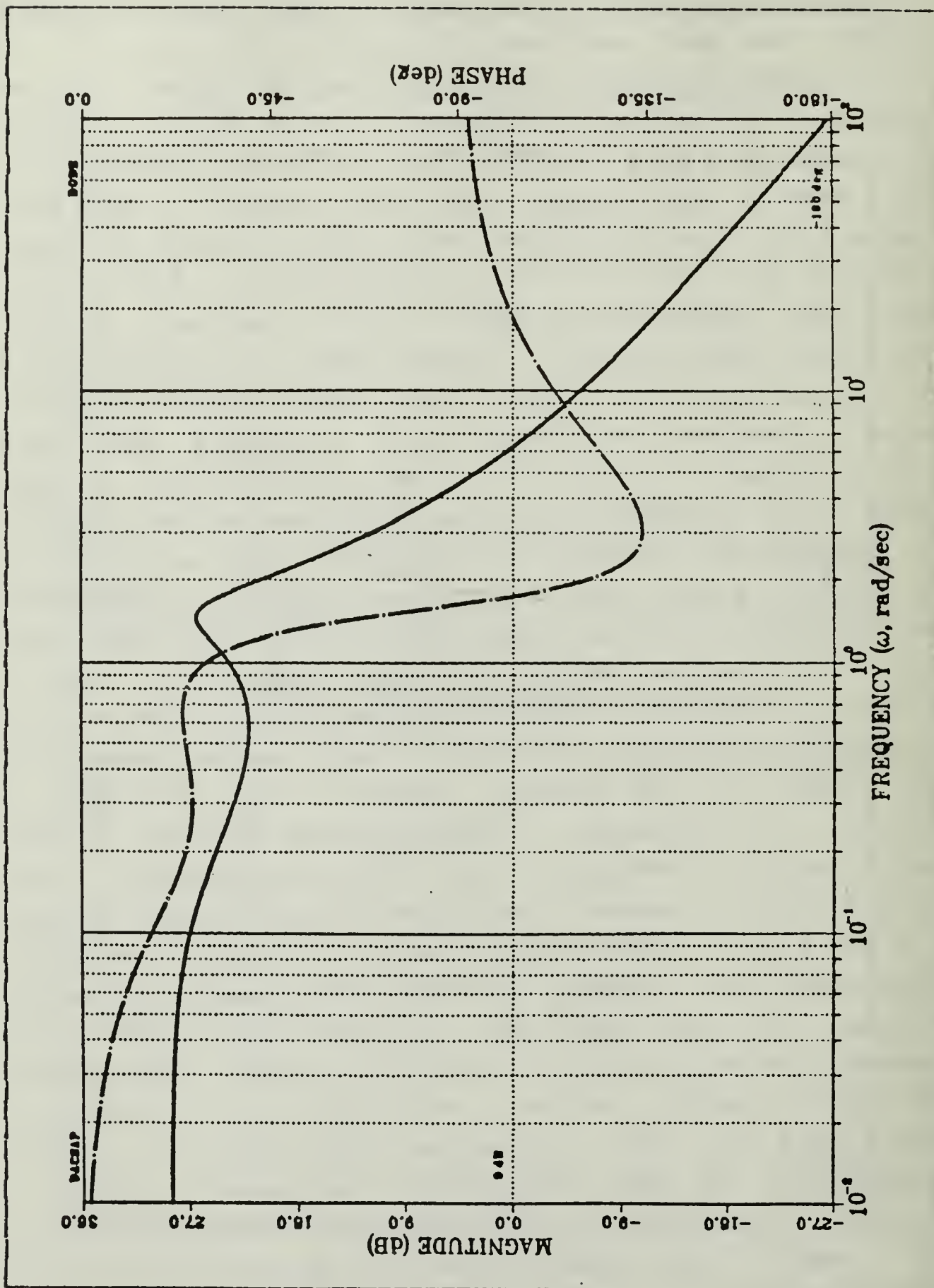


Figure 6.6 Pole Placement Only Design $F*G$ 1:1.

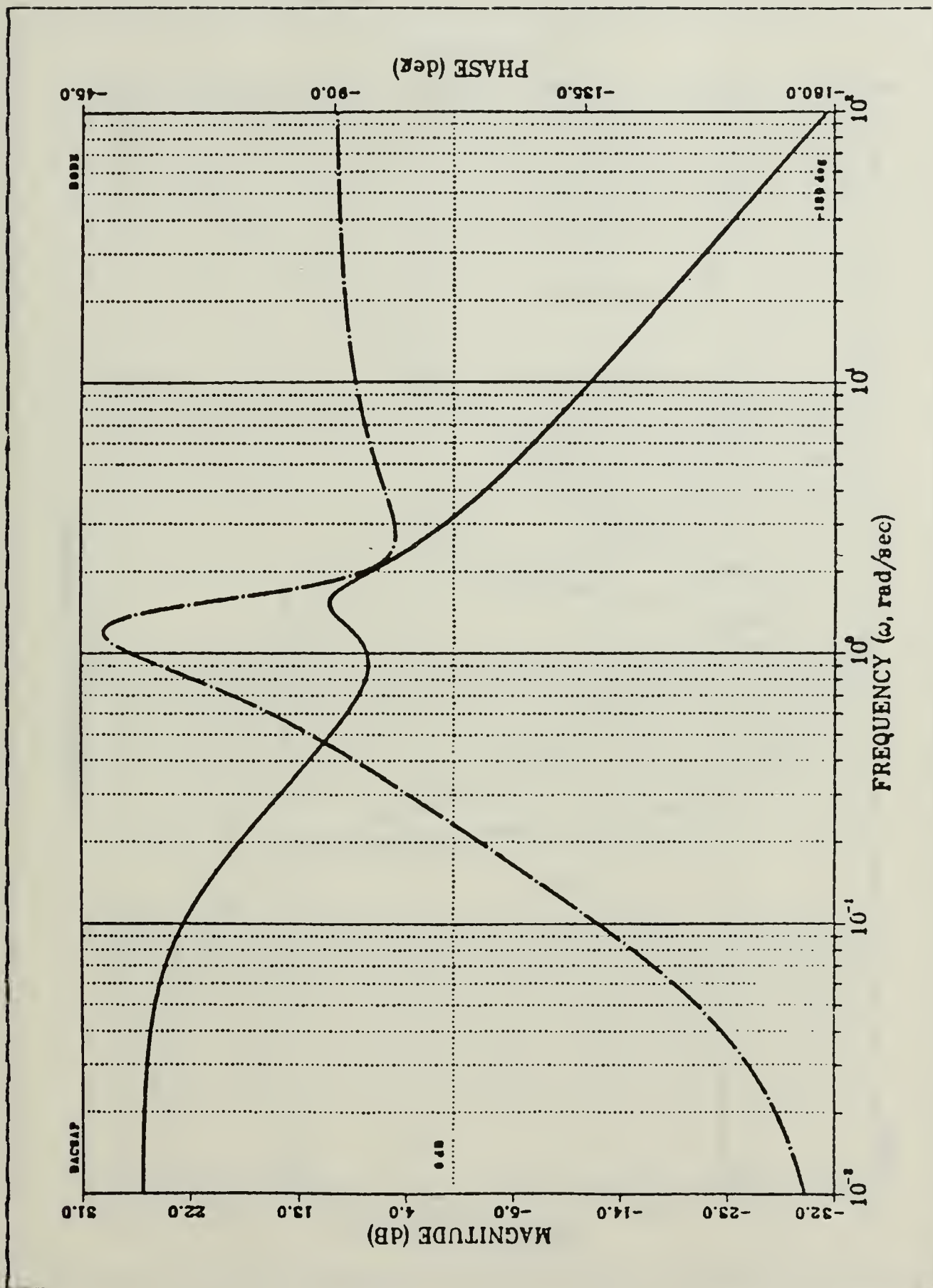


Figure 6.7 Robustness Design F*G 1:1.

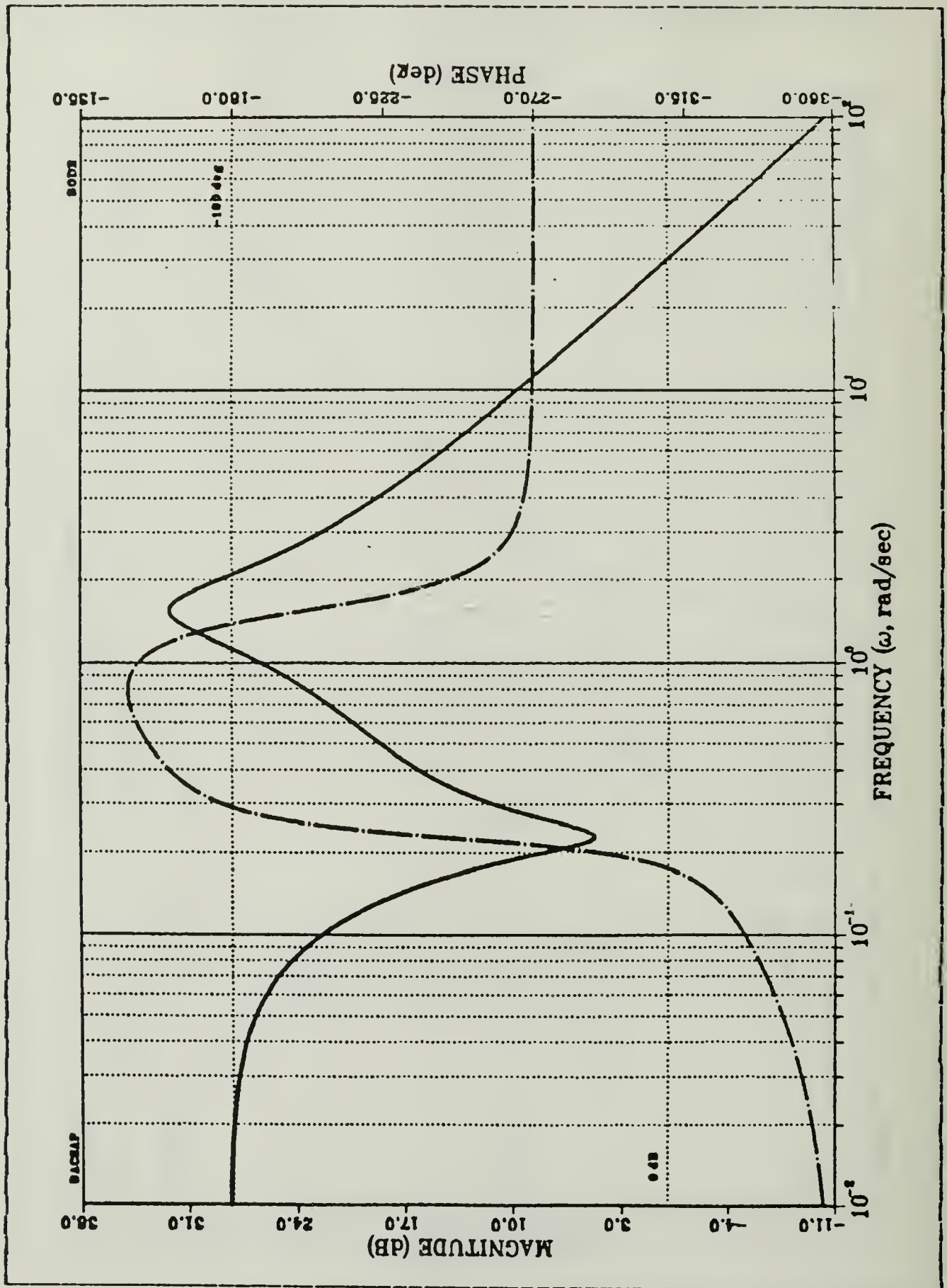


Figure 6.8 Pole Placement Only Design $F*G$ 1:2.

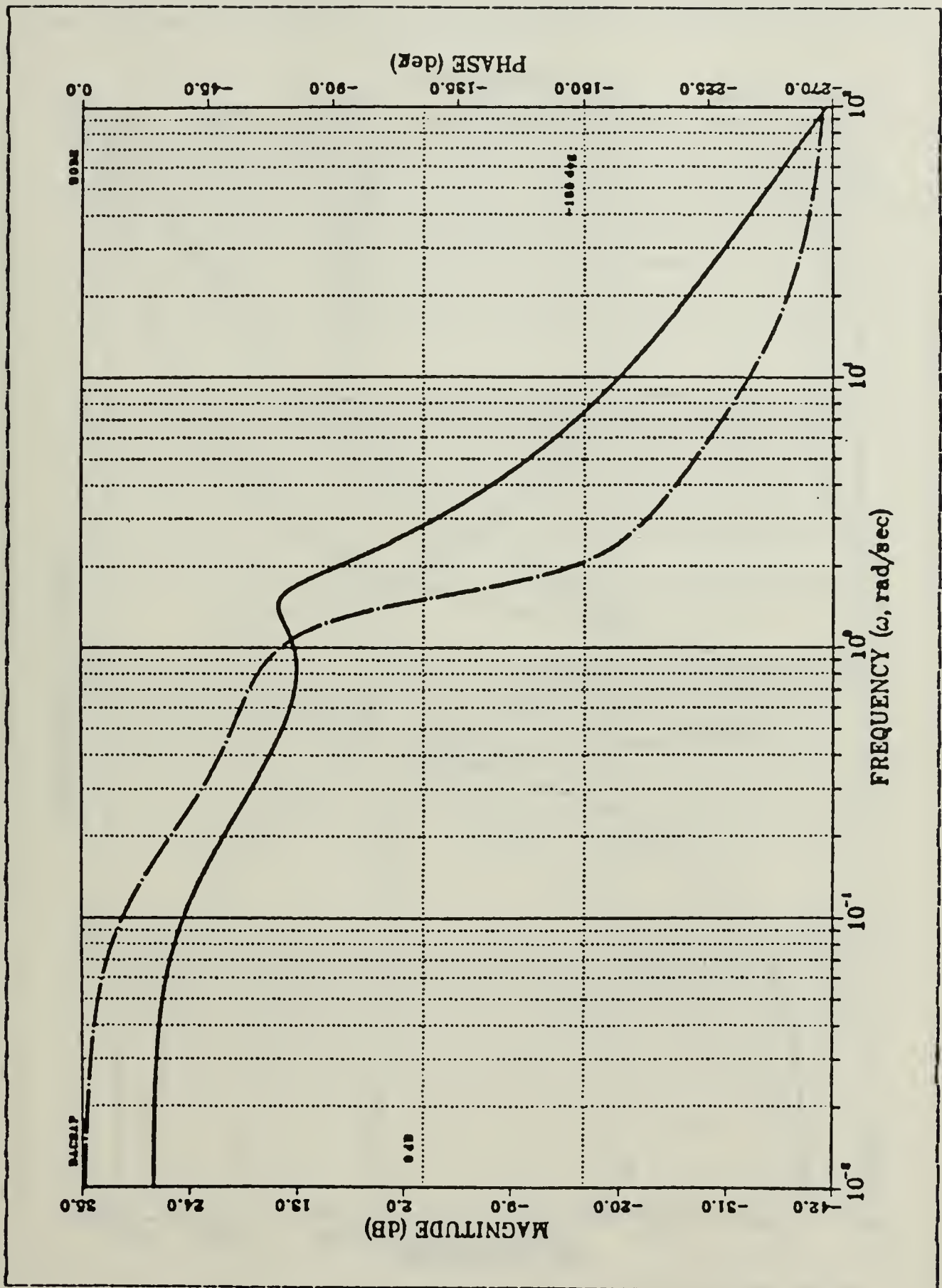


Figure 6.9 Robustness Design F*G 1:2.

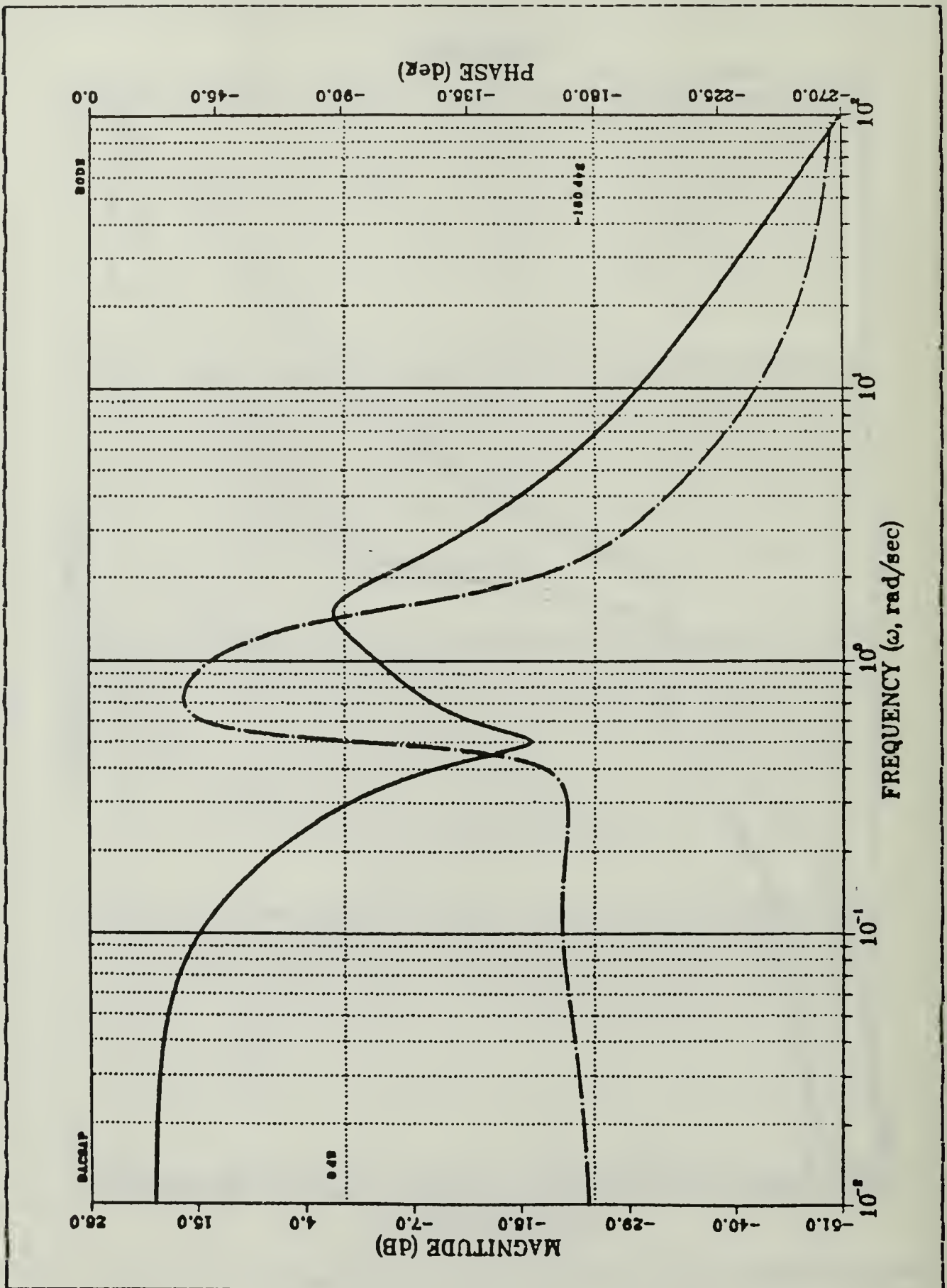


Figure 6.10 Pole Placement Only Design $F*G$ 2:1.

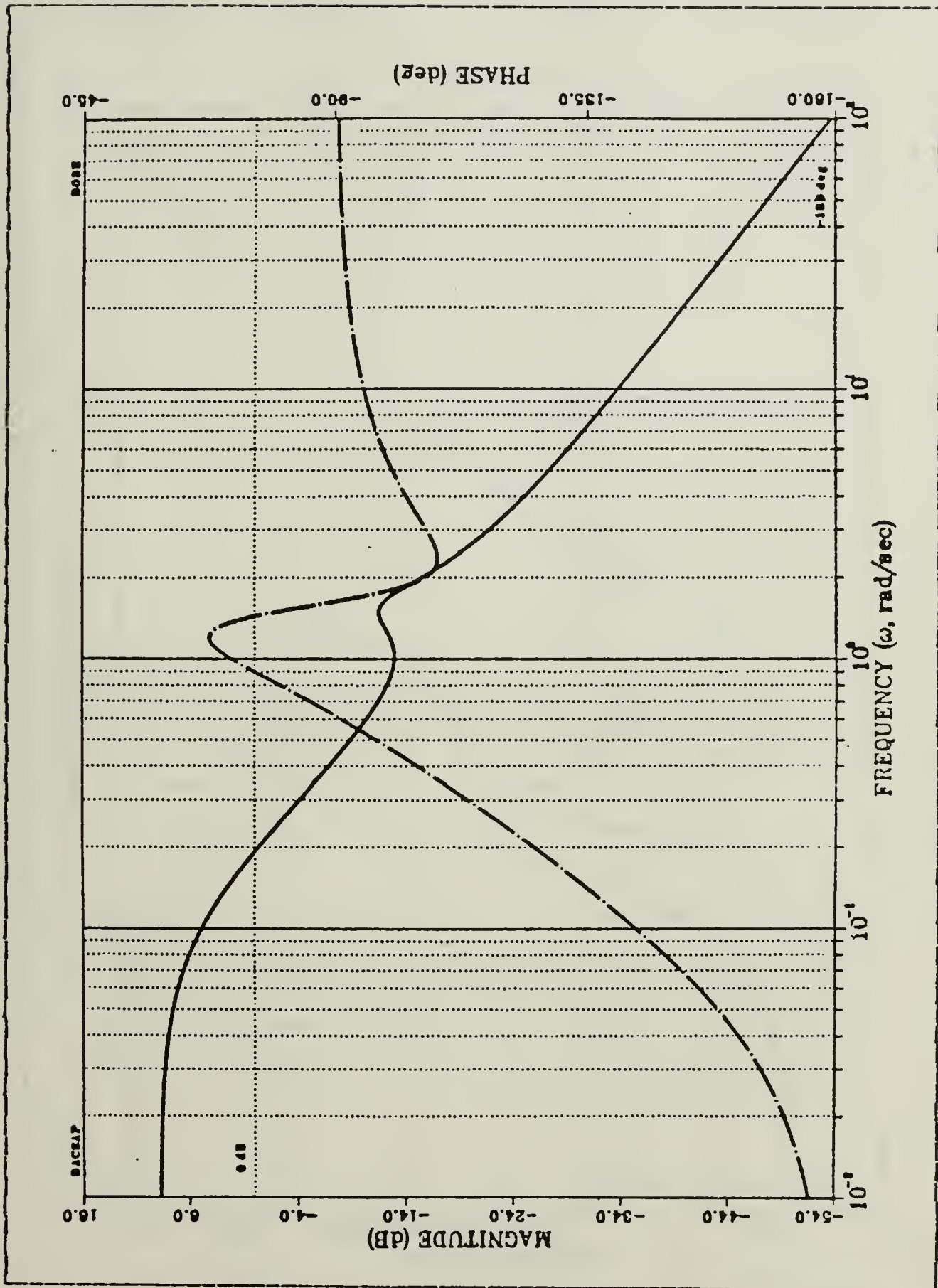


Figure 6.11 Robustness Design F*G 2:1.

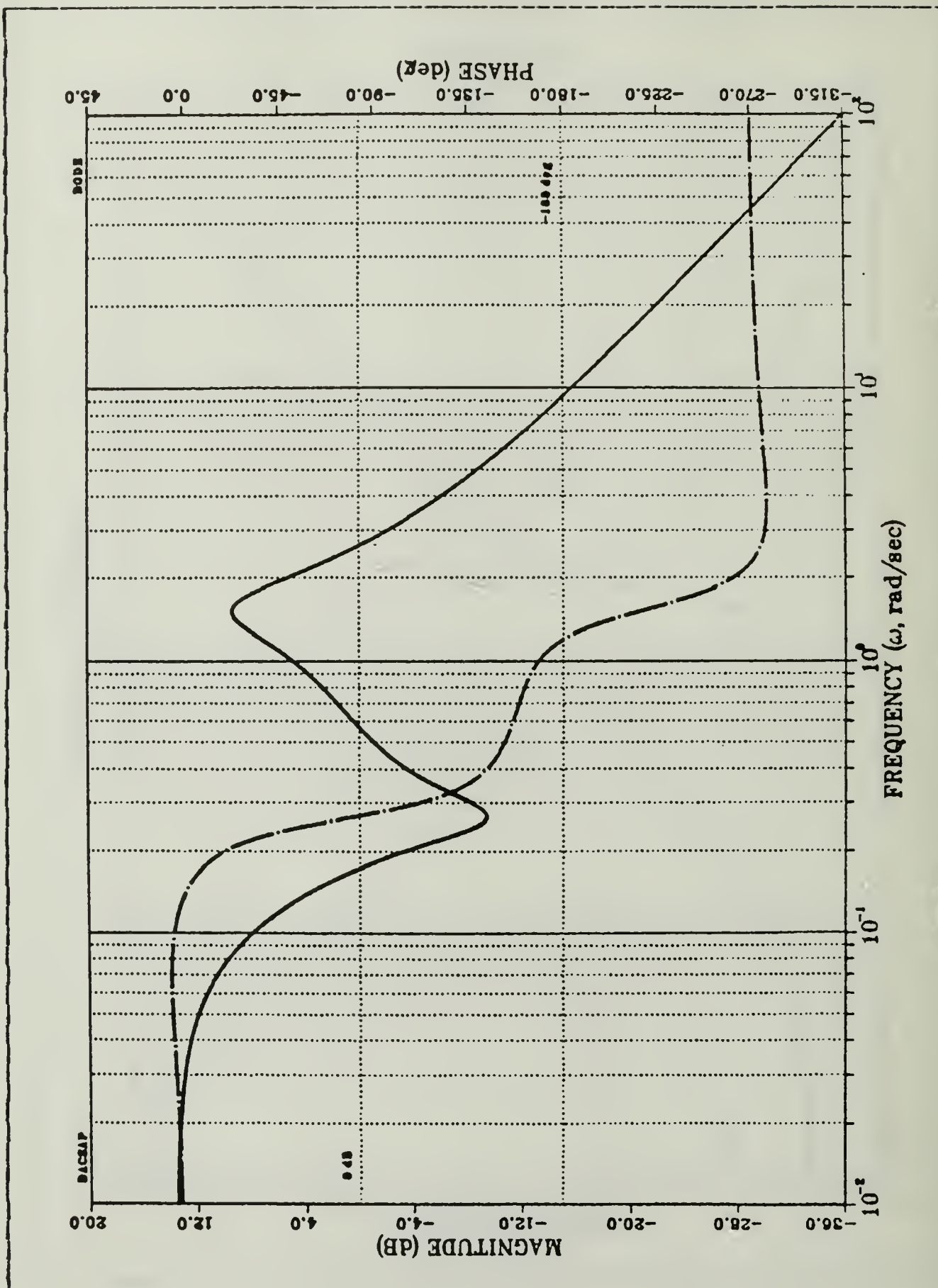


Figure 6.12 Pole Placement Only Design F*G 2:2.

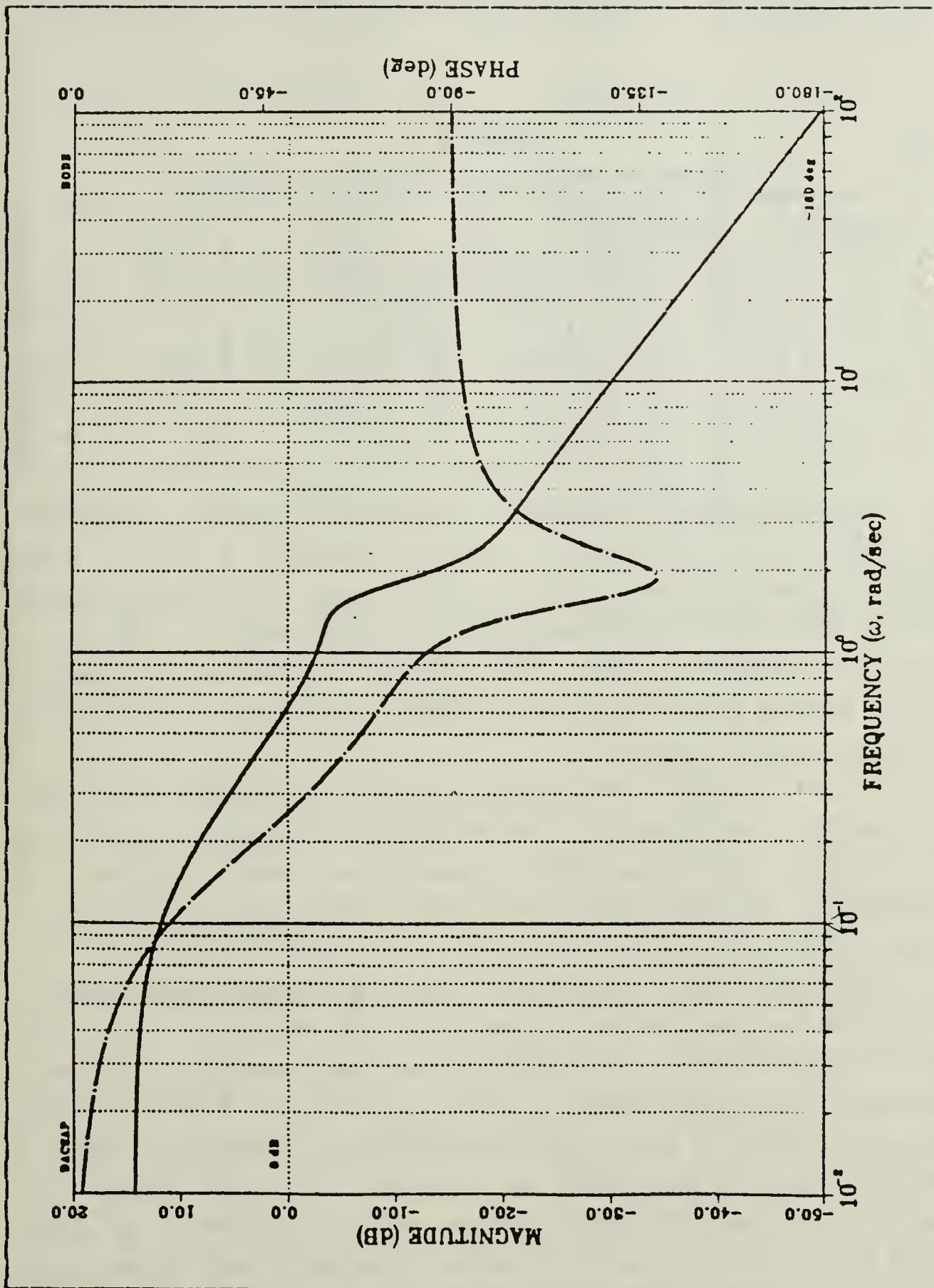


Figure 6.13 Robustness Design F*G 2:2.

The F*G transfer functions bode plot numerical results are shown in Table 4.

TABLE 4
F*G Transfer Functions Bode Plot Results

Channel	Bandwidth		PM		GM		Gain	
	pole	rad/sec SV	pole	degree SV	pole	SV	pole	SV
1 : 1	6.1	3.2	58	80	.	.	34	25.7
1 : 2	30	2.83	89.7	-20	-32	-7.2	28	27.6
2 : 1	0.3	0.19	9.5	53	8.8	.	19.4	8.6
2 : 2	0.17	0.64	170	106	-7.3	.	13.5	14.1

The most noticed change in the overall system, however, is in the transfer function input 1 output 2. This is the change at the minimum singular value position, which greatly reduces the gain and bandwidth in this channel through a change in feedback gain. The optimizer routine brings the entire system gains to more balanced conditions and recovers a highly robust design.

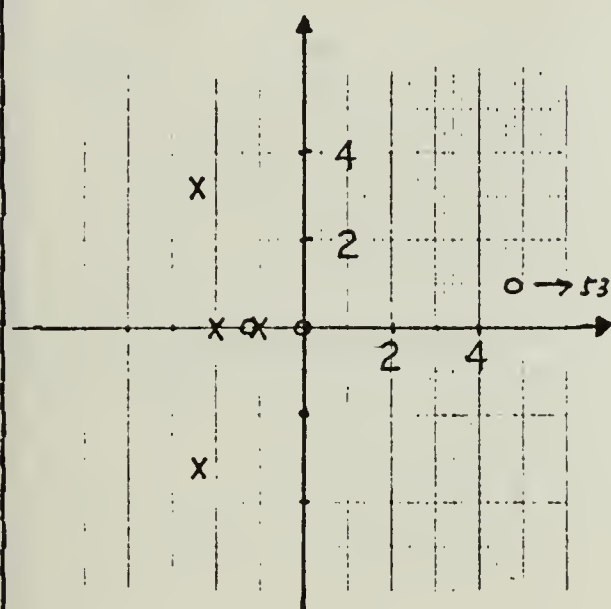
The gain changes associated with the robustness improvement cause the zeros of the various closed-loop pole-zero diagram of the closed-loop transfer matrices to move. A comparison of the eight pole-zero diagrams is shown in Figures 6.14 to 6.17.

The significant feature of these pole-zero diagrams is the shift in the zeros of the optimized design in a direction that attempts to equalize or balance the frequency response for frequencies in the vicinity of the minimum singular values. The pole-zero diagram of channel input 1 output 2 will be discussed as an example of this effect. In figure 6.12 the pole only design zeros are located at about -0.31 and -0.78. When the pole placement and robustness routine has completed the feedback gain modification these

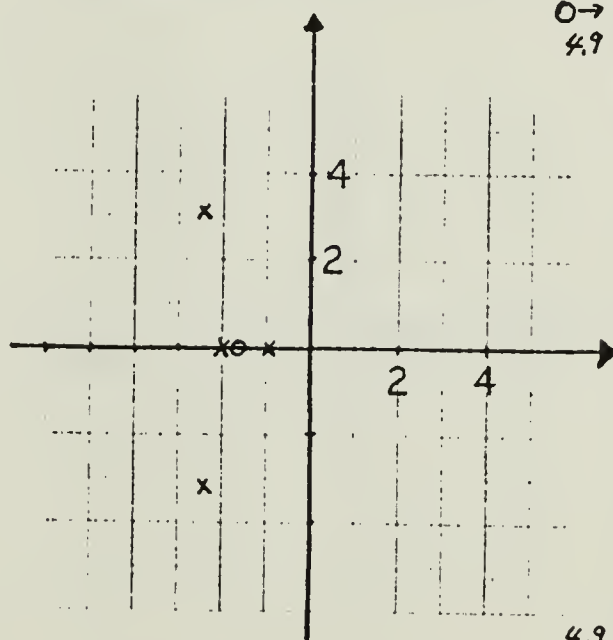
POLE ONLY DESIGN

ROBUSTNESS DESIGN

0 → 4.9

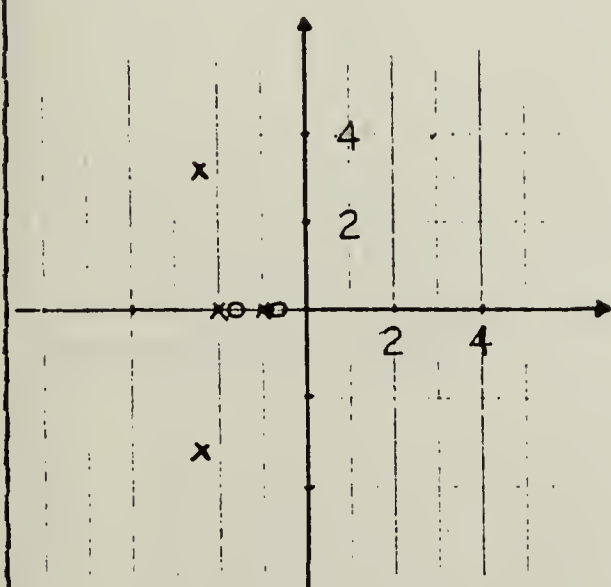


$\mathcal{G}_e - U(1 : 1)$

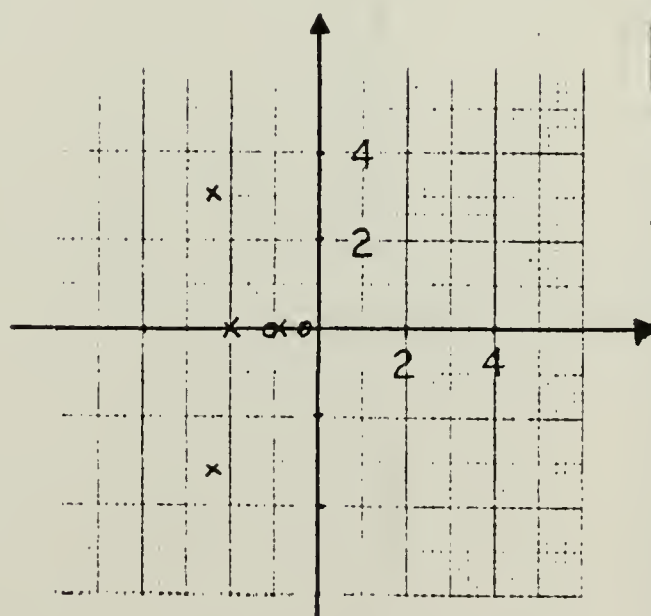


$\mathcal{G}_e - U(1 : 1)$

4.9 0 →



$\mathcal{G}_e - W(1 : 2)$

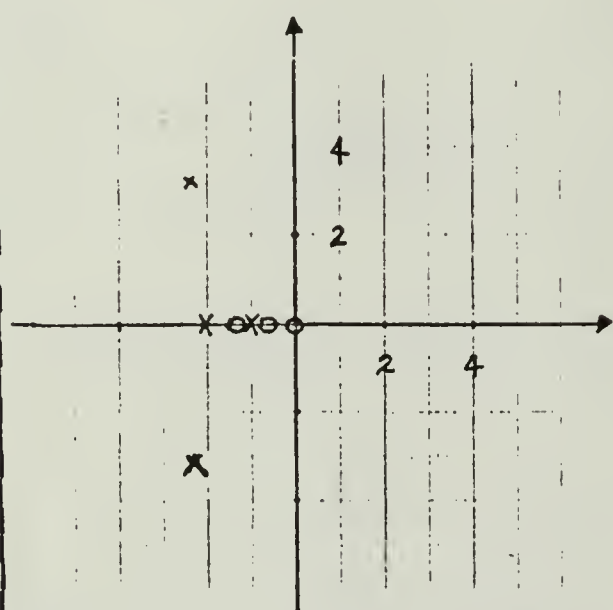


$\mathcal{G}_e - W(1 : 2)$

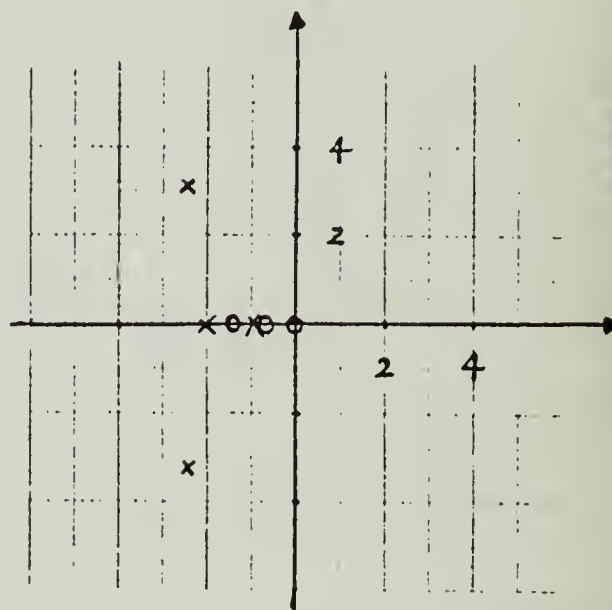
Figure 6.14 Pole-Zero Map for 1:1 and 1:2.

POLE ONLY DESIGN

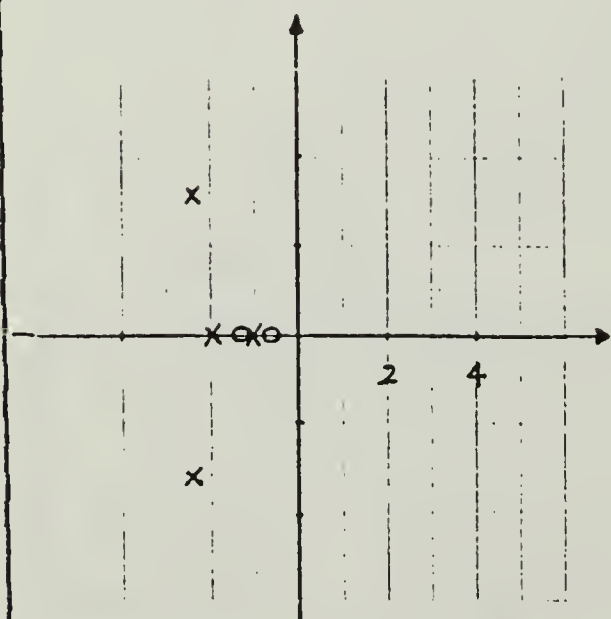
ROBUSTNESS DESIGN



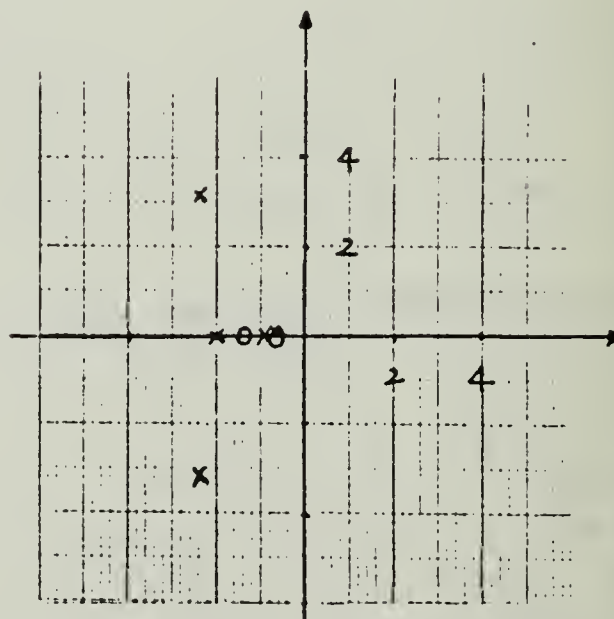
$$\hat{d}_e - Q(1 : 3)$$



$$\hat{d}_e - Q(1 : 3)$$



$$\hat{d}_e - \theta(1 : 4)$$



$$\hat{d}_e - \theta(1 : 4)$$

Figure 6.15 Pole-Zero Map for 1:3 and 1:4.

POLE ONLY DESIGN

ROBUSTNESS DESIGN

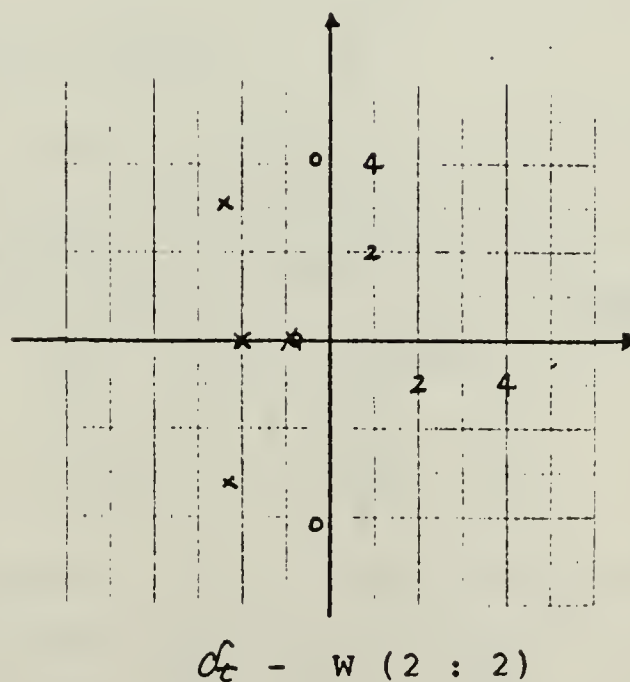
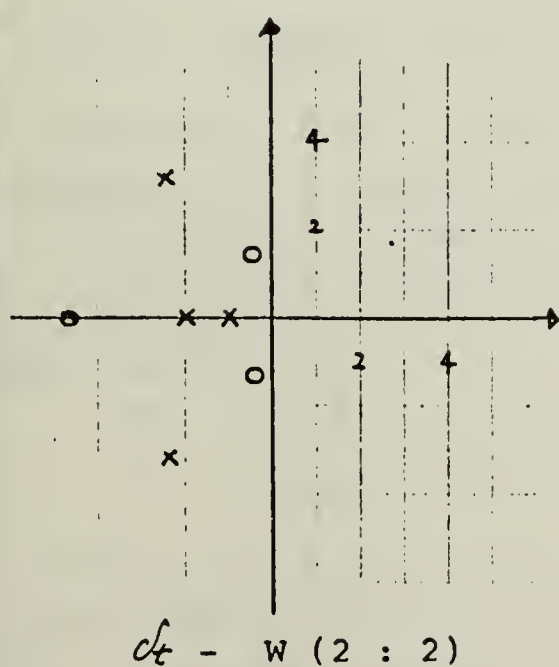
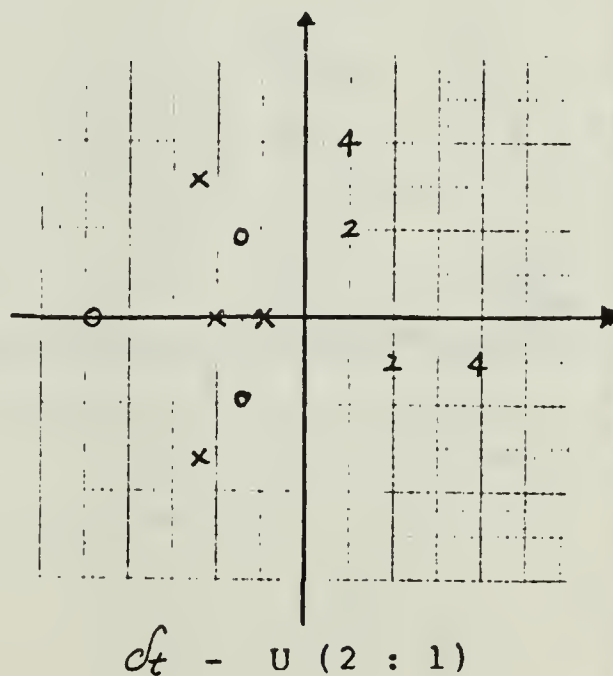
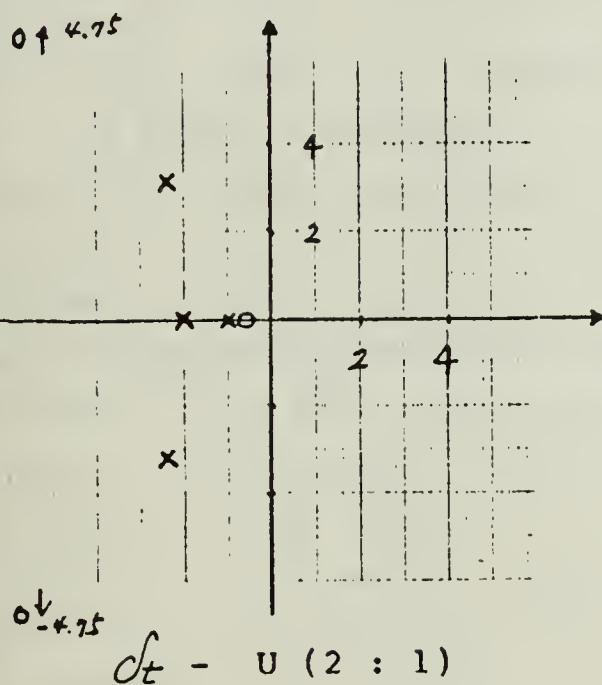
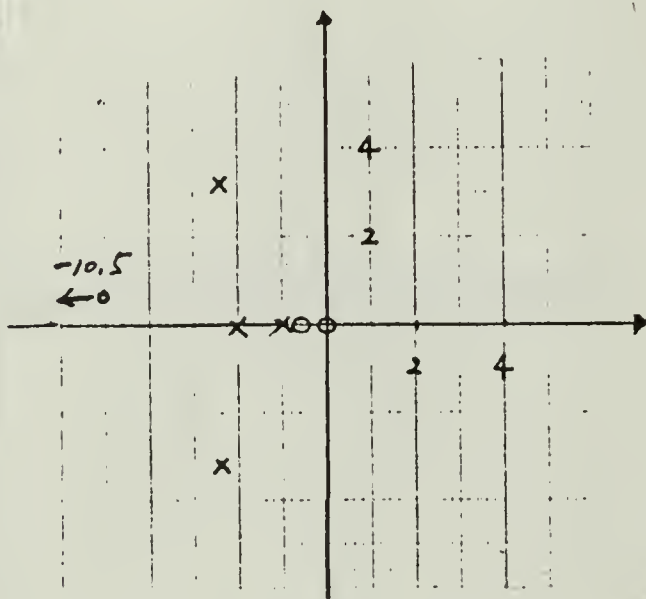


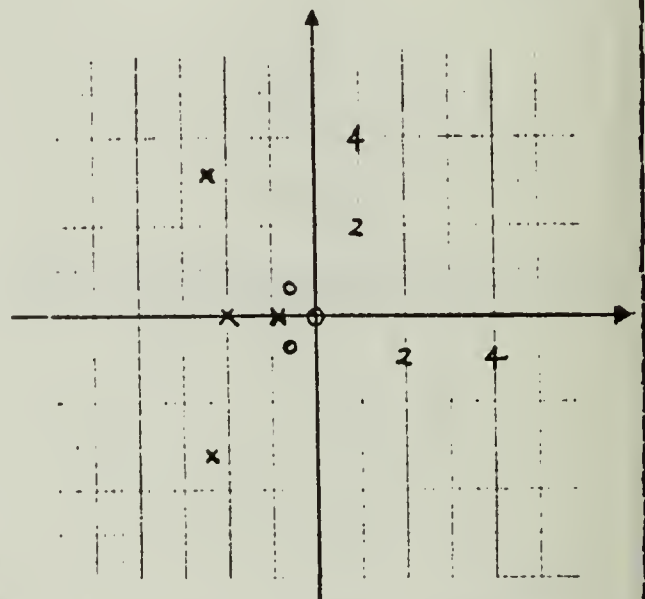
Figure 6.16 Pole-Zero Map for 2:1 and 2:2.

POLE ONLY DESIGN

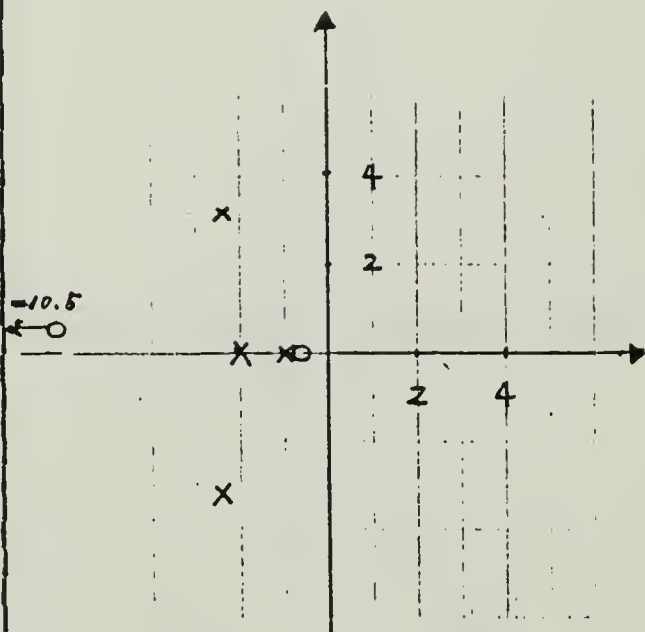
ROBUSTNESS DESIGN



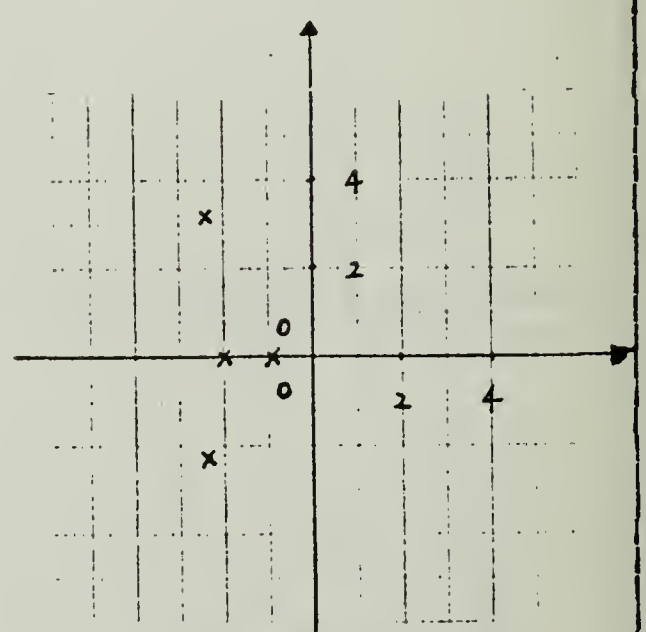
$$\hat{d}_t - Q(2 : 3)$$



$$\hat{d}_t - Q(2 : 3)$$



$$\hat{d}_t - \theta(2 : 4)$$



$$\hat{d}_t - \theta(2 : 4)$$

Figure 6.17 Pole-Zero Map for 2:3 and 2:4.

zeros have shifted to -0.17 and -0.56. The effect of these zero shifts is to combine with the pole locations to equalize the frequency response and increase DC gain of 14 db for the same bandwidth, at the minimum singular value frequency 1 rad/sec as depicted in Figures 6.18 and 6.19. Zero shifts for the remainder of the transfer functions provide similar results in the other channels. By moving toward the frequencies associated with the minimum singular values the zeros have balanced the overall frequency response of the system in each channel. While the channel gain modification is the primary mechanism for robustness recovery, the zero shift associated with the feedback gain changes is directly related to the overall frequency response of the system. A robustness design meeting the required pole locations and a robustness singular value level of 0.6 rad provides adequate gain and phase margin for the design.

B. OUTPUT TRANSFER FUNCTION G*F ANALYSIS

Using the NPGS 'CONXSU' program [Ref. 9], to get the desired output transfer function feedback constants, the pole placement only program was first run to get the desired pole and the computed pole (see Table 2). the feedback matrix F is

$$F = \begin{bmatrix} -0.10853 & 0.50675 & 13.97235 & 7.73604 \\ 0.19809 & -0.10997 & -90.41902 & 12.42874 \end{bmatrix}$$

the objective function is 0.0002 and the additive output minimum singular value vs frequency is seen in Figure 6.20. This plot shows that pole placement only G*F design has very low minimum singular values for the return difference

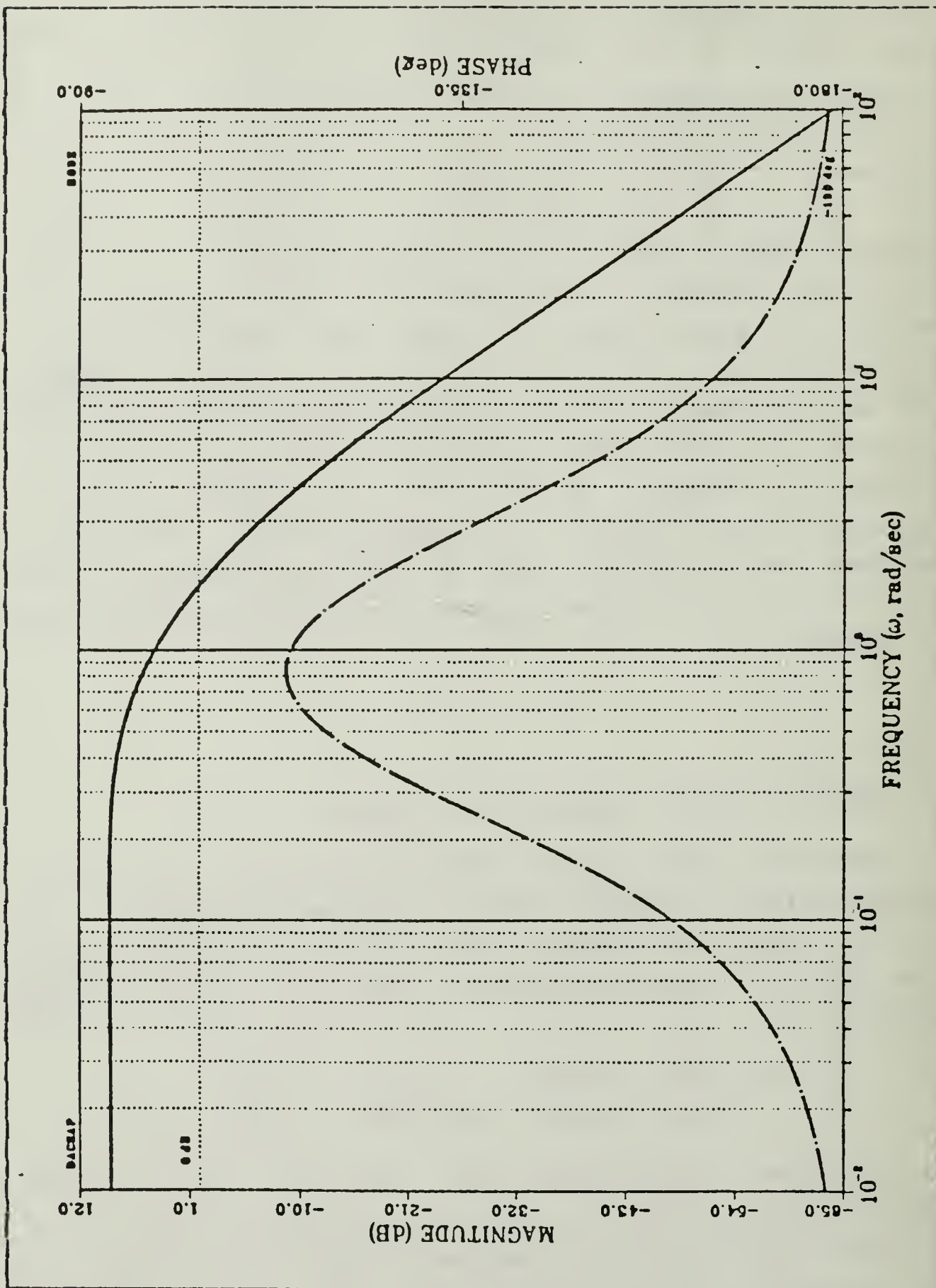


Figure 6.18 Pole Placement Only Design $F*G$ Closedloop 1:2.

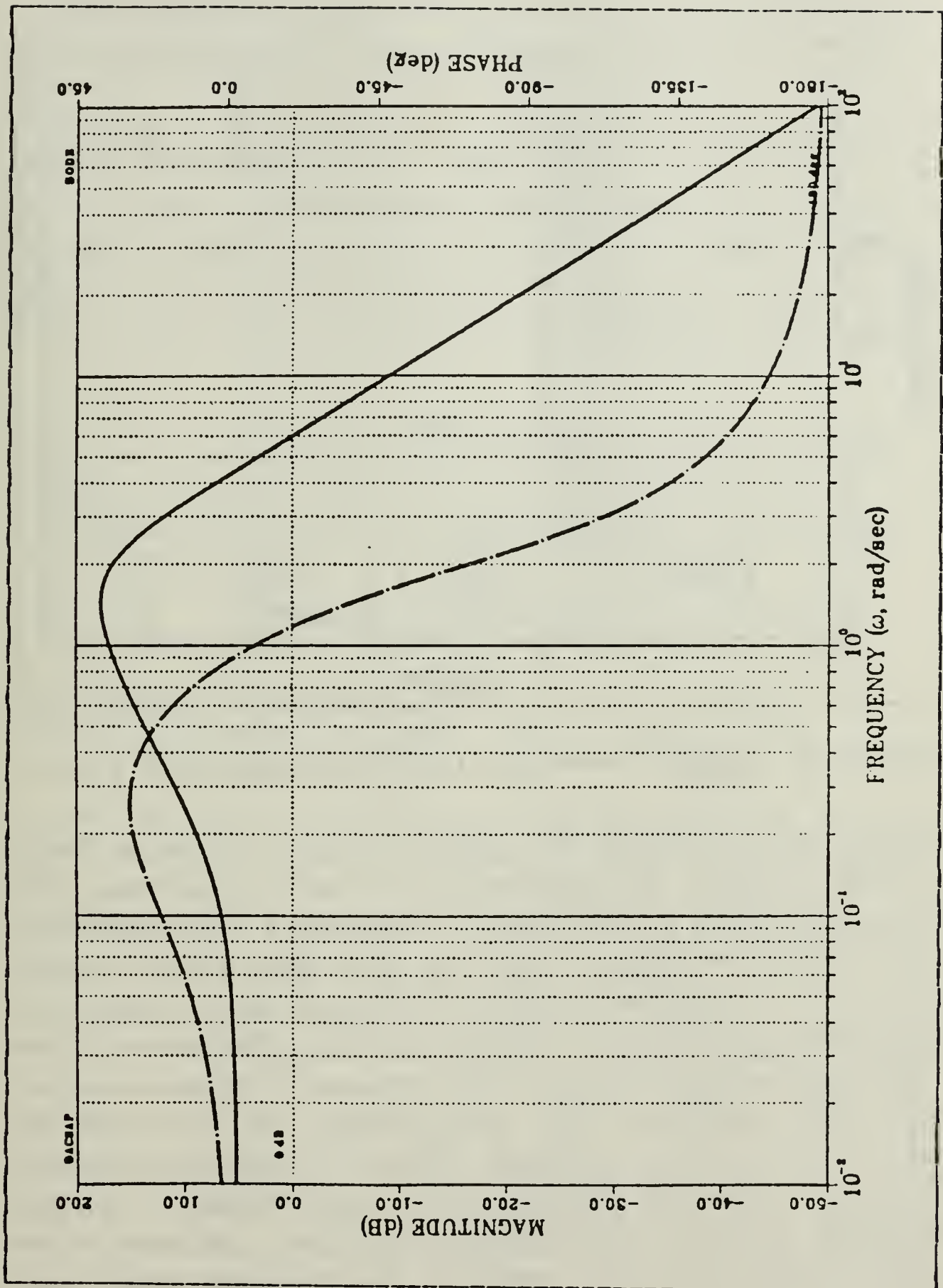


Figure 6.19 Robustness Design F*G Closedloop 1:2.

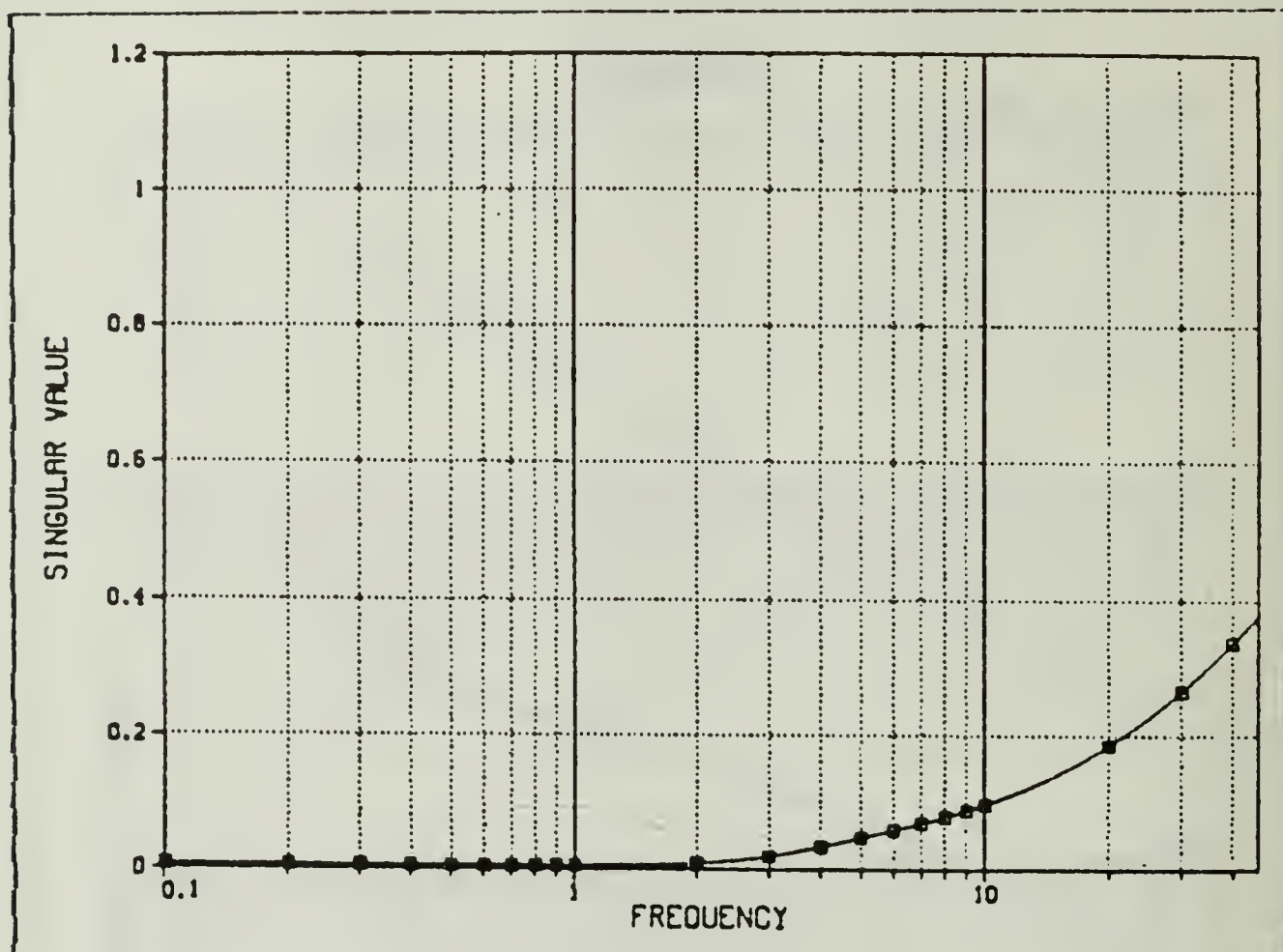


Figure 6.20 Pole placement only G*F Singular Value Plots.

matrix. Pole placement only goes as low as -48 db or 0.004 rad near 1 rad/sec in frequency. Using the universal gain and phase diagram as discussed in Chapter 5 this equates to a gain margin of about -0.003 db to 0.003 db and a phase margin of 0.5 degrees. These phase and gain margins are quite small, showing the need to run a pole placement and robustness design program. It is assumed that the eigenvalues (pole locations) of the system, as developed in [Ref. 7], are the required poles for the performance criteria. Once the pole locations are set (see Table 5), robustness criteria curve discussed earlier, singular value levels are made for this problem. The singular value level chosen is 0.6 rad. This corresponds to a gain margin of -4.0 db to 8 db and a phase margin of about 35 degrees.

For a singular value level of 0.6 rad the pole placement and robustness design routine places the poles as shown in Table 5. There is a trade off between performance and robustness in many control problems. IN output transfer function $G*F$ singular value calculation, the shift in this pole can have a significant effect on the performance, it was found necessary to move the pole at -0.5 to -0.05 in order to achieve the desired robustness. The slight differences in these pole locations an insignificant effect on the

TABLE 5

$G*F$ Pole Placement and Robustness Design Pole Locations

Desired pole		Computed pole	
-1.2	-1.6j	-1.20944	1.58904j
-1.2	-1.6j	-1.20944	-1.58904j
-1.0		-1.02955	
-0.05		-0.05836	

performance. The feedback matrix F is

$$F = \begin{bmatrix} -0.27091 & 0.18869 & 0.0 & 0.0 \\ 1.88298 & -1.60017 & 0.0 & 0.00914 \end{bmatrix}$$

The objective function is 0.0002 and the additive output singular value vs frequency is seen in Figure 6.21. This plot shows that in the robustness design the gain adjustment moves the minimum singular value from about 0.004 rad, with very poor phase and gain margins, to a level of 0.612 rad, close enough to the desired values of gain and phase. After obtaining the feedback gains the NPGS 'OPTSYS' program was used to obtain the necessary data, Bode plot, pole-zero map, and time response plot. The $G*F$ robustness design time response plot is shown in Figure 6.22. The response of pitch rate is relatively good but sluggish response of pitch attitude to δ_c step input. The performance of the pitch attitude was degraded. It is possible that a

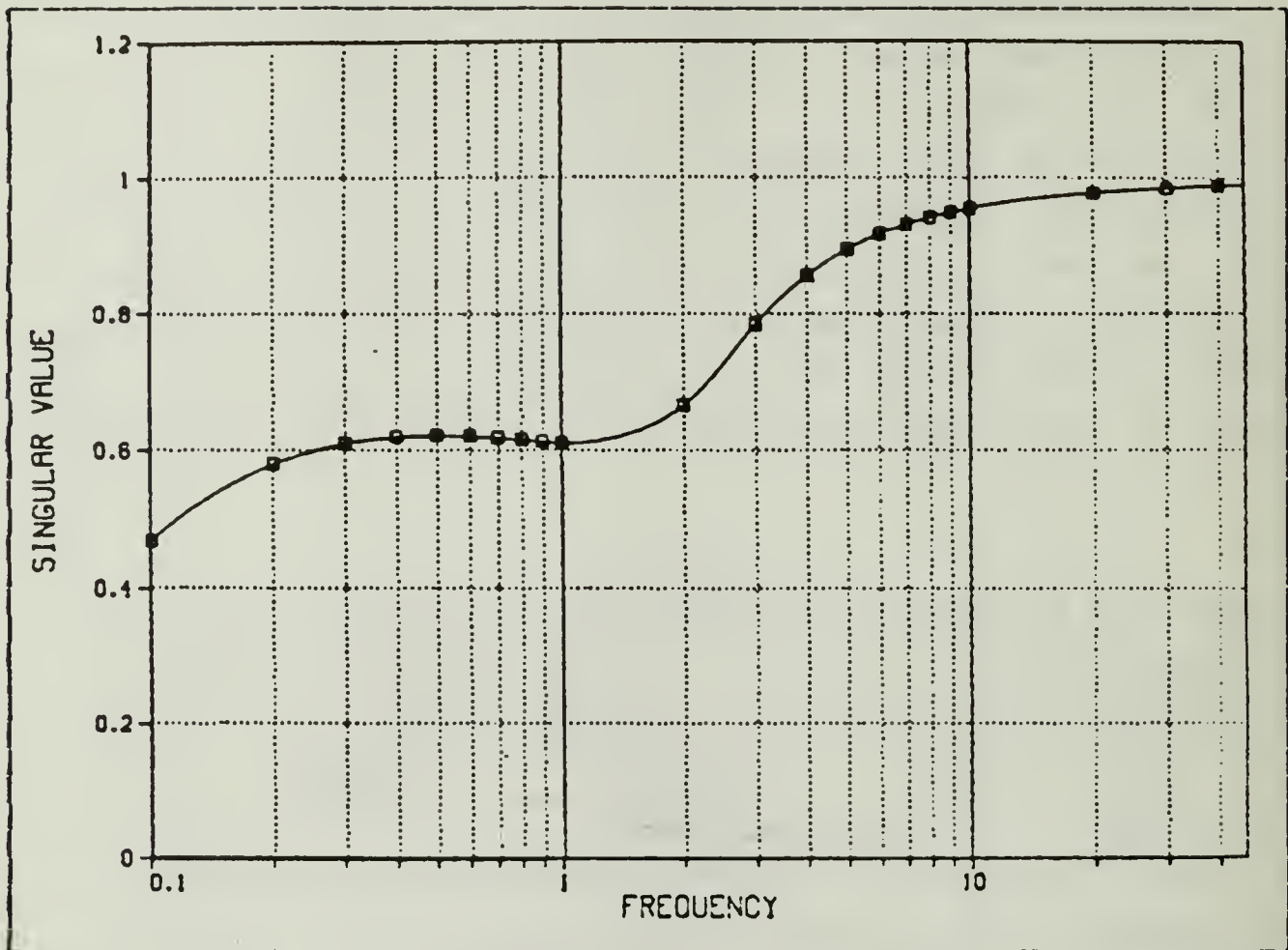


Figure 6.21 Robustness Design $G*F$ Singular Value Plots.

further change in the pole location could achieve better performance and still meet the robustness criteria. The body axis forward velocity and vertical velocity perturbation responses are the same as in the pole placement only design(see Figure 6.4). Comparing the loop Bode plots of the pole placement and robustness design transfer function, $G*F$, shows an increase in robustness.

Considering a SISO Bode analysis, the channel input 1 output 1 bode plot are shown in Figure 6.23 and 6.24. The bandwidth(BW) shows a small increase, 0.6 rad/sec, and the phase margin decrease of 26 degrees. The DC gain drops from 21.4 db to 17.3 db, a 4 db decrease and the slope change is similar to the pole only design as seen in Figures 6.23 and 6.24. This channel only shows a smooth curve.

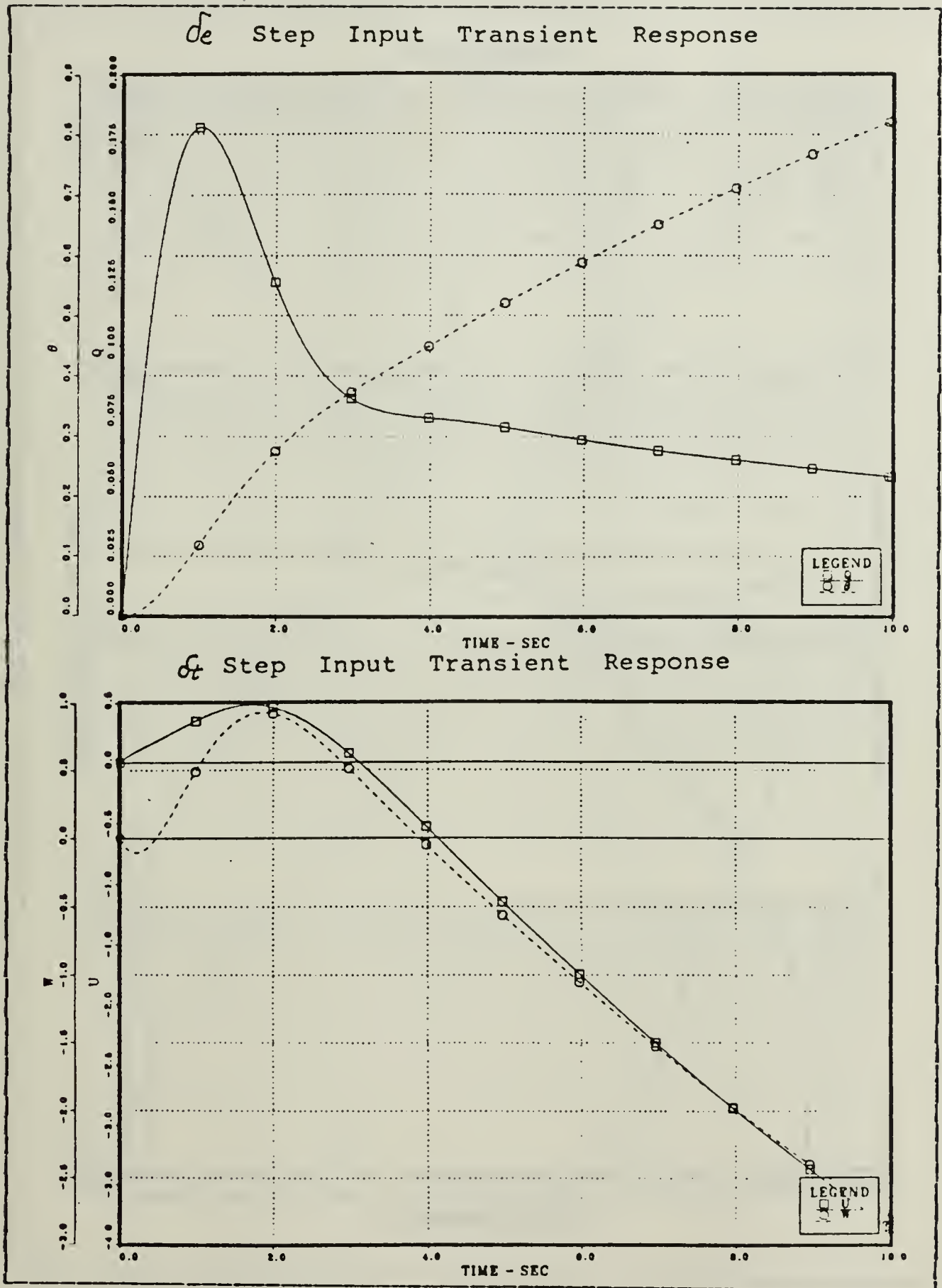


Figure 6.22 G*F Robustness Design Time Response.

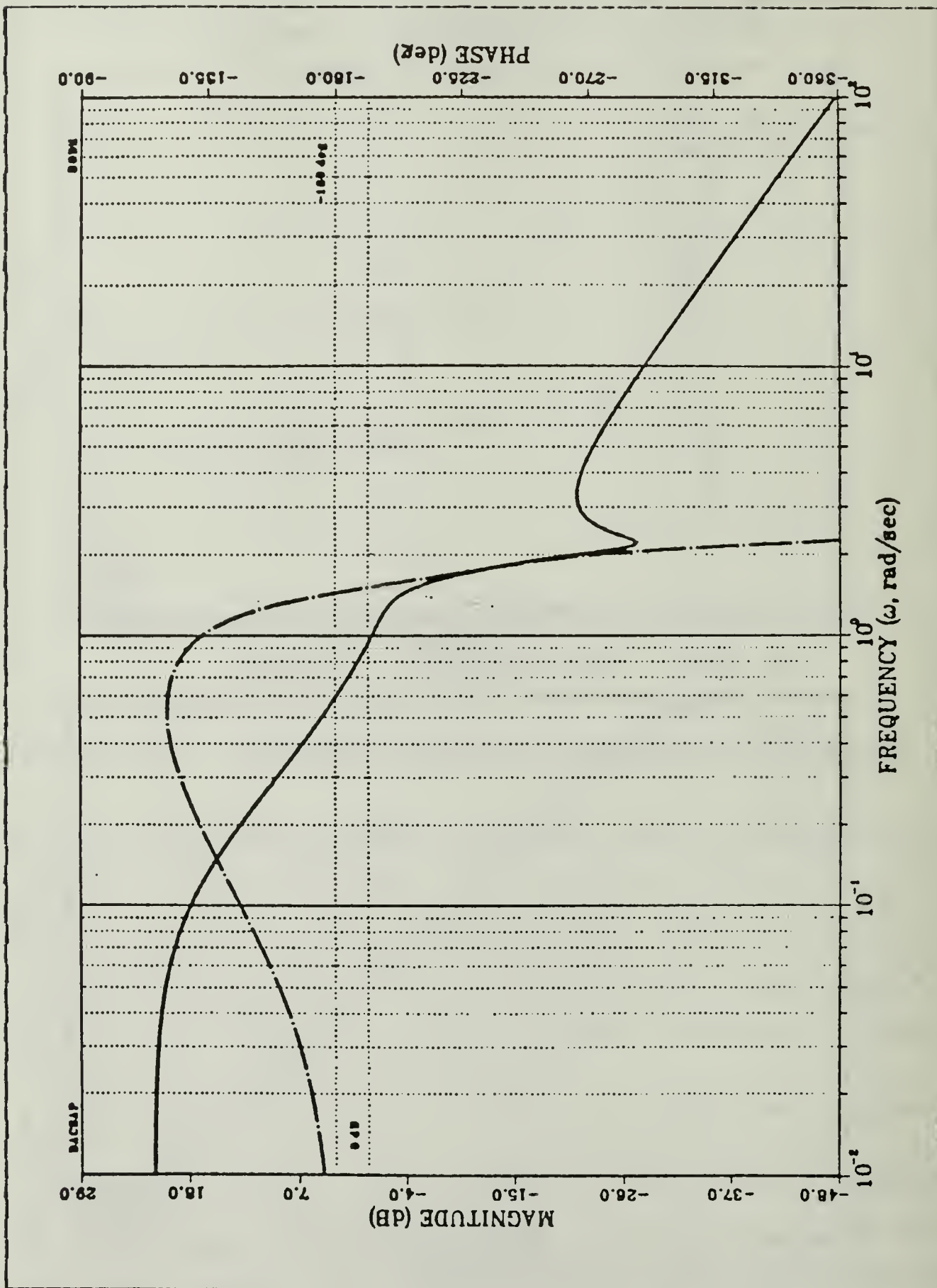


Figure 6.23 Pole Placement Only Design $G*F$ 1:1.

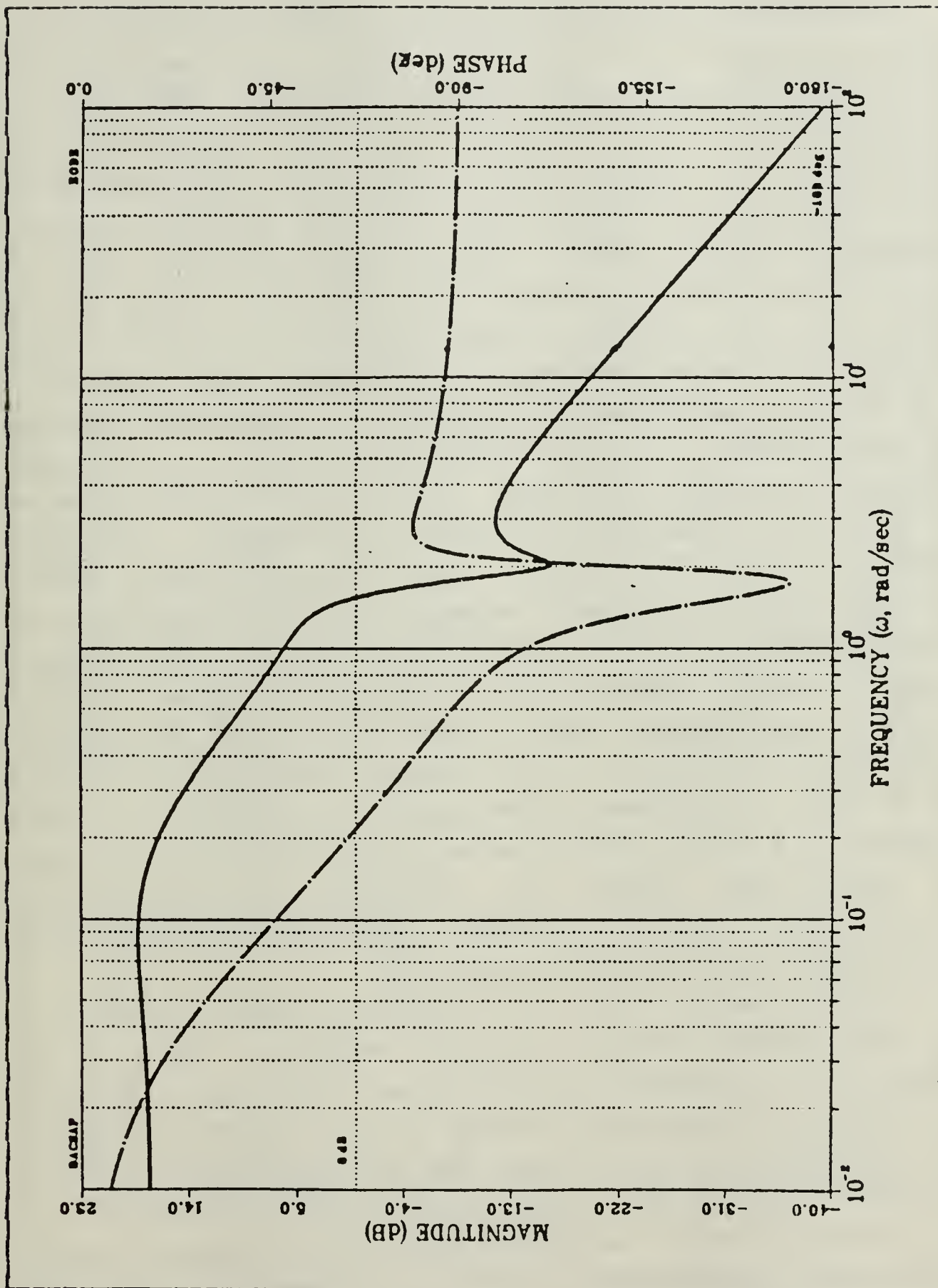


Figure 6.24 Robustness Design G*F 1:1.

Considering the channel input 1 output 2 with bode plots shown in Figures 6.25 and 6.26, a shift in the bandwidth(BW) from 2.4 rad/sec to 3.2 rad/sec is shown. The DC gain increases from 12.7 db to 15.8 db at the minimum singular frequency of 1 rad/sec and an increase in the phase margin of 28 degrees. Figures 6.25 and 6.26 show the similar frequency response curve, slope changes by zeros move the one pole position 0.8 rad/sec for pole-zero cancel and the other one zero move to close the minimum singular value frequency 1 rad/sec and two pole location. The increase in the DC gain and phase margin yields an increased tolerance to perturbation. The channel input 2 output 1 bode plots are shown in Figures 6.27 and 6.28. The DC gain decreases 16 db and the bandwidth shifts left 0.8 rad/sec, increasing the phase margin 151 degrees. The zero shift has the effect of smoothing the frequency response curve in the vicinity of the frequency of the minimum singular value. The channel input 2 output 2 bode plots are shown in Figures 6.29 and 6.30. These figures show a small shift left in the bandwidth from 4.5 rad/sec to 2.8 rad/sec. The DC gain decreases 12 db with an increased phase margin of 56 degrees. This results in a smooth curve, caused by the zero location shift in the same manner as previous channels(channels 1;1,2;1,2;2). The G*F transfer functions bode plot numerical results are provided in Table 6.

The noticeable change in the overall system, however, is in the transfer function input 1 output 2. This is the change at the minimum singular value position, increasing the gain and phase margin through a change in feedback gain. The optimizer routine brings the system gains to a more balanced condition and recovers a highly robust design.

The gain changes associated with the robustness improvement cause the zeros of the various closed-loop pole-zero diagram of the closed-loop transfer matrix to move. A

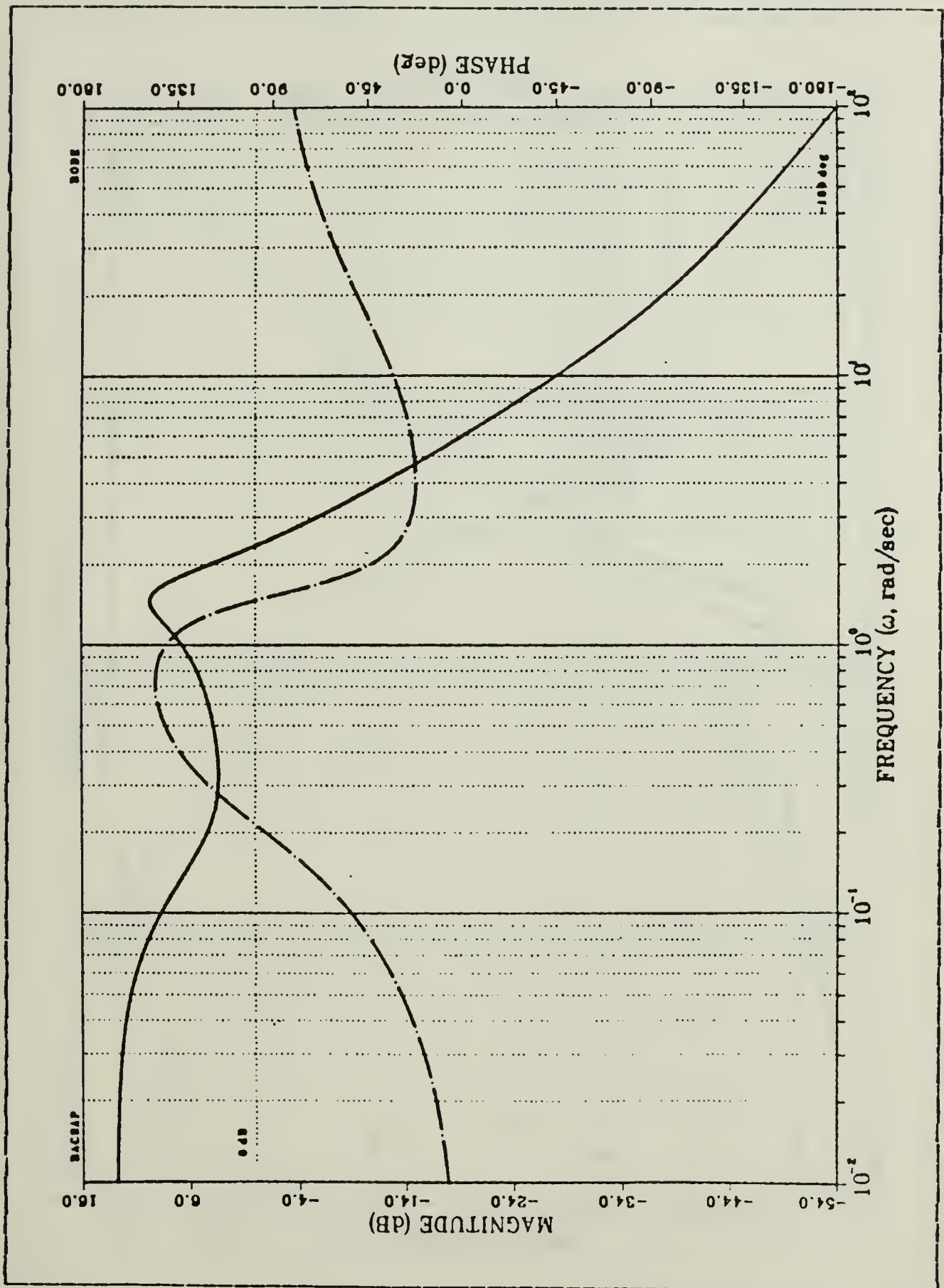


Figure 6.25 Pole Placement Only Design $G \cdot F$ 1:2.

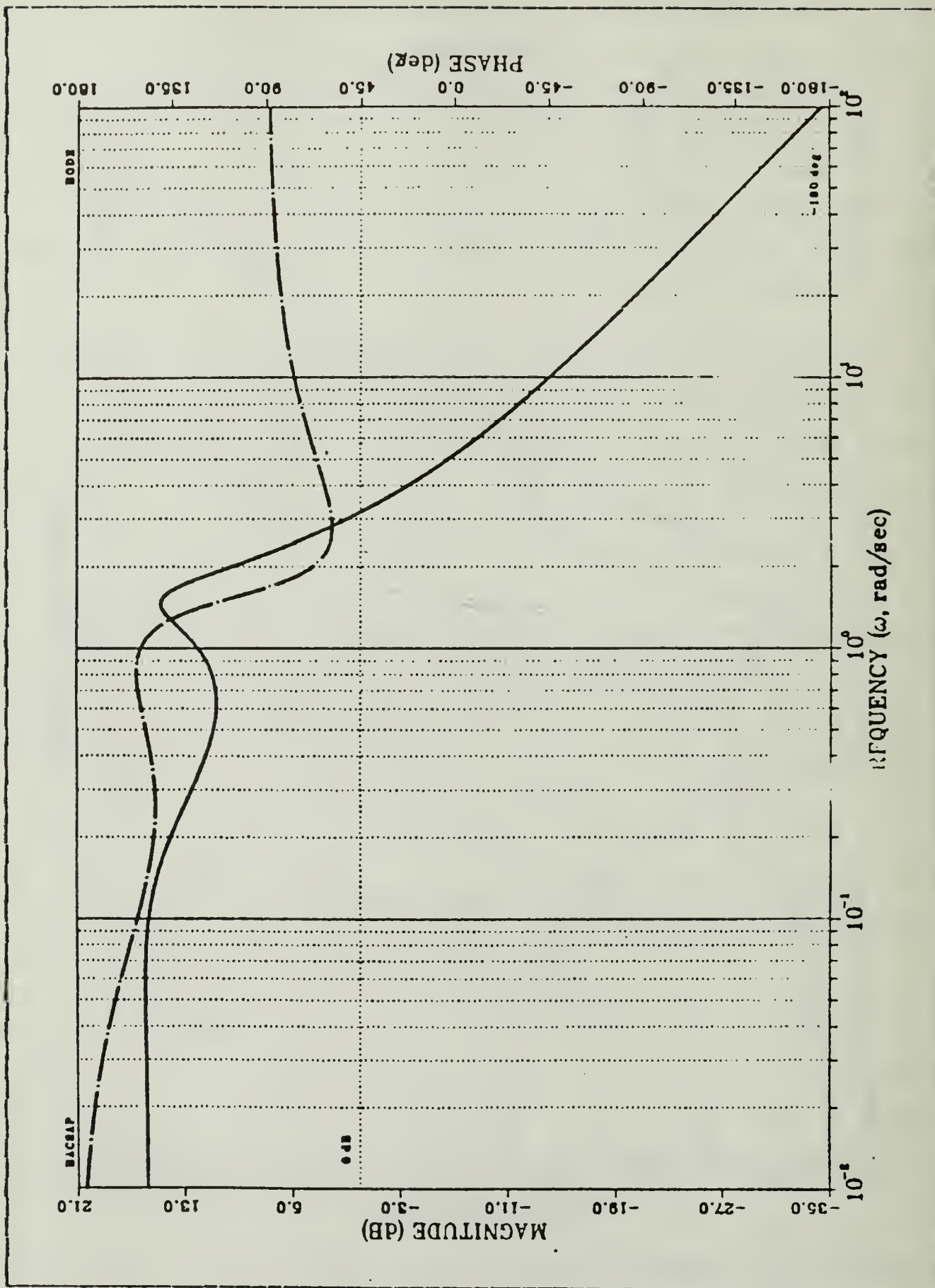


Figure 6.26 Robustness Design $G*F$ 1:2.

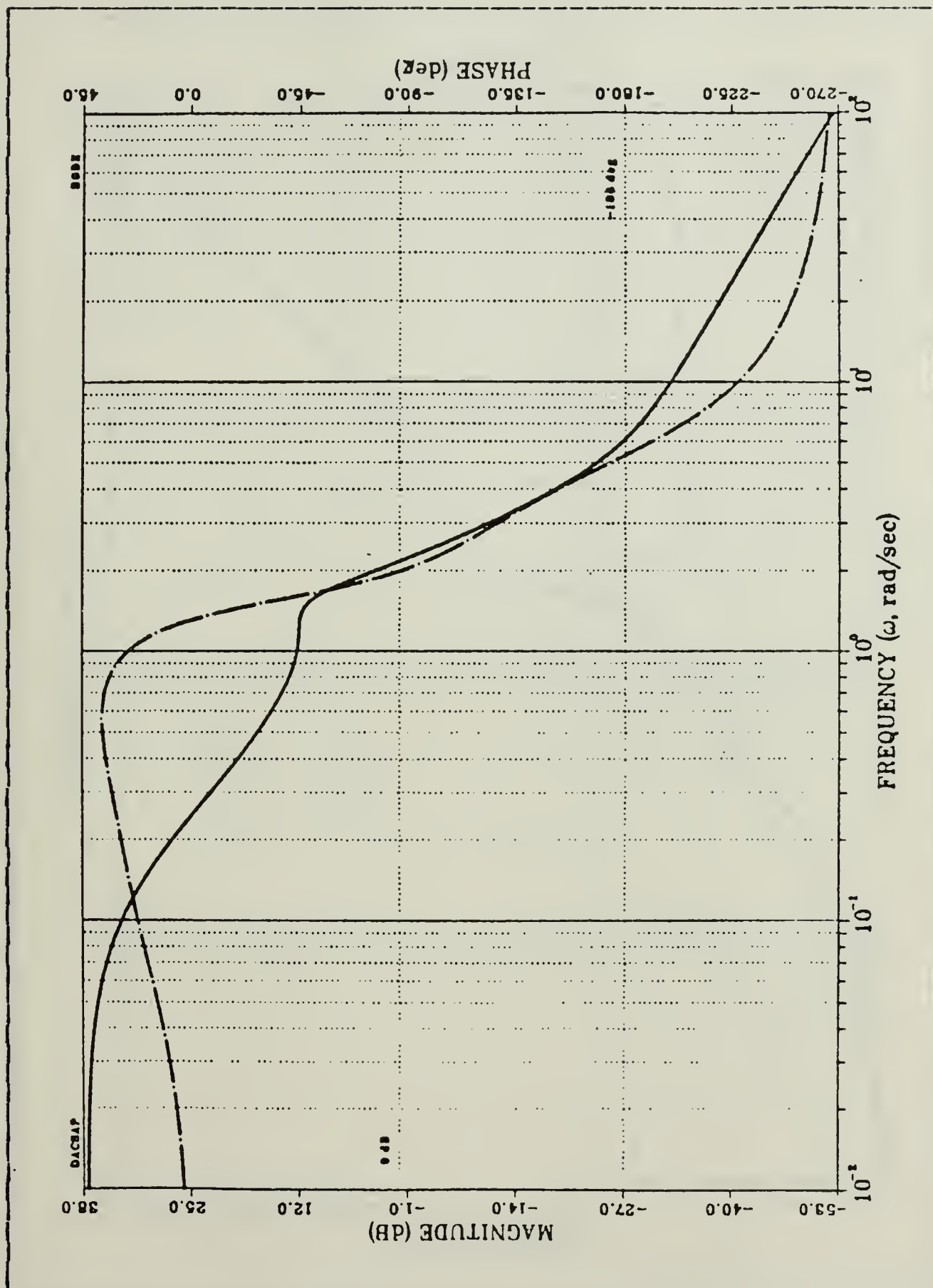


Figure 6.27 Pole Placement Only Design $G*F$ 2:1.

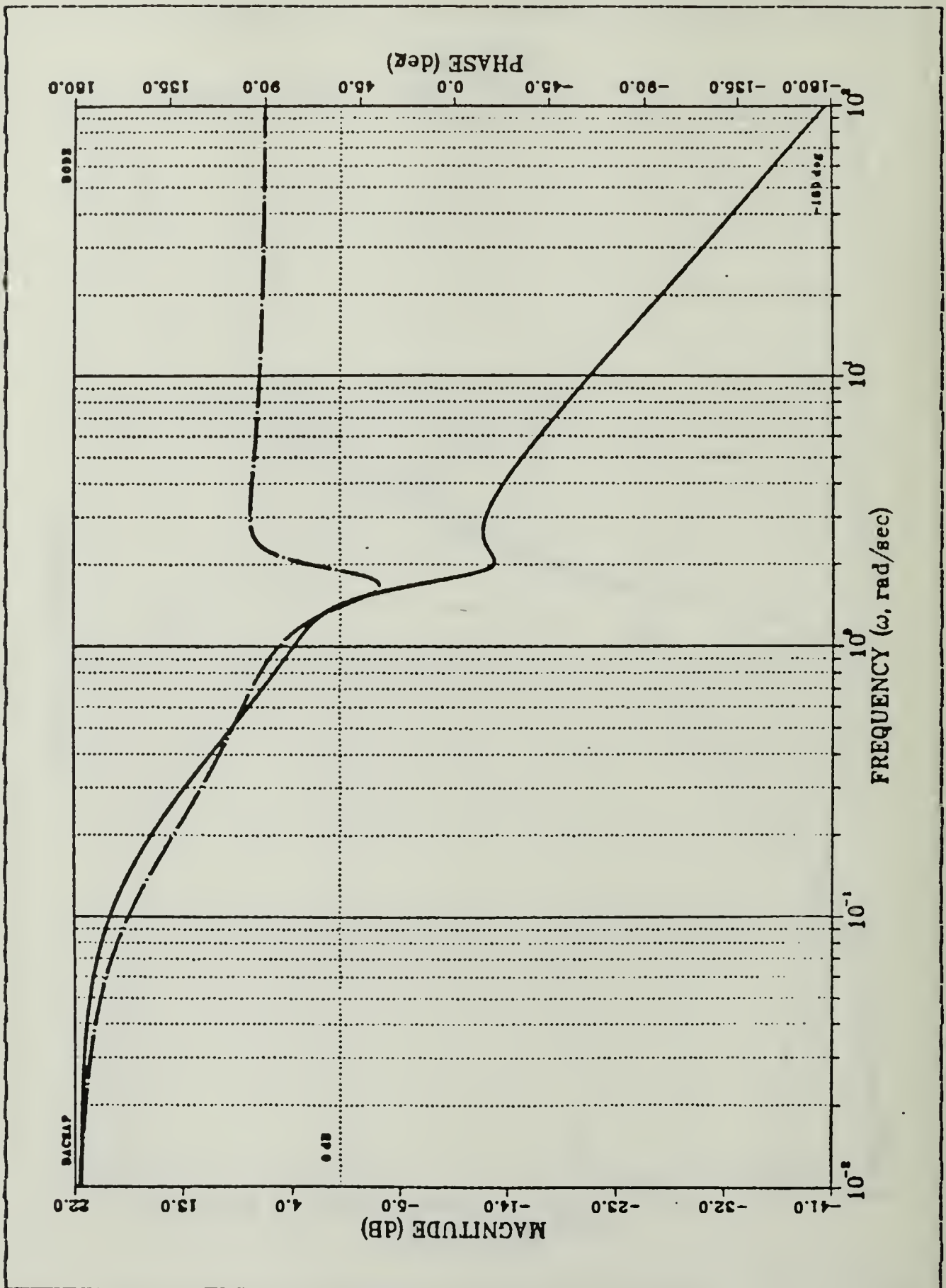


Figure 6.28 Robustness Design G*F 2:1.

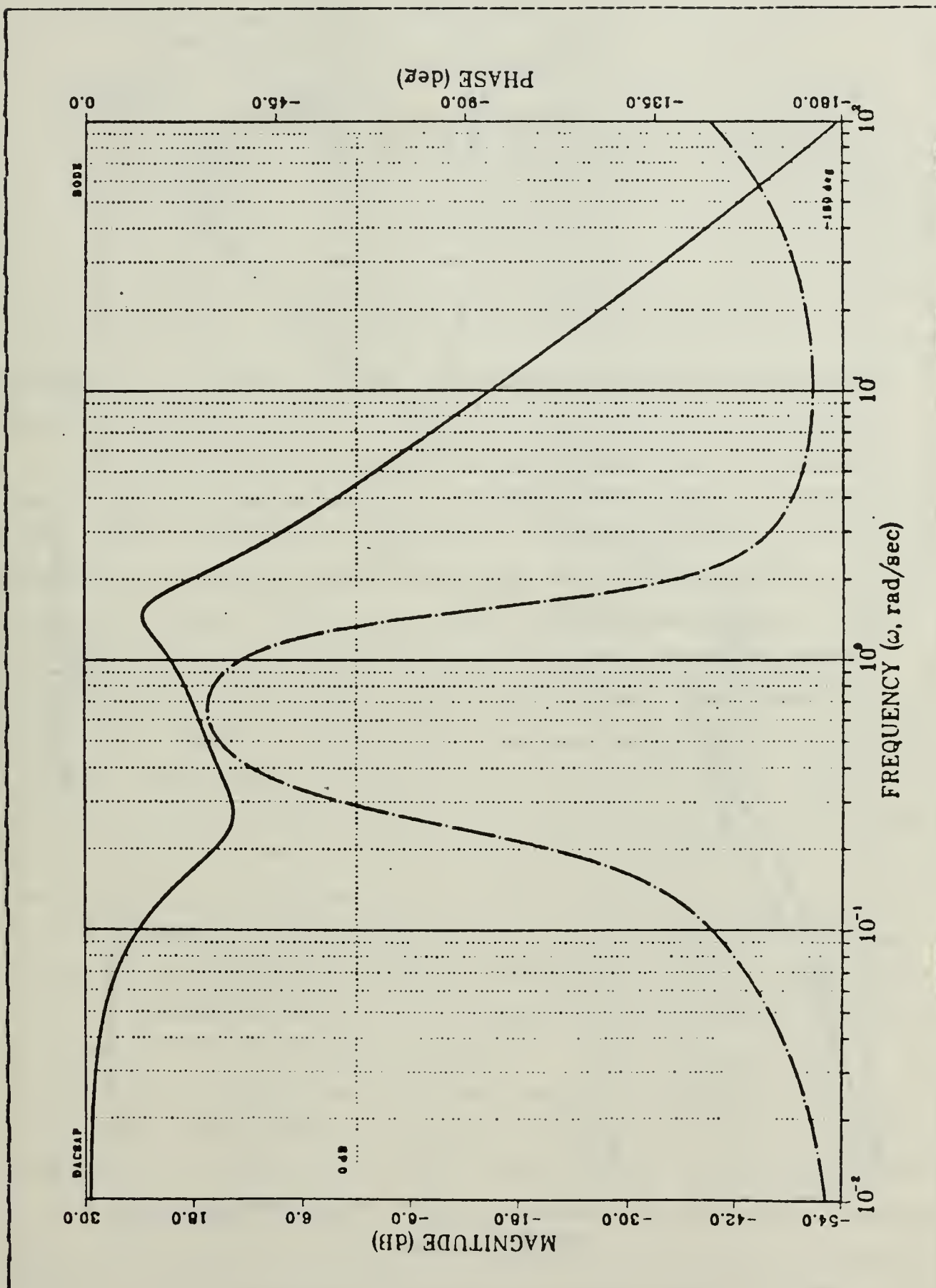


Figure 6.29 Pole Placement Only Design G*F 2:2.

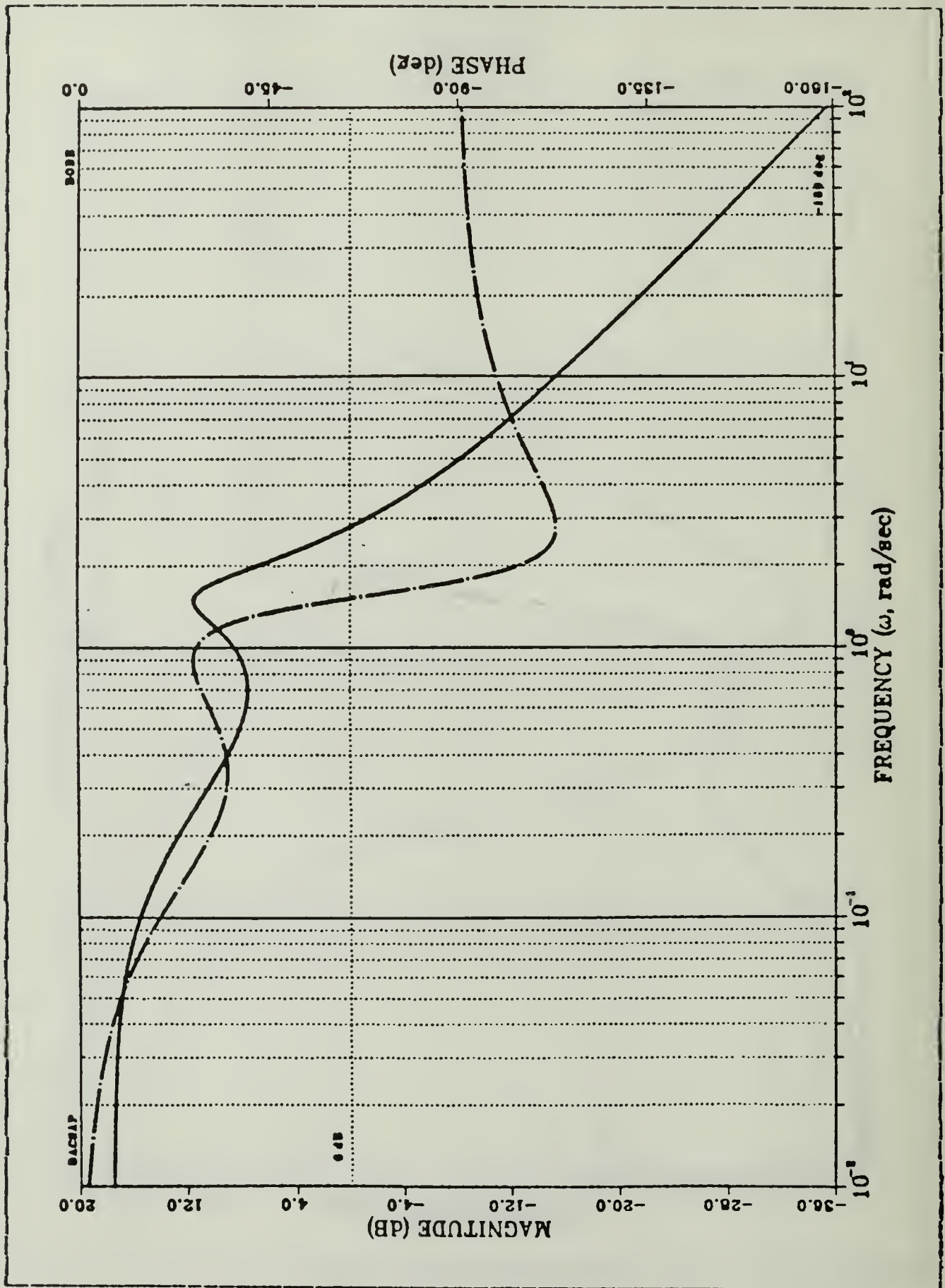


Figure 6.30 Robustness Design $G*F$ 2:2.

TABLE 6
G*F Transfer Functions Bode Plot Results

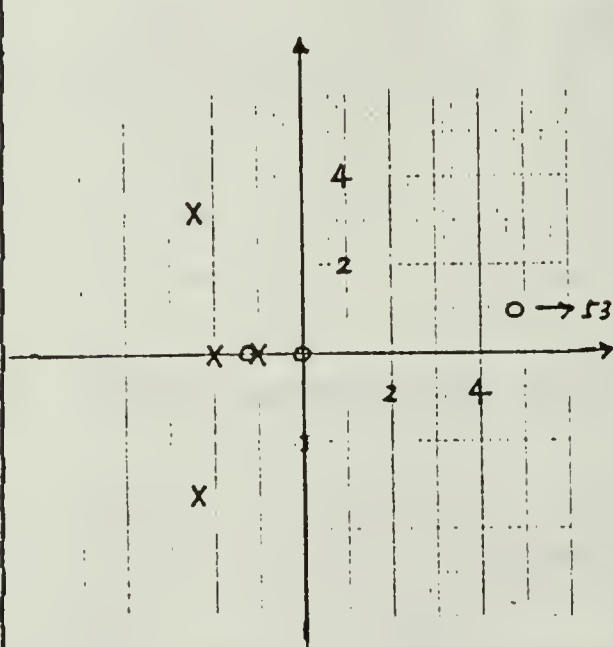
channel	Bandwidth		PM		GM		Gain	
	pole	rad/sec SV	pole	degree SV	pole	SV	pole	SV
1 : 1	0.95	1.56	49	23	3.9	.	21.4	17.3
1 : 2	2.36	3.2	211.3	239	.	.	12.6	15.8
2 : 1	2.2	1.43	80	231	.	.	37.3	21.5
2 : 2	4.5	2.8	10.7	17.5	.	.	29.1	17.5

comparison of the eight pole-zero diagrams is shown in Figures 6.31 to 6.34.

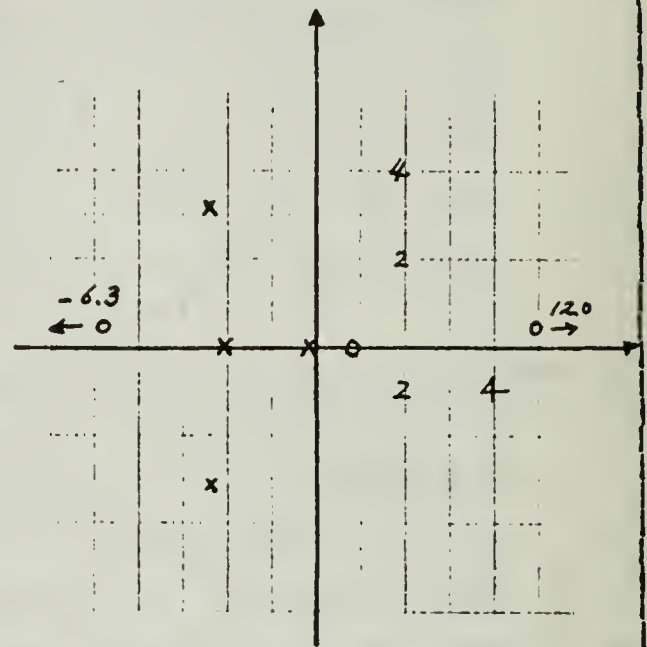
The significant feature of these pole-zero diagrams is the shift of the zeros of the optimized design in a direction that attempts to equalize or balance the frequency response for frequencies in the vicinity of the minimum singular values. The pole-zero diagram of channel input 1 output 2 will be discussed as an example of this effect. In figure 6.30, the pole only design zeros are located about -0.31 and -0.78. When the pole placement and robustness routine completes the feedback gain modification these zeros shift close to -1.7 and 0.28. The effect of these zeros shifting is to combine with the pole locations to equalize the frequency response and increase the DC gain 25 db at the same bandwidth and the minimum singular value frequency 1 rad/sec, as depicted in Figures 6.35 and 6.36. Zero shifts for the remainder of the transfer functions provide similar results in the other channels. By moving toward the frequencies associated with the minimum singular values the zeros have balanced the overall frequency response of the system in each channel. While the channel gain modification is the primary mechanism for robustness recovery the zero shift associated with the feedback gain changes is directly related to the overall frequency response of the system.

POLE ONLY DESIGN

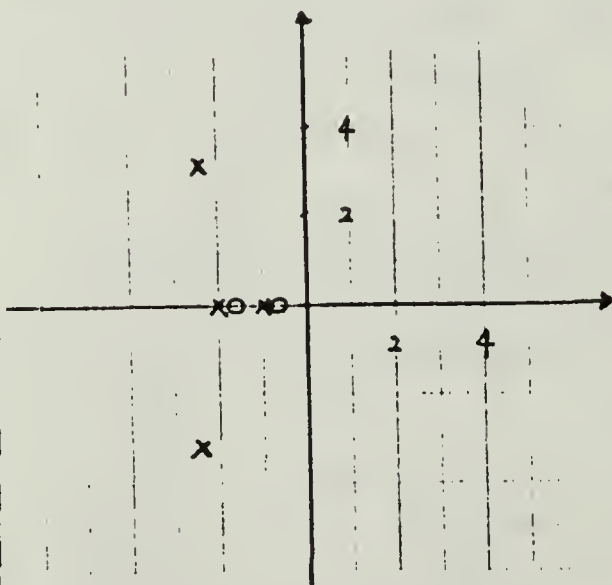
ROBUSTNESS DESIGN



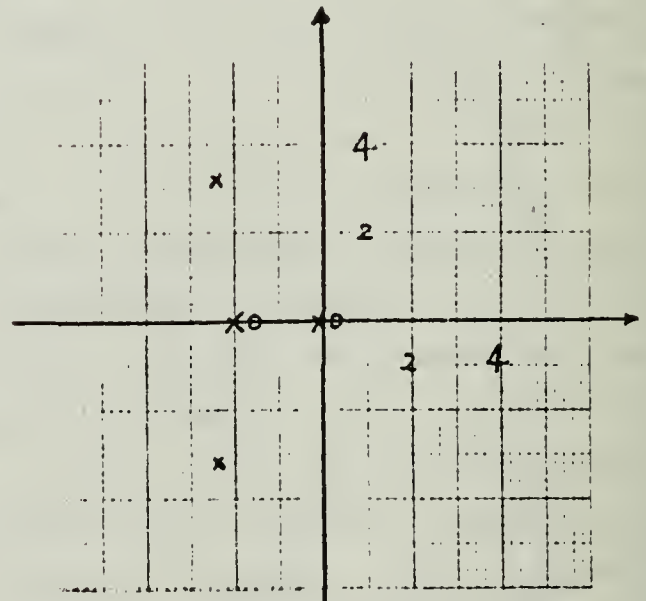
$$\hat{d}_e - U(1 : 1)$$



$$\hat{d}_e - U(1 : 1)$$



$$\hat{d}_e - W(1 : 2)$$

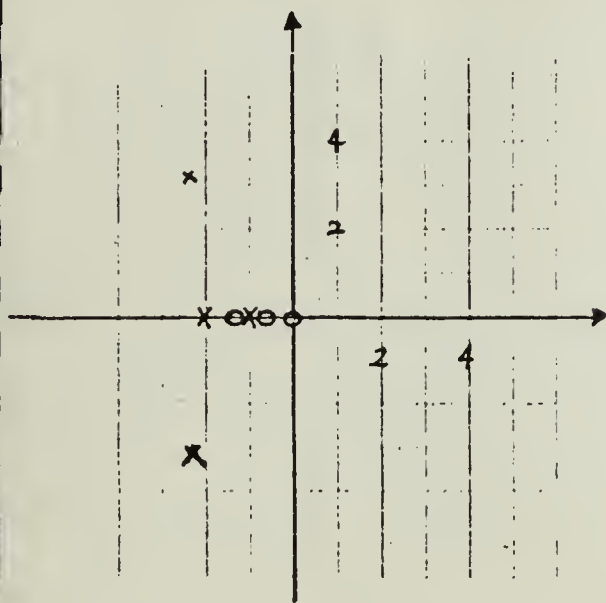


$$\hat{d}_e - W(1 : 2)$$

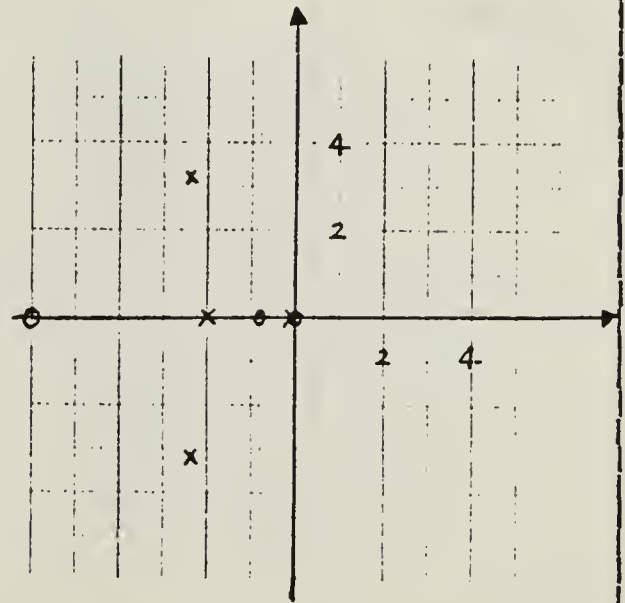
Figure 6.31 Pole-Zero Map for 1:1 and 1:2.

POLE ONLY DESIGN

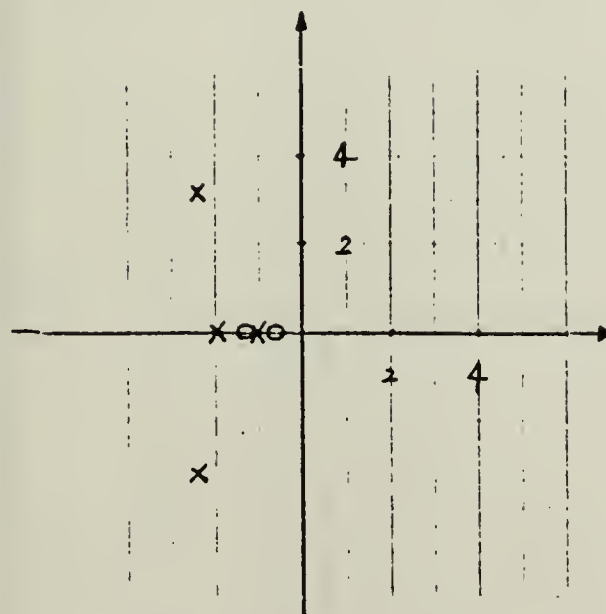
ROBUSTNESS DESIGN



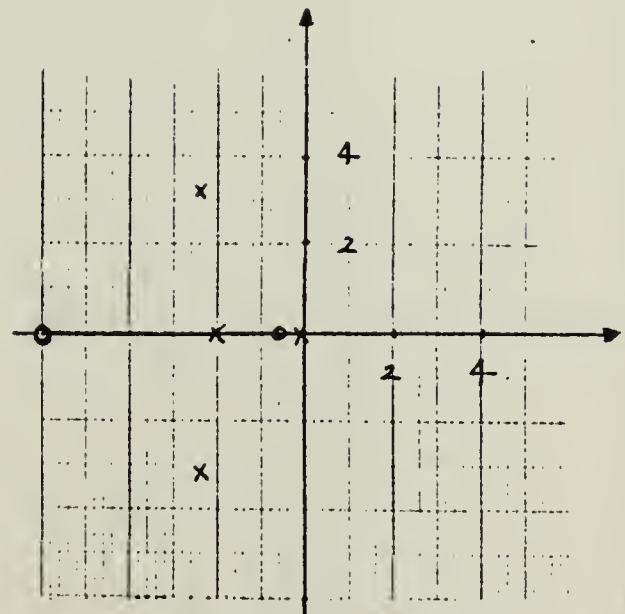
$$\hat{d}_e - Q(1 : 3)$$



$$\hat{d}_e - Q(1 : 3)$$



$$\hat{d}_e - \theta(1 : 4)$$



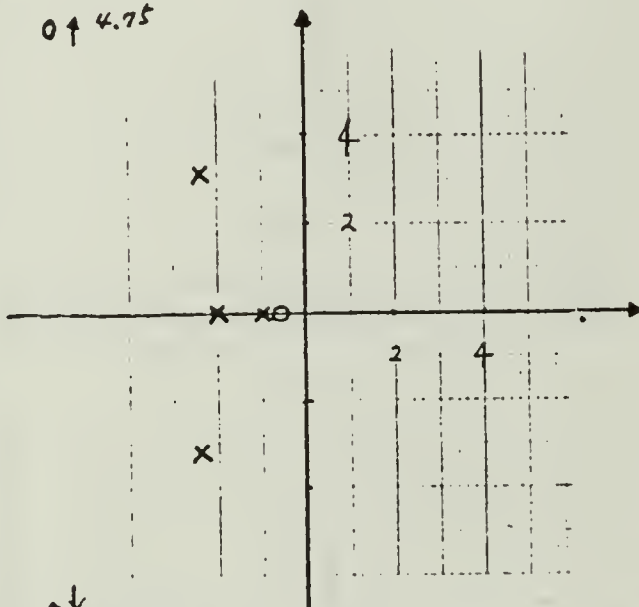
$$\hat{d}_e - \theta(1 : 4)$$

Figure 6.32 Pole-Zero Map for 1:3 and 1:4.

POLE ONLY DESIGN

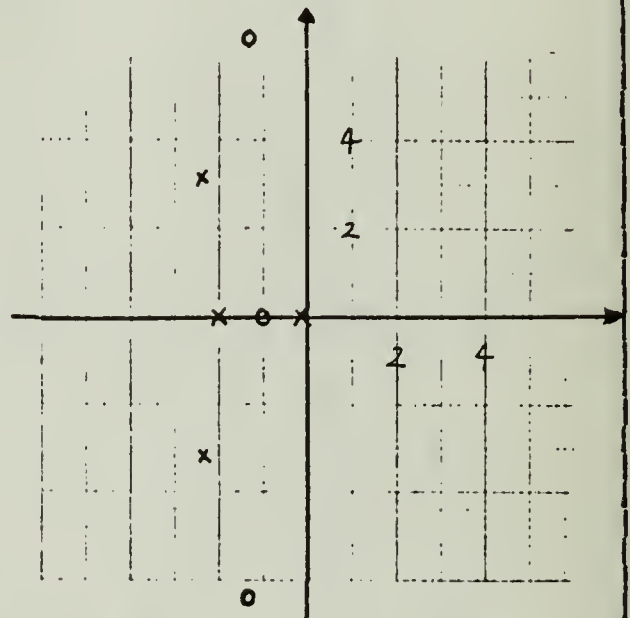
ROBUSTNESS DESIGN

$0 \uparrow 4.75$

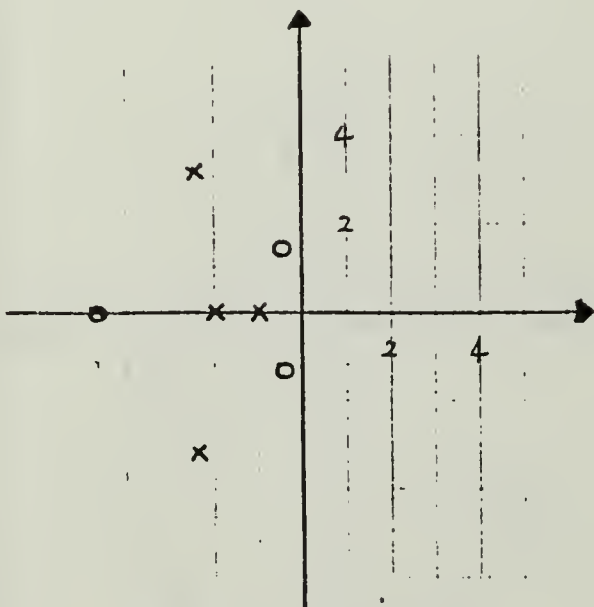


$0 \downarrow 4.75$

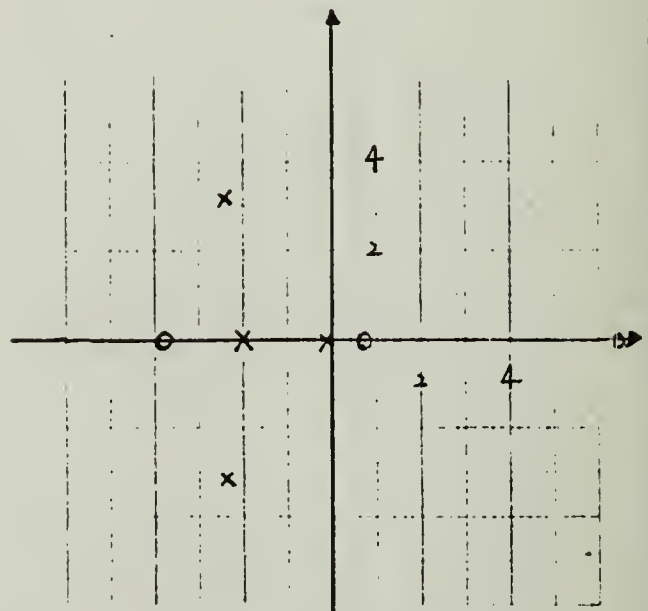
$\delta_t - U(2 : 1)$



$\delta_t - U(2 : 1)$



$\delta_t - W(2 : 2)$

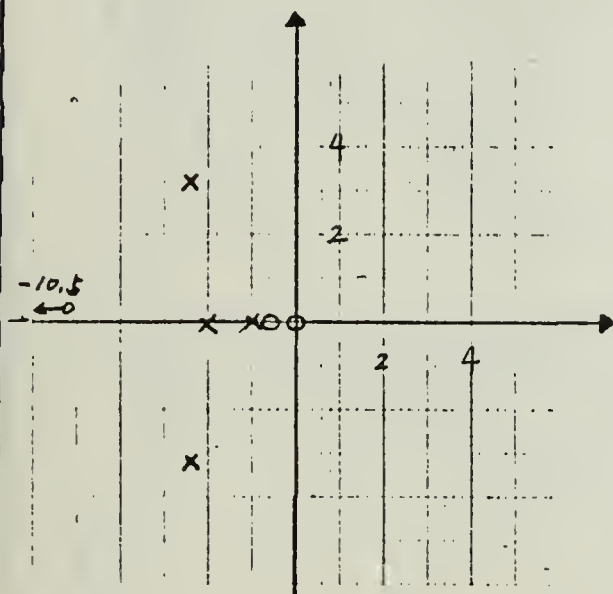


$\delta_t - W(2 : 2)$

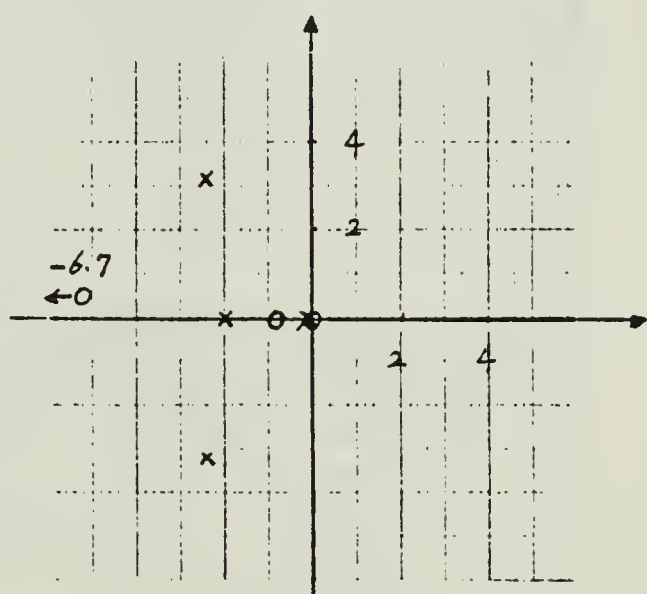
Figure 6.33 Pole-Zero Map for 2:1 and 2:2.

POLE ONLY DESIGN

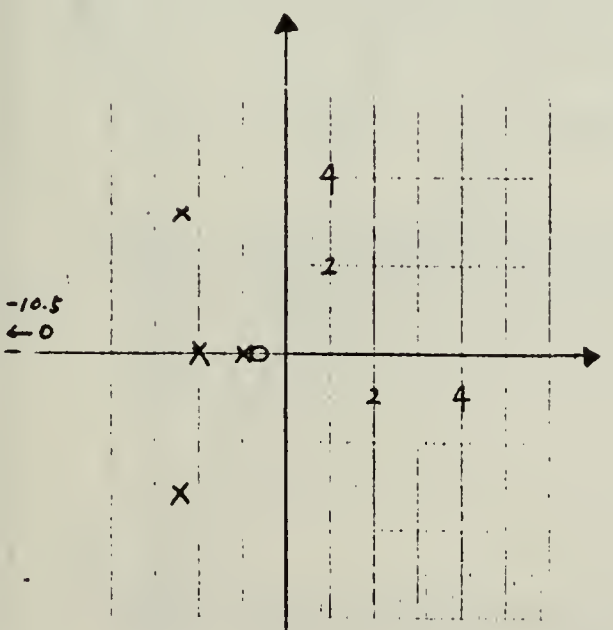
ROBUSTNESS DESIGN



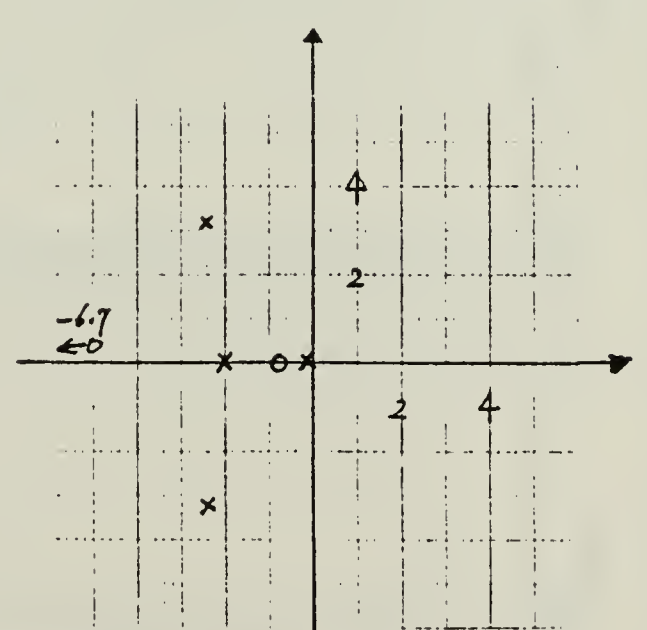
$$\hat{d}_t - Q(2 : 3)$$



$$\hat{d}_t - Q(2 : 3)$$



$$\hat{d}_t - \theta(2 : 4)$$



$$\hat{d}_t - \theta(2 : 4)$$

Figure 6.34 Pole-Zero Map for 2:3 and 2:4.

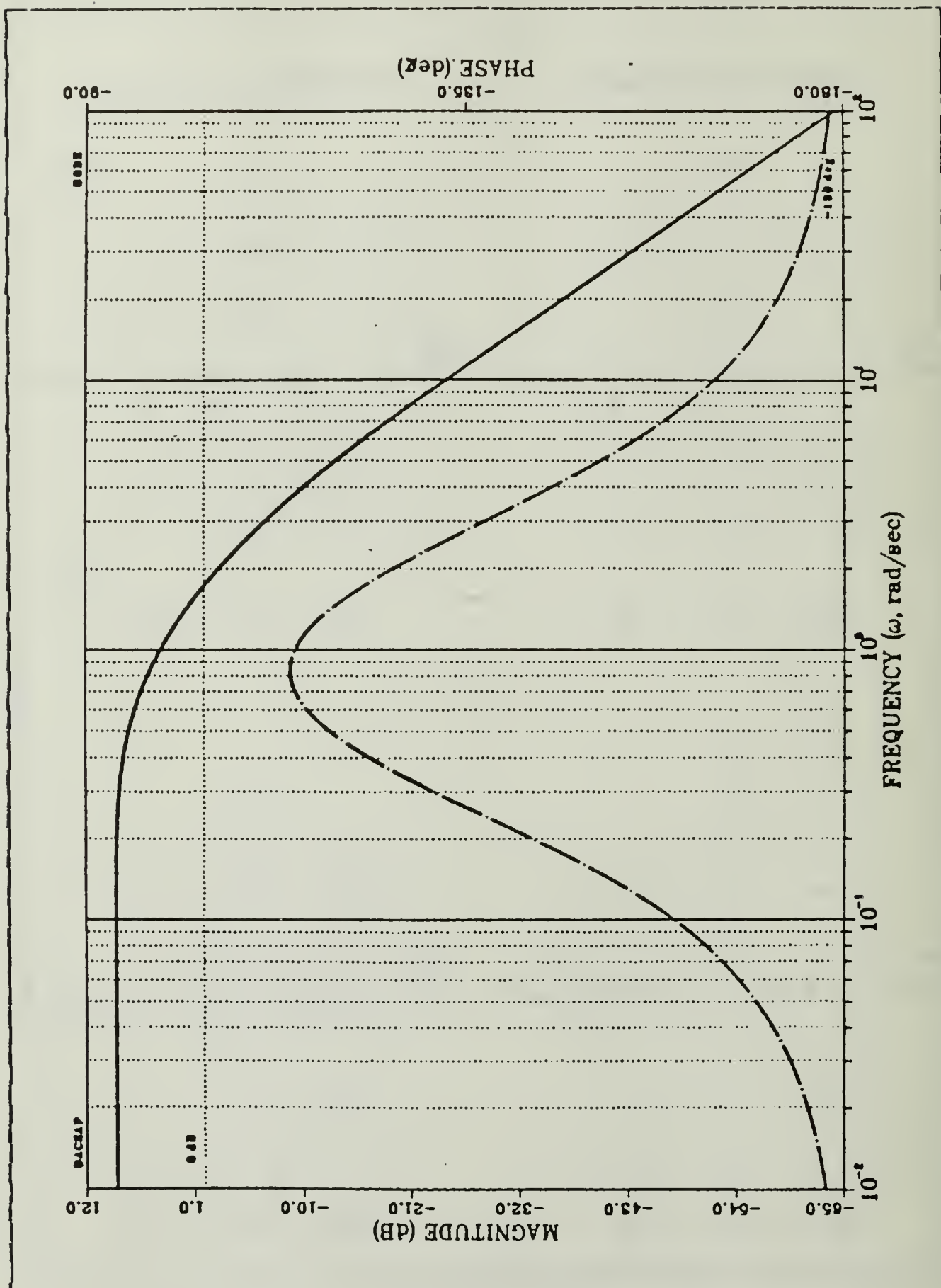


Figure 6.35 Pole Placement Only Design G*F Closedloop 1:2.

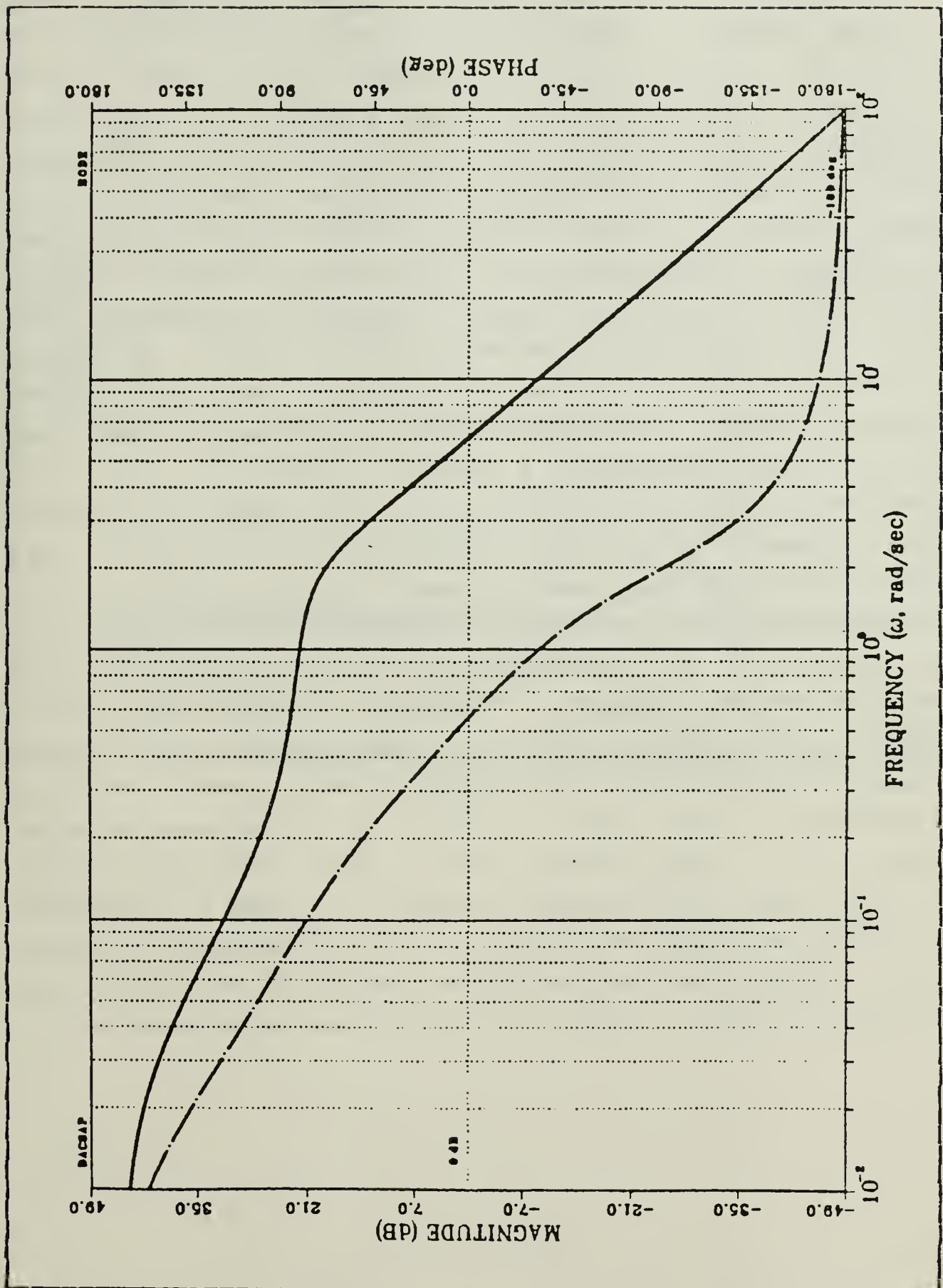


Figure 6.36 Robustness Design G^*F Closedloop 1:2.

To summarize this analysis, a given performance level has been chosen in terms of pole locations. The level of robustness has been set for a desired gain and phase margin based on the universal gain and phase margin curve. The pole placement and robustness routine improves the robustness level by changing the feedback gains that affect the channel input 1 output 2 cross-coupling. This robustness recovery is affected by modification of the system feedback gains in such a manner that cross coupling gains are reduced so that small cross-coupling perturbations do not drive the system into instability. The open-loop transfer function plots are used to indicate how this mechanism operates and have been shown to be an alternative indicator of channels that may be affected by crossfeed perturbations. The pole-zero diagrams of the closed-loop transfer functions of the transfer matrix further indicate that zero movement is in a direction that equalizes the gain level of the frequency response curves in the vicinity of the lowest singular values providing a more balanced system response. Finally, a comparison of the input transfer function $F*G$ output singular value and output transfer function $G*F$ input singular value plots are shown in Figures 6.37 and 6.38. The $F*G$ output minimum singular value is too low (0.0076 rad). The $G*F$ input minimum singular value is also its own low (0.1 rad). Therefore both transfer functions control only own function's robustness. Further analysis would be needed if robustness were required in both the input and output case simultaneously.

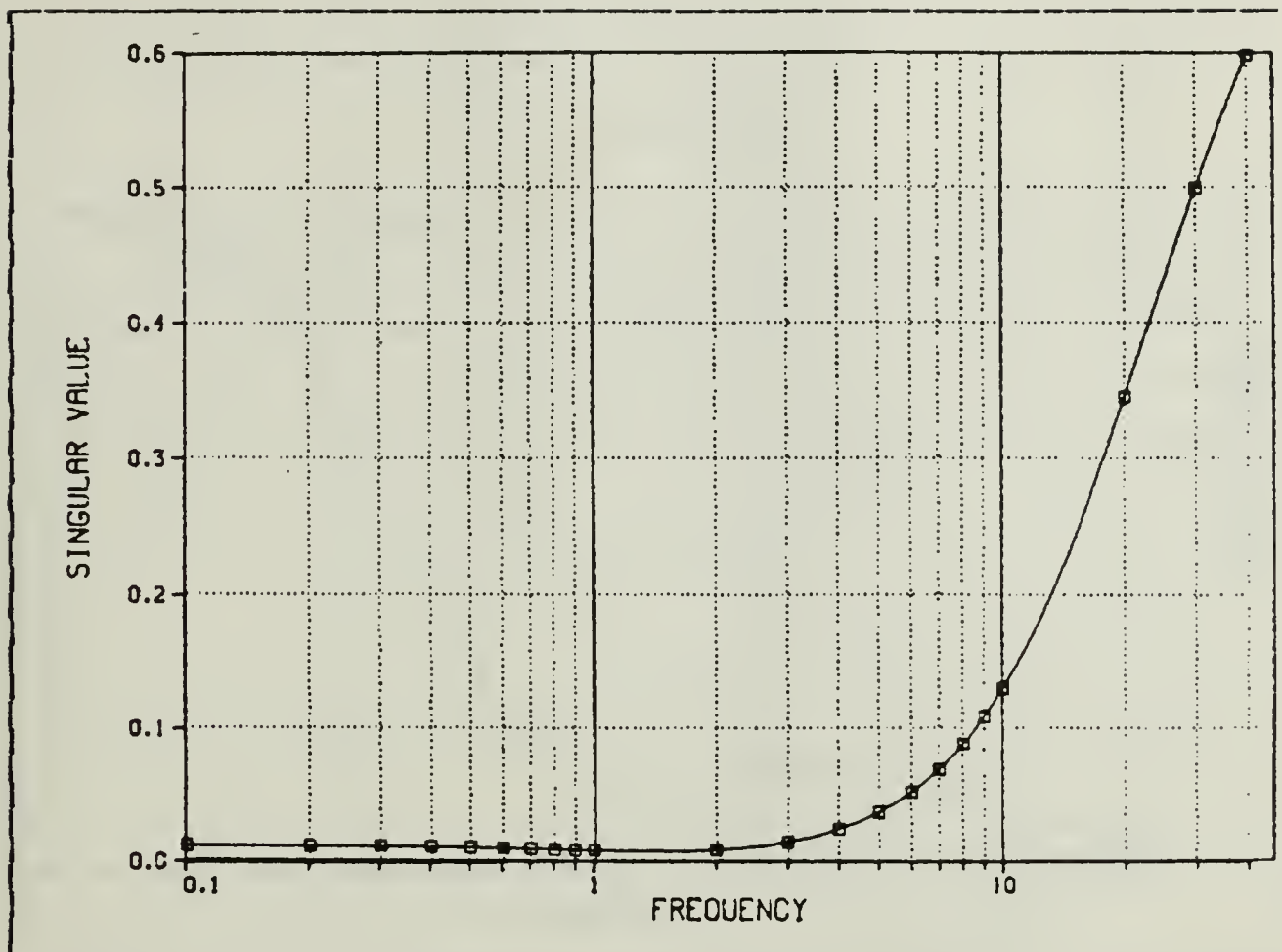


Figure 6.37 Robust Design F*G Output Singular Value Plots.

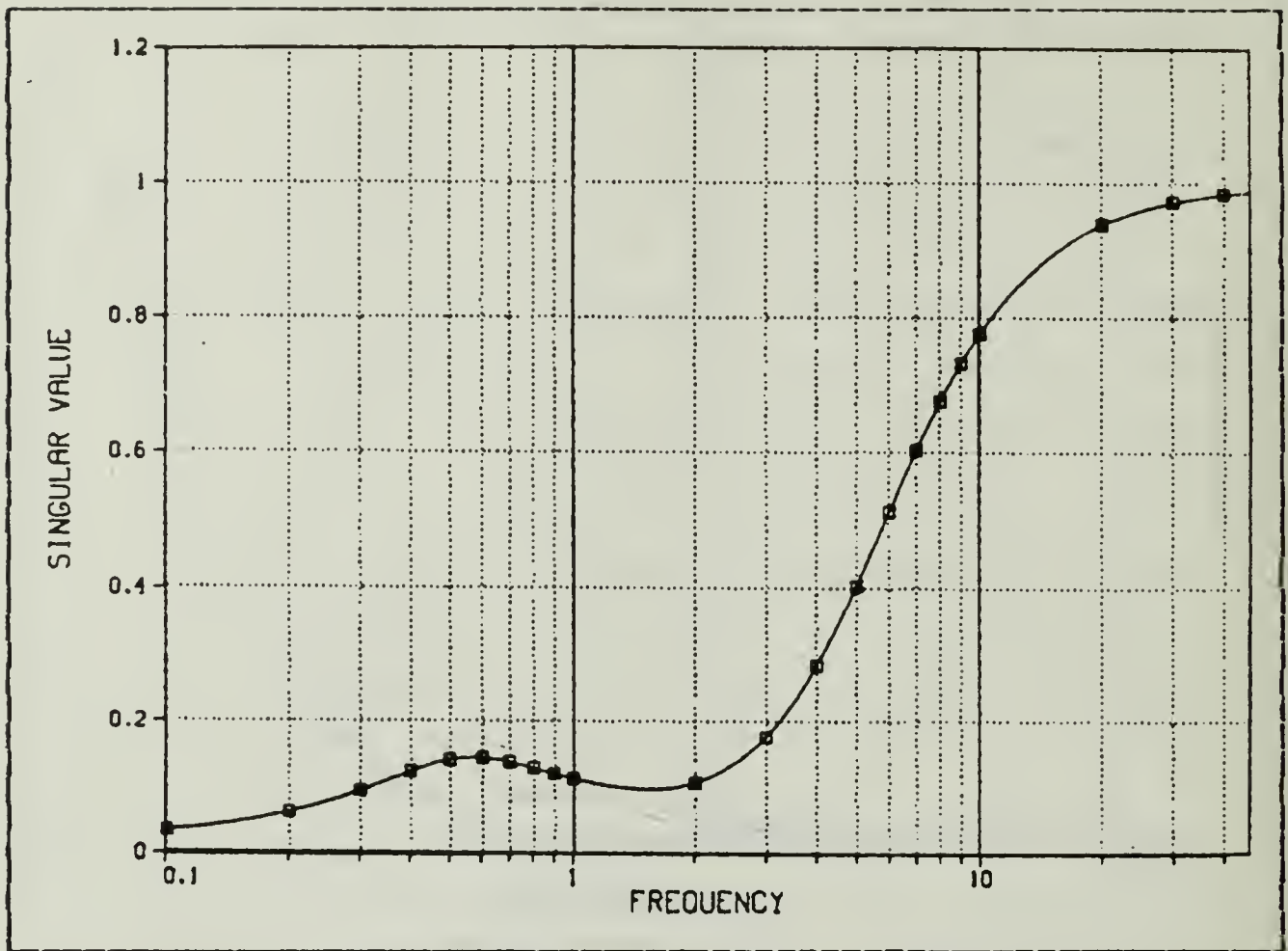


Figure 6.38 Robust design $G*P$ Input Singular Value Plots.

VII. CONCLUSIONS

The pole placement and robustness design routine coupled with the Automated Design Synthesis program provides the designer an excellent tool with which to attack the robust design problem. The pole placement and robustness design routine has demonstrated the capability of providing designs that solve the X22A V/STOL A/C longitudinal dynamic problem caused by cross-coupling perturbations which reduce robustness in multivariable systems. This design improvement is accomplished by modifying the system feedback gains in such a manner that the gain in channels that are affected by cross-coupling perturbations is equalized with other system gains to reduce this cross-coupling effect. The gain changes are accompanied by zero shifts which also influence the gain distribution and frequency response of the system.

The lack of robustness can be discovered in two ways. The first method is to plot the open-loop Bode plots of each element of the transfer matrix and look for extremely high gains or bandwidths relative to the other transfer functions. The second method examines the singular values of the return difference matrix for magnitude. The joint analysis method tells where the robustness problem occurs in the design. Low singular values correspond to low robustness. The pole placement and robustness design routine can increase robustness by modifying feedback gains to reduce the effect of cross-coupling within the system. Observing the gain modification made by the pole placement and robustness routine the critical channel within the system that affects the robustness can be determined from the Bode plots. The pole placement and robustness routine feedback gain changes also cause zero shifts during the robustness

recovery. The gain on the open loop Bode plot for the affected cross-coupling channel is adjusted and the closed-loop zeros, as seen on the pole-zero diagram, are shifted. This zero shift is in a direction which will combine with system poles to smooth the frequency response diagram in the vicinity of the minimum singular value. The performance of the robustness design input transfer function $F*G$ provides the best response, but the output transfer function $G*F$ indicates the performance of the pitch attitude is degraded. It is possible that a further change in the pole location would provide better performance and still meet the robustness criteria.

LIST OF REFERENCES

1. Doyle, J. C. and Stein, G., "Multivariable Feedback Design: Concepts for a Classical/Modern Synthesis", IEEE Trans. Auto. Control, Vol AC-26, No.1, pp4-16, Feb 1981.
2. Safanov, M. G. and Athans, M., "Gain and Phase Margin of Multiloop LOG Regulators", IEEE Trans. Auto. Control, April 1977.
3. Sandell, N. S., Jr., Lehtomaki, N. A., and Athans, M., "Robustness Results in Linear Quadratic Gaussian Based Multivariable Control Designs", IEEE Trans. Auto. Control, Vol 26, No. 1, pp75-92, Feb. 1981.
4. Lehtomaki, N. A., Practical Robustness Measures in Multivariable Control System Analysis, Ph.D. Thesis, Massachusetts Institute of Technology, Cambridge, Mass 1981.
5. National Aeronautics and Space Administration TM - 84524, Application of Matrix Singular Value Margins of Multiloop Systems, by Mukhopadhyay, V. and Newsom, J., July 1982.
6. Mukhopadhyay, V. and Newsom, J., "The use of Singular Value Gradients and Optimization Techniques to Design Robust Controllers for Multiloop Systems", AIAA Guidance and Control Papers, August 1983.
7. Alphatech Inc., TR - 121, Multivariable Stability Margins for Vehicle Flight Control Systems, by Sandell, N. R., Jr., et al, Dec. 1981.
8. Cunningham, T. B., "Eigenspace Selection Procedures for Closed Loop Response Shaping with Modal Control", IEEE Trans. Decision & Control, Vol 1 PP178 - 186, 1980.
9. Gordon, V. C., "Utilization of Numerical Optimization Techniques in the Design of Robust Multi-input, Multi-output Control Systems", Ph.D. Thesis, Naval Postgraduate School, Monterey, California 1984.

INITIAL DISTRIBUTION LIST

	No.	Copies
1. Defense Technical Information Center Cameron Station Alexandria Va 22314	2	
2. Chairman, Code 67 Department of Aeronautics Naval Postgraduate School Monterey, Ca 93943	1	
3. Library, Code 0142 Naval Postgraduate School Monterey Ca 93943	2	
4. Professor D.J. Collins Code 67Co Department of Aeronautics Naval Postgraduate School Monterey, Ca 93943	5	
5. Hur, Joongil (Chang, jin hwa) 648-103 (14 tong 7 ban) Jeon-nong -1 dong, Dong-dae-moon gu Seoul, Korea	2	
6. Personnel Management Office Air Force Headquarters Dae-bang dong, Gwan-ak gu Seoul, Korea	2	
7. Lee, Chungwon SMC #2825 Naval Postgraduate School Monterey, Ca 93943	1	

1 3 5 3 7 5

8

211175

T Thesis
C C37152 Chang
C c.1 Analysis of control
system from a view-
point of desired pole
placement and desired
degree of robustness.

27 JAN 87

30949

211175

Thesis
C37152 Chang
c.1 Analysis of control
system from a view-
point of desired pole
placement and desired
degree of robustness.

Analysis of control system from a viewpo



3 2768 002 09709 9

DUDLEY KNOX LIBRARY